Macroscopic Traffic Flow Modelling on Roundabouts and Optimization

By

Legesse Lemecha

SUBMITTED IN PARTIAL FULFILMENT OF THE REQUIREMENTS FOR THE DEGREE OF DOCTOR OF PHILOSOPHY

AT

ADDIS ABABA UNIVERSITY

ADDIS ABABA, ETHIOPIA

ADDIS ABABA UNIVERSITY
DEPARTMENT OF
MATHEMATICS

The undersigned hereby certify that they have read and recommend to the Faculty of Graduate Studies for acceptance a thesis entitled " **Macroscopic Traffic Flow Modelling on Roundabouts and Optimization** " by **Legesse Lemecha Obsu** in partial fulfilment of the requirements for Doctor of Philosophy Degree **Ph.D.**

Date: July 10, 2015

Examining Committee

External Examiner: _____

Prof. Ahmed Mohammed (Ph.D)
Ball State University, USA

Supervisors:

_____

Semu Mitiku (Ph.D)

_____

Paola Goatin (Ph.D)

Internal Examiner:

_____

Tadesse Abdi (Ph.D)
Addis Ababa University

Chair Person:

_____

Zelalem Teshome (Ph.D)
Head, Department of Mathematics, AAU

ADDIS ABABA UNIVERSITY

Date: July 10, 2015

Author: Legesse Lemecha Obsu
Title: **Macroscopic Traffic Flow Modelling on Roundabouts and Optimization**
Department: Mathematics
Degree: Ph.D Convocation: July 10 Year: 2015

Signature of Author

This work is dedicated for the memory of my brother Hata'u Lemecha who lost by car accident on February 4, 2013.

Acknowledgements

First of all, I would like to express my heartfelt thanks to my research supervisors Dr. Semu Mitiku and Dr. Paola Goatin for their constant encouragement and invaluable guidance during the preparation of this dissertation. In particular, I am indebted to Dr. Semu Mitiku, who gave me the opportunity to join this PhD Program. Since I have known him, he is an exceptional mentor and ready to help me throughout the study period. I am also sincerely grateful to Dr. Paola Goatin for her continued intellectual and professional guidance, and her sincere care during research visit. They have spent countless hours going through every detail of my work, and giving me constructive feedback on the direction of my research. Further I am deeply grateful to Prof. Dr. Axel Klar, TU Kaiserslautern, for guidance and valuable support during the research visit.

My heartfelt gratitude also goes to Maria Laura Delle Monache, Mathias Mimault, Dr. Raule Borsche, and Anne Meurer for their remarkable ideas and constructive comments during this work. Also I have special thanks to my best friends Dr. Shiferaw Feyissa and Mezgabu Angessa for their continuously nurturing my family during the study period.

I am also grateful to Prof. Abdulkadir Hassen and Prof. Ahmed Mohammed for material support and continuous encouragement. I would also like to acknowledge all my friends Addis Ababa University, Adama Science and Technology University and all staff members of Mathematics department of Addis Ababa University for continuously encouraging me during this work.

My special thanks goes to the Deutscher Akademischer Austausch Dienst (DAAD), International Science Program, Sweden(ISP), African Mathematics Millennium Science Initiative(AMMSI) and INRIA for their financial support to complete this research work.

On the personal front, I am heartily grateful to my wife Derartu Tolossa and my sons Obsinet and Jinenus for their understanding, patience and support during the entire period of my study.

Abstract

This dissertation is motivated by practical problem of traffic flow on roundabouts. The study aimed at modelling traffic flow on roundabouts, proposing an optimization strategy for traffic flow on roundabouts and investigating the impact induced by short stay of pedestrians on the crosswalk on the performance of the roundabout in regulating traffic flow problem. To this end, macroscopic approach of traffic modelling has been used. To be specific, first the roundabout was modelled as a sequence of 2×2 junctions with one main lane and secondary incoming and outgoing roads. The evolution of traffic flow on the road networks of the roundabout was modelled by Lighthill-Whitham-Richards model. Then, we considered two cost functionals: the total travel time and the total waiting time, which give an estimate of the time spent by drivers on the network section. These cost functionals were minimized with respect to the right of way parameter for the incoming roads. For each cost functional, the analytical expression was given at each junction. We then solved numerically the optimization problem and the traffic behaviour was studied on the whole roundabout. The approach was numerically tested on a simple roundabout with three incoming and three outgoing roads. Two different choices of parameters were considered: instantaneously locally optimal and a well chosen but fixed values. The simulation results have shown that the local optima parameter value outperform the other choices, in improving the performances of the network. This result indicate the effectiveness of the optimization strategy compared to the case of fixed constant right of way parameters. In the second case, we formulated the problem in discrete form. Then a cost functional that measures the total travel time spent by drivers on the roundabout in discrete form were introduced. Numerical tests were conducted for a roundabout with four incoming and four outgoing roads. The simulation results show that gradient based instantaneous optimal choice of the priority parameters produce better results in improving the performance of the roundabout compared to the fixed choices of priority parameters. In the third case, we considered the roundabouts as alternatively periodic sequences of 2×1 and 1×2-type junctions and external incoming and outgoing roads. The evolution of traffic flow on the road networks of the roundabout was modelled by Lighthill-Whitham-Richards model with extended flux to capture the presence of pedestrians on crosswalk. To this end, we introduced three cost functionals that measure the total mass of vehicle , average velocity, and total flux respectively on the network. Then we analyzed the performance of the roundabout with and without pedestrian through numerical simulation using Godunov scheme. The simulation result indicated that, the presence of pedestrians on the crosswalk reduces the performance of roundabout in controlling traffic flow problem.

Contents

List of Figures

List of Tables

Notation and Abbreviations

$\mathbb{N}$	the set of natural numbers
$\mathbb{R}^+$	the set of positive real numbers
$\mathbb{R}$	the set of real numbers
$\mathbf{L^1}$	the set of Lebesgue integrable functions
Tot. Var	the total variation of a function
C^0	the set of continuous function
C_c^1	the set of continuous and differentiable functions with compact support
BV	the set of functions with bounded variation
$W^{1,\infty}$	$\{\rho \in \mathbb{L}^\infty : D\rho \in \mathbb{L}^\infty\}$
LWR	Lighthill-whitham- Richards
ODE	Ordinary Differential Equations
PDE	Partial Differential Equations
TTT	Total travel time
TWT	Total waiting time
TWT_{loc}	Local Total Waiting Time
TTT_{loc}	Local Total Travel Time
CGP	Coclite-Garavello-Piccoli
FIFO	First in first out

Chapter 1
Introduction

In the recent years, a wide range of traffic flow theories and models have been developed by scientists and engineers. Nevertheless, in the transportation sector, the issue of traffic congestion is still one of the main environmental and economical problem in the current years. For example, according to the 2011 Urban Mobility Report of Texas Transportation Institute [63], congestion caused urban Americans to travel 4.8 billion hours more and to purchase an extra 1.9 billion gallons of fuel for a congestion cost of $101 billion. Further, in the report it was estimated that congestion cost will grow from $101 billion to $133 billion in 2015 and $175 billion in 2020. This report shows that the impact of congestion increases every year in the US.

Similar to other countries, traffic congestion is widely observed in Ethiopia particularly in Addis Ababa. It is sever at intersections and roundabouts especially during peak hours. However, due to lack of well structured facilities, documented data on traffic congestion and absence of significant research made in this filed, it is hard to figure out the effects of congestion on urban Ethiopians in terms of economic impact, and environmental pollution.

In addition to the increasing demand of mobility among our society, the steady growth of traffic volume, and the occurrence of traffic jams on the road network remains prompt us to consider traffic flow problem.

Roundabouts are special forms of road network having short links and connected to external incoming and outgoing roads. Traffic evolution on the roundabout also differ from other road networks due to priorities given for traffic on the main road. Modern roundabouts are considered as an alternative traffic control device that can improve safety and operational efficiency at intersections when compared to other conventional intersection controls [27]. This implies, studying traffic flow on the roundabout play vital role in improving sustain-

ability and safety issues of the society. Therefore, traffic flow modeling and optimization on the roundabout are the core theme of this dissertation.

Traffic flow models can be considered as a theoretical substitution of a real traffic system. It provides a better understanding of traffic evolution, in particular the formation and propagation of traffic congestion. Broadly speaking, there are three main ways in which traffic models can be used:

- in traffic flow prediction and estimation
- in control strategies such as roundabout, traffic light and ramp metering.
- in assessing different design options and in choosing most cost-effective strategy.

Traffic flow models are broadly classified into three main categories based on level of detail, representation of the process, and scale of application. The classifications are: Microscopic, Mesoscopic, and Macroscopic traffic flow model.

Microscopic traffic flow model concentrates on the behavior of each individual vehicle. The driver will adjust his or her velocity and acceleration according to the conditions ahead. These models are often called Follow-the-Leader models. In Follow-the-Leader models each vehicle is influenced directly by the one in front, as often happens in real traffic flow. Thus, vehicle position is treated as a continuous function and each vehicle moves according to an ordinary differential equation normally dependent on its speed and the distance to the next vehicle [3, 32]. The solution of a large system of ordinary differential equations can provide the desired description of the flow conditions on the road. However, when the number of vehicles become large this model is not computationally feasible.

The mesoscopic approach is based on a statistical description that closely related to the kinetic theory of gases. Kinetic theory describes the state of the system by a probability distribution function of the position and velocity of the vehicles. Mathematical models use integro-differential type equations. The kinetic equations for vehicular traffic discussed by various authors, see for example in [48, 56] and references therein.

The macroscopic approach studies features of traffic flows such as flow rate f, traffic density ρ and travel speed v globally which are assumed to be continuous. Mathematical models are stated in terms of nonlinear partial differential equations derived from hyperbolic conservation laws, and phenomenological models are used for their closure. It provide better understanding on the forma-

tion and dissipation of traffic jams. The advantage of macroscopic models are their tractable mathematical structure and low number of parameters.

Each of the modelling approach that has been presented above is characterized by advantages and disadvantages. None of them is absolutely good or absolutely bad in capturing all the observed traffic phenomena. Regardless of its technical limitations, in this dissertation we follow macroscopic approach that are derived from fluid dynamics because it seems appropriate to describe phenomena such as shock formation and propagation.

1.1 Structure of the Dissertation

This dissertation is organised as follows. We begin with reviewing important related literature and its basic mathematical properties in Chapter 1. Then we briefly recall important mathematical preliminaries and its derivation in chapter 2. We present traffic flow optimization on roundabouts by modelling roundabout as a concatenation of junctions with its detail analysis in Chapter 3. In Chapter 4 we addressed impacts of pedestrians' on the performance of the roundabout in regulating traffic problem. Finally we present conclusions and future work in Chapter 5.

1.2 Background of the Study

The origins of macroscopic traffic flow models date back to 1950's, when the seminal works of Lighthill and Whitham [53] and Richards [61] proposed a fluid dynamic model for vehicular traffic flow on an infinite single road, commonly denoted as LWR. The main mathematical challenge to the LWR, and more generally systems of conservation laws, is the development of discontinuities, which can occur in finite time even from smooth initial conditions [8, 30]. The existence and uniqueness of an initial value problem (Cauchy problem) for conservation laws on infinite domain are achieved through a suitable entropy condition introduced in the pioneering works of Oleinik [58] and Kruzkov [50].

The LWR model has been extended to road networks by several authors in most recent years, see [11, 13, 16, 25, 29] and references therein. In the network setting, one-dimensional hyperbolic systems of conservation laws are also an efficient framework for modeling gas pipeline flow [2], data networks [23], and

supply chains [35]. These models have also been utilized for the optimization of vehicular traffic flow on road networks through various approaches, see for example [10, 12, 24, 40, 60]. Optimal control of traffic flow on networks have been investigated by different authors using different optimization techniques; detailed presentation and analysis can be found for example in [38] and reference therein.

The scalar LWR traffic flow model has some limitation in capturing all the properties of traffic phenomenon. For example, the model can not efficiently describe observed traffic behavior in light traffic [5, 30]. To harmonize some of the limitations of first-order models Payne [59] and independently Whitham [65]came up with second order traffic model that couple the mass conservation equation with a momentum equation. Usually denoted as PW in the literature. The PW model written as

$$\begin{cases} \frac{\partial \rho}{\partial t} + \frac{\partial \rho v}{\partial x} = 0 \\ \frac{\partial v}{\partial t} + v\frac{\partial v}{\partial x} + \frac{1}{\rho}\frac{\partial (A_e(\rho))}{\partial x} = \frac{1}{\tau}(V_e(\rho) - V) \end{cases} \tag{1.1}$$

where

(a) $V_e(\rho)$ is the equilibrium value of the speed,
(b) $\frac{1}{\rho}\frac{\partial (A_e(\rho))}{\partial x}$ represents the anticipation term proposed differently by different authors.
(c) $\frac{1}{\tau}(V_e(\rho) - V)$ denotes relaxation term of V with in a certain time $\tau > 0$ towards its equilibrium value $V_e(\rho)$.

However, the model has several limitations from engineering point of view as Daganzo detailed in [20]. Motivated by Daganzo's criticisms, Aw and Rascle [1] introduced a new macroscopic model which reads

$$\begin{cases} \rho_t + (\rho v)_x = 0 \\ (v + p(\rho))_t + v(v + p(\rho))_x = 0 \end{cases} \tag{1.2}$$

where the quantity $p(\rho)$ plays the role of an "anticipation factor "that takes into account the reactions of the drivers to what happens in front of them. These models avoid several inconsistencies of previous models, like wrong way traffic and missing bounds on the density. Nevertheless, as pointed out by the authors, the Aw-Rascle model is not well-posed near the vacuum $\rho = 0$. This fact is intended to reproduce instabilities that might appear in real situations at low car densities, but it is a source of difficulties from the mathematical point of view. This model has been intensively investigated in the last decade by different researchers, see for example [28, 31, 33]. Other higher or-

der traffic flow model have been also introduced and investigated, see for example [14, 16, 30] and references therein. In addition to analytical discussions, numerical methods have been studied for macroscopic traffic flow models for example in [9, 18, 46, 49, 51, 64].

Compared to higher order models, the LWR model is simple, robust, and sufficient to describe correctly most of the important behavior of traffic phenomena and situations. It admits analytical solutions for most traffic situations and is presently the only traffic flow model for which a fairly complete theory and numerical techniques are available. Therefore, this is the model we used in this dissertation.

1.2.1 The LWR Model

In this subsection, we briefly recall the mathematical descriptions of vehicular traffic based on nonlinear hyperbolic conservation laws. Macroscopic models describe the evolution of vehicle in terms of macroscopic variables such as the density and average speed of cars. The basic assumption is that the road is considered as a line with infinite in length and car's size is assumed negligible compared to the road's length. A unidirectional road is modelled by an interval $I = (a,b) \subset \mathbb{R}$, $a < b$. The density $\rho(t,x)$ and the average velocity $v(t,x)$ depend on the time $t \in \mathbb{R}^+$ and position $x \in I$.

The first model of this type was due to the pioneer work of Lighthill and Whitham [53] and independently Richards [61]. The conservation of the number of vehicles leads to the following scalar hyperbolic partial differential equations

$$\rho_t + f(\rho)_x = 0 \tag{1.3}$$

where $\rho = \rho(t,x)$ is the mean traffic density defined as the number of vehicles per unit length, and $f(\rho)$ is the traffic flow usually denotes the number of vehicles per unit time. The flux is assumed to depend only on the density and can be written as

$$f(\rho) = \rho v(\rho) \tag{1.4}$$

where the mean velocity v is a non-negative, non-increasing function. This phenomenological relation is valid in steady state conditions, and it is not realistic in more complicated situations. Experimental measurements [47] revealed that the closure relation at steady state only hold for small values of the density. Otherwise the fundamental diagram becomes multi-valued and leads to free flow and congested region. Further analysis can be found in [5, 30, 39] and references

therein. R. Colombo [14, 16] introduced a second order model that includes the ideas of a congested and free-flow region and discussed transition between the two regions. For the detailed derivation and analysis of nonlinear hyperbolic conservation laws we refer to [8, 19, 26, 45, 49].

1.2.2 LWR Model for Traffic Networks

In this subsection, we review some of the literature on LWR model which has been implemented on road networks for later reference. The idea to consider the LWR model on a road network was first proposed in [44] by Holden and Risebro. Then there has been a growth of interest among researchers [9, 13, 22] in modelling traffic on road networks using macroscopic model. More recently, several authors proposed models on networks that are able to describe the dynamics at intersections, see [16, 25, 29] and references therein.

In the network setting, one-dimensional hyperbolic systems of conservation laws have been utilized for the optimization of vehicular traffic flow on road networks through various approaches, see for example [10, 12, 17, 38, 40, 60]. Furthermore, optimal control of traffic flow on networks have been investigated by different authors using different optimization techniques; see for example in [38] and references therein.

First let us briefly recall the definition of road network and definitions of solution at junctions on the network.

Definition 1.1. Road networks consist a couple$(\mathscr{I}, \mathscr{J})$ where $\mathscr{I}$ denotes a finite collection of unidirectional roads and $\mathscr{J}$ is the set of junctions. Each road is modelled by an interval $I_i = [a_i, b_i] \subseteq \mathbb{R}, \quad i = 1, \ldots, n$, possibly with either $a_i = -\infty$ or $b_i = +\infty$, while each junction $J \in \mathscr{J}$ is the union of two non empty subsets **Inc(J)** and **Out(J)** of $1, \ldots, n$ respectively represents the incoming and outgoing roads.

The term unidirectional in this definition is for formality purpose since a two way road is described through two distinct unidirectional roads. The vehicular dynamics on each road segment is governed by hyperbolic conservation laws [8, 30] away from the junctions

$$\begin{cases} \partial_t \rho_i + \partial_x f(\rho_i) = 0, \forall i \in \mathscr{I}, x \in (a_i, b_i), \quad t \in \mathbb{R}^+, \\ \rho_i(0, x) = \rho_{i,0}(x), \quad \forall x \in (a_i, b_i), \end{cases} \tag{1.5}$$

where the function $\rho_i = \rho_i(t,x) \in [0, \rho_{max}]$ describe the density of vehicular traffic on road i, and ρ_{max} is the maximal density of the vehicles on the road under consideration. The traffic flux

$$f : [0, \rho_{max}] \to \mathbb{R}^+$$

is assumed to be differentiable, strictly concave and $f(0) = f(\rho_{max}) = 0$.

Definition 1.2. Let J be a junction with incoming roads, say $I_1, \ldots, I_n$, and outgoing roads, say $I_{n+1}, \ldots, I_{n+m}$. A weak solution at J is a collection of functions $\rho_i : I_i \times [0, +\infty) \to \mathbb{R}, i = 1, \ldots, n+m$, such that

$$\sum_{i=1}^{n+m} \left(\int_0^{+\infty} \int_{a_i}^{b_i} \left(\rho_i \frac{\partial \varphi_i}{\partial t} + f(\rho_i) \frac{\partial \varphi_i}{\partial x} \right) dxdt + \int_{a_i}^{b_i} \rho_{i,0}(x) \varphi_{i,0}(x) dx \right) = 0, \tag{1.6}$$

for every $\varphi_i, i = 1, \ldots, n+m$ smooth having compact support in the set $(a_i, b_i] \times (0, +\infty)$ for $i = 1, \ldots, n$ (incoming roads) and in $[a_i, b_i) \times (0, +\infty)$ for $j = n+1, \ldots, n+m$ (outgoing roads), that are also smooth across the junction, i.e.

$$\varphi_i(., b_i) = \varphi_j(., a_j), \qquad \frac{\partial \varphi_i(., b_i)}{\partial x} = \frac{\partial \varphi_j(., a_j)}{\partial x},$$

where $i \in \{1, \ldots, n\}$ and $j \in \{n+1, \ldots, n+m\}$

The formulation of a well−defined problem at each junction on the road network needs Rankine-Hugoniot condition for the existence of weak solutions. This leads to the following Lemma.

Lemma 1.1. *Let $\rho = (\rho_1, \ldots, \rho_{n+m})$ be a weak solution of (1.5)at the junction such that $x \to \rho_i(t,x)$ has bounded variation. Then ρ satisfies the Rankine-Hugoniot condition at the junction J, namely*

$$\sum_{i=1}^{n} f(\rho_i(t, b_i)) = \sum_{j=n+1}^{n+m} f(\rho_j(t, a_j)) \tag{1.7}$$

for almost every $t > 0$.

This result confirms the conservation of vehicles at a junction. For the technical proof we refer ([30], page 98).

Definition 1.3 (Weak solution of a Riemann Problem at a Junction). By a weak solution of the Riemann problem for a junction $J_j \in \mathscr{J}$ we mean a weak solution of the initial value problem (1.5) for the road network consisting of the single junction with n incoming and m outgoing roads all extending to infinity [44]. The initial data are given by

$$\rho_{i,0}(x) \equiv \rho_{i,0} \quad \forall x \in [a_i, b_i], \quad i = 1, \ldots, n+m.$$

where $\rho_{i,0}$ are constants.

The existence of weak solution alone can not be sufficient unless it meet the required physical meaning for a given junction. In the study of traffic flow on a road network, the main challenging task is the definition of suitable additional coupling conditions at junction in order to recover a unique weak solution of the Riemann problem. To this aim, a variety of approaches has been suggested, see for example [13, 25, 29, 43, 44]. For completeness we review some of the main ideas suggested in these references and defer others for the next chapter.

Coclite-Garavello-Piccoli (CGP) approach

In this approach [13] , the authors considered a junction with n incoming and m outgoing roads. For a given initial data $\rho_{i,0}$, the authors restricted the possible values of $\hat{\rho}_{i,0}$ in order to obtain the correct wave speed , and then solved a Riemann problem on each road as follows

$$\hat{\rho}_{i,0} \in \begin{cases} \{\rho_{i,0}\} \cup (\tau(\rho_{i,0}), 1] & \text{if } 0 \leq \rho_{i,0} < \rho_c \quad i = \ldots, n, \\ [\rho_c, 1], & \text{if } \rho_c \leq \rho_{i,0} \leq 1 \end{cases} \tag{1.8}$$

and

$$\hat{\rho}_{j,0} \in \begin{cases} [0, \rho_c] & \text{if } 0 \leq \rho_{j,0} \leq \rho_c \\ \{\rho_{j,0}\} \cup [0, \tau(\rho_{j,0})) & \text{if } \rho_c \leq \rho_{j,0} \leq 1 \quad j = n+1, \ldots, n+m. \end{cases} \tag{1.9}$$

where $\tau(\rho) \neq \rho$ denotes a unique number such that $f(\tau(\rho)) = f(\rho)$ for every $\rho \neq \rho_c$. Further the authors introduced a traffic distribution matrix by assuming that:

(A) there are some prescribed preference of drivers, that is the traffic from incoming roads is distributed on outgoing roads according to fixed coefficients. Precisely, there exists a traffic distribution matrix

$$A = \{\beta_{j,i}\}_{j=n+1,\ldots,n+m,1,\ldots,n} \in \mathbb{R}^{m \times n},$$

such that

$$\beta_{ji} \neq \beta_{ji'}, \forall i \neq i', \quad 0 < \beta_{jn} < 1, \quad \sum_{j=n+1}^{n+m} \beta_{ji} = 1 \tag{1.10}$$

where β_{ji} is the percentage of the drivers arriving from the i^{th} incoming road and take the j^{th} outgoing road for each $i' \neq i = 1, \ldots, n$ and $j = n+1, \ldots, n+m$.

(B) respecting rule (A), drivers choose so as to maximize fluxes.

Then the following coupling condition is assumed to be satisfied for the junction $J \in \mathscr{J}$,

$$\hat{\gamma}_i = f(\hat{\rho}_i)$$

$$f(\hat{\rho}_j) = \sum_{j=n+1}^{n+m} \beta_{ji} f(\hat{\rho}_i) = \sum_{j=n+1}^{n+m} \beta_{ji} \hat{\gamma}_i, \quad \forall j = n+1, \ldots, n+m. \tag{1.11}$$

The function E was introduced to measure the flux function on the incoming roads as follows,

$$E : (\gamma_1, \ldots, \gamma_n) \in \mathbb{R}^n \mapsto \sum_{i=1}^{n} \gamma_i$$

and the sets

$$\Omega_i := \begin{cases} [0, f(\rho_{i,0})], & \text{if } 0 \le \rho_{i,0} \le \rho_c \\ [0, f(\rho_c)], & \text{if } \rho_c \le \rho_{i,0} \le 1, \end{cases} i = 1, \ldots, n,$$

$$\Omega_j := \begin{cases} [0, f(\rho_c)], & \text{if } 0 \le \rho_{j,0} \le \rho_c \\ [0, f(\rho_{j,0})], & \text{if } \rho_c \le \rho_{j,0} \le 1, \end{cases} j = n+1, \ldots, n+m,$$

$$\Omega := \left\{ (\gamma_1, \ldots \gamma_n) \in \Omega_1 \times \cdots \times \Omega_n : A \cdot (\gamma_1, \ldots, \gamma_n)^T \in \Omega_{n+1} \times \cdots \times \Omega_{n+m} \right\}.$$

Then proved that

$$E(\hat{\gamma}_1, \ldots, \hat{\gamma}_n) = \max_{(\gamma_1, \ldots, \gamma_n) \in \Omega} E(\gamma_1, \ldots, \gamma_n) \quad \text{subjected to } (1.8) - (1.11).$$

has a unique solution in the sense of Definition 1.3. Because of condition (1.10) this approach do not include a junction with two incoming and one outgoing roads. More precisely, one can treat the problem where the number of incoming roads is greater than the number of outgoing ones. In this case, if not all cars can go through the junction then there should be a yielding rule between incoming roads. This corresponds to fix right of way parameters, which permit to find a unique solution. For the details about priority parameter rule we refer to [30]. Also, the authors proved the existence of solutions to the Cauchy problem and showed the Lipschitz continuous dependence on initial data does not hold in general, but it does hold under special assumptions.

Herty-Lebacque-Moutari Approach

In this approach, the authors extended the models introduced in [13, 44] for intersections using a description in terms of supply and demand functions by

introducing a buffer of finite storage capacity at a junction. This approach is motivated by an effort for a relevant modeling of complex intersections such as roundabout and on-ramps.

The characteristics of the buffer is defined by making the assumptions that: junction has a certain limited capacity so that vehicles can enter the junction and get stuck provided that no car should be lost inside the buffer. The instantaneous rate of change of the buffer load at a junction is governed by the difference between the inflow and outflow of the traffic at a junction. This leads to the following Cauchy problem for a given junction J:

$$\partial_t \rho_{\mathrm{i}} + \partial_x f(\rho_{\mathrm{i}}) = 0, \tag{1.12}$$

$$\rho_i(0,x) = \rho_{\mathrm{i},0} = \begin{cases} \rho^-_{\mathrm{i},0} & \text{for } x < b_{\mathrm{i}} \quad \text{if i} \in \mathscr{I}^- \\ \rho^+_{\mathrm{i},0} & \text{for } x > a_{\mathrm{i}} \quad \text{if i} \in \mathscr{I}^+ \end{cases} \tag{1.13}$$

$$\dot{l}(t) = \sum_{i \in \mathscr{I}^+} f(\rho_i(t,b_i)) - \sum_{i \in \mathscr{I}^-} f(\rho_i(t,a_{\mathrm{i}})), \quad \forall t \geq t_0, \tag{1.14}$$

$$l(0) = l_0, \quad 0 \leq l_0 \leq l_{max}, \tag{1.15}$$

Herein $\mathscr{I}^-$ and $\mathscr{I}^+$ denotes the set of incoming and outgoing roads respectively. In this setting, equation (1.12) describes traffic evolution on incoming and outgoing roads.

Set the rules for entering and exiting the junction as follows.

- If the buffer is not empty, the demand of the buffer is constant, regardless of the current number of cars in the buffer and thus, the exiting flow from the buffer is idealized to be constant.
- If the buffer is not full, the supply of the buffer is constant, regardless of the current number of cars in the buffer. Hence, the flow entering the buffer is idealized to be constant.

For a junction with multiple outgoing roads, the authors considered traffic distribution matrix as in [13]. Whereas in the case of multiple incoming roads and a completely filled buffer they follow the approach given in [41] to deal with the matter of priorities on the incoming roads. Eventually, the modeling approach modified so that the actual fluxes $q_i := f(\rho_i(t,b_i))$ if $i \in \mathscr{I}^+$ and $q_j := f(\rho_j(t,a_j))$ if $j \in \mathscr{I}^-$ satisfy for *a.e.* time $t > 0$

$$q_i = min\{\frac{1}{\sum_i d_i} s_B, d(\rho_i(t,b_i))\}, \quad q_j = min\{\beta_j d_B, s(\rho_j(t,a_j))\}, \tag{1.16}$$

$$d_B = \begin{cases} \mu & \text{if } 0 < l(t) \leq l_{max}, \\ min\{\sum_{i\in\mathscr{I}^+} d(\rho_i(t,b_i)), \mu\} & \text{if } l(t) = 0, \end{cases} \tag{1.17}$$

$$s_B = \begin{cases} \mu & \text{if } 0 < l(t) \leq l_{max}, \\ min\{\sum_{j\in\mathscr{I}^-} min(s(\rho_j(t,a_j)), \beta_j\mu)\} & \text{if } l(t) = l_{max}, \end{cases} \tag{1.18}$$

$$\dot{l}(t) = \sum_{\mathrm{i}\in\mathscr{I}^+} f(\rho_{\mathrm{i}}(t,b_{\mathrm{i}})) - \sum_{\mathrm{j}\in\mathscr{I}^-} f(\rho_{\mathrm{j}}(t,a_{\mathrm{j}})), \forall t \geq t_0, \tag{1.19}$$

Equations(1.16)-(1.19) define a Riemann solver at a single junction where roads are extended to infinity while equation (1.16) states that the actual flow on the incoming road is bounded by the demand in order to obtain the correct wave speeds. According to the authors, if the supply of the buffer s_B is less than the total demand $\sum_i d_i$, then the right-of-way rule applies. Similarly, the outgoing fluxes q_j : are bounded by the supply on the corresponding road, $s(\rho_j(t,a_j))$, and by the maximal inflow toward this road, $\beta_j d_B$. The demand of the buffer d_B is equal to μ, whenever the buffer is not empty. If the buffer is empty we require that at most the demand of the incoming roads is used to determine the actual outflows. In the case of a full buffer only the minimum of $\beta_j\mu$ and $s(\rho_j(t,a_j))$ is allowed as throughput through the buffer.

Unfortunately, the authors remarked that well-posedness for an arbitrary number of incoming and outgoing roads is not achieved except for a single incoming and single outgoing roads as special case. For this special case, the exist of a unique weak entropy solution established in [43] Lemma 3.1.

In addition to well-poesedness limitation for arbitrary number of incoming and outgoing roads, all cars entering the same buffer might loose the information about their origins and destinations due to the proposed model contains buffer inside the junction.

However, in [29] the authors considered the same approach and proved the existence and well posedness of solutions at the node with buffer for an arbitrary number of incoming and outgoing roads.

In order to achieve the result, the authors established the following technical definitions for entropy admissible solution, Riemann problem and Riemann solver which we are going to recall briefly.

The following consecutive definitions are taken from [29].

Definition 1.4. A function $\rho_i \in C([0,+\infty[;L^1_{loc}(I_i))$ is an entropy admissible solution to (1.12) in the arc I_i if, for every $k \in [0,1]$ and every $\varphi : [0,+\infty[\times I_i \to \mathbb{R}$ which is smooth, positive and with compact support in $]0,+\infty[\times(I_i \setminus \{0\})$, it holds

$$\int_0^{+\infty} \int_{I_i} (|\rho_i - k|)\,\partial_t \varphi + sgn(\rho_i - k)(f(\rho_i) - f(k))\partial_x \varphi dx dt \geq 0. \tag{1.20}$$

Definition 1.5. A collection of functions $\rho_i \in C([0,+\infty[;L^1_{loc}(I_i))$ where $i \in \{1,\dots,n+m\}$ and $l \in W^{1,\infty}$ is a weak solution at J if

1. for every $i \in \{1,\dots,n+m\}$, the function ρ_i is an entropy admissible solution to (1.12) in I_i ;
2. for every $i \in \{1,\dots,n+m\}$ and for $a.e.t > 0$, the function $x \mapsto \rho_i(t,x)$ has a version with bounded variation;
3. for $a.e.t > 0$
$$\dot{l}(t) = \sum_{i=1}^{n} f(\rho_i(t,0^-)) - \sum_{i=n+1}^{n+m} f(\rho_i(t,0^+))$$
where ρ_i stands for the version with bounded variation.

Consider a node J with a buffer, whose demand and supply are equal to a constant $\mu \in (0, \max\{n,m\} f(\rho_c))$. Then fix $\rho_{1,0},\dots,\rho_{n+m,0} \in [0,1]$, $\quad l_0 \in [0, l_{max}]$ and consider the following Riemann problem at J

$$\begin{cases} \partial t \rho_i + \partial_x f(\rho_i) = 0 \\ \rho_i(0,.) \equiv \rho_{i,0} \\ \dot{l}(t) = \sum_{i=1}^{n} f(\rho_i(t,0^-)) - \sum_{i=n+1}^{n+m} f(\rho_i(t,0^+)), \quad i \in \{1,\dots,n+m\} \\ l(0) = l_0 \end{cases} \tag{1.21}$$

The real valued function $l(t) \in [0, l_{max}]$ denotes the total number of cars in the buffer inside the junction J at time t.

Definition 1.6. A solution to the Riemann problem (1.21) is a weak solution at J, in the sense of Definition 1.5, such that $\rho_i(0,x) = \rho_{i,0}$ for every $i \in \{1,\dots,n+m\}$ and for $a.e.\ x \in I_i$ and such that $l(0) = l_0$.

Furthermore, the authors considered the concept of Riemann solver at junction as in [30] in order to fix the correct wave speed.

Definition 1.7. A Riemann solver $\mathscr{RS}$ is a function

$$\begin{aligned} \mathscr{RS} : \quad & [0,1]^{n+m} \to [0,1]^{n+m} \\ & (\rho_{1,0},\dots,\rho_{n+m,0}) \mapsto (\bar{\rho}_1,\dots,\bar{\rho}_{n+m}) \end{aligned}$$

satisfying the following

1. for every $i \in \{1,\dots,n\}$, the classical Riemann problem

$$\begin{cases} \partial_t \rho + \partial_x f(\rho) = 0, \quad x \in \mathbb{R}, t > 0. \\ \rho(0,x) = \begin{cases} \rho_{i,0}, & \text{if } x < 0, \\ \bar{\rho}_i, & \text{if } x > 0, \end{cases} \end{cases}$$

is solved with waves with negative speed;
2. for every $j \in \{n+1,\dots,n+m\}$, the classical Riemann problem

$$\begin{cases} \partial_t \rho + \partial_x f(\rho) = 0, \quad x \in \mathbb{R}, t > 0. \\ \rho(0,x) = \begin{cases} \rho_{j,0}, & \text{if } x < 0, \\ \bar{\rho}_j, & \text{if } x > 0, \end{cases} \end{cases}$$

is solved with waves with positive speed;

Using these concepts and formulations the authors precisely set the Cauchy problem at J:

$$\begin{cases} \partial_t \rho_i + \partial_x f(\rho_i) = 0, \quad x \in I_i \setminus \{0\}, t > 0 \\ \rho_i(0,x) = \rho_{i,0}(x) \\ \dot{l}(t) = \sum_{i=1}^{n} f(\rho_i(t,0^-)) - \sum_{i=n+1}^{n+m} f(\rho_j(t,0^+)), \quad i \in \{1,\dots,n+m\} \\ l(0) = l_0 \end{cases} \tag{1.22}$$

where $\rho_{1,0},\dots,\rho_{n,0} \in \mathrm{BV}(]-\infty,0];[0,1])$ are fixed initial data on the incoming arcs, $\rho_{n+1,0},\dots,\rho_{n+m,0} \in \mathrm{BV}([0,+\infty[;[0,1])$ m- initial data on the outgoing arcs and $l_0 \in [0, l_{max}]$.

Theorem 1.1. *For every $T > 0$, the Cauchy problem* (1.22) *admits a weak solution at $J(\rho_1,\dots,\rho_{n+m},l)$ such that*

1. *for every $i \in \{1,\dots,n+m\}$, ρ_i is a weak entropic solution of*

$$\partial_t \rho_i + \partial_x f(\rho_i) = 0$$

in $[0,T] \times \mathscr{I}_i$;
2. *for every $i \in \{1,\dots,n+m\}$, $\rho_i(0,x) = \rho_{i,0}(x)$ for a.e $x \in \mathscr{I}_i$;*
3. *for a.e $t \in [0,T]$*

$$\mathscr{RS}_{l(t)}(\rho_1(t,0-),\dots,\rho_{n+m}(t,0+)) = (\rho_1(t,0-),\dots,\rho_{n+m}(t,0+));$$

4. *for a.e $t \in [0,T]$*

$$\dot{l}(t) = \sum_{i=1}^{n} f(\rho_i(t,0^-)) - \sum_{i=n+1}^{n+m} f(\rho_j(t,0^+)).$$

Then proved existence and well-posedness of the solutions by using the wave-front tracking technique and the generalized tangent vectors. For the detail technical analysis we refer to [29]. More recently, modelling junction with ramp buffer was introduced in [25] and proved the existence and uniqueness of solutions of the Riemann problem at the junction by solving a Linear Programming (LP) optimization problem. In chapter 3 , this is the model we modified to study traffic flow on a roundabout.

The first macroscopic pedestrian flow model was due to the seminal work of Hughes [62] where the preferred direction of motion is given by the solution of an Eikonal Equation

$$f(\xi)||\nabla\phi|| = 1 \tag{1.23}$$

where the function $f(\xi)$ is given by

$$f(\xi) = U_{max}\left(1 - \frac{\xi}{\xi_{max}}\right).$$

Here U_{max} is the maximal velocity, ξ_{max} the maximal density of the pedestrian and $\xi = \xi(t,x)$ denotes the pedestrian density in bounded domain. Furthermore, in [15] the authors presented a model for the flow pedestrians that describes features such as the fall due to panic in the outflow of people through a door. More recently, the coupling of traffic flow networks with pedestrian motion on the street has been studied in [6, 7].

1.3 Contributions

The main contribution of this dissertation is in the macroscopic traffic flow modeling and optimization on roundabouts which include: Macroscopic traffic flow optimization on roundabouts, Gradient-based instantaneous traffic flow optimization on a roundabout and Pedestrians' impact on the performance of a roundabout. From these contributions, one of them published, one accepted, submitted and the last in preparation.

Chapter 2
Derivation of Scalar Conservation Law

2.1 The Scalar Conservation Law

Physical quantities are said to be conserved in certain process if the amount of substance before the process remains the same also after the process ends. Based on this assumption, the equation of scalar conservation law is already derived in standard books. For instance properties and detailed analysis of nonlinear hyperbolic conservation laws can be found in [4, 8, 19, 26, 45, 49, 54, 55].

To recall, a road is considered to be a line with infinite length and size of a vehicle is assumed to be negligible compared to the road length. Furthermore, assume that vehicles do not enter or leave the section of the road at any of its points. The conservation law states that the change in the total amount of a physical quantity contained in any region of space must be equal to the net flux of that quantity across the boundary of that region. Fix any two distinct points x_1 and x_2 on the section of the road. Then the number of vehicles between x_1 and x_2 varies according to the law

$$\frac{d}{dt}\int_{x_1}^{x_2}\rho(t,x)\,dx = \int_{x_1}^{x_2}\frac{\partial}{\partial t}\rho(t,x)\,dx \tag{2.1}$$

This rate of change must be equal to the net flux across x_1 and x_2 which is given by

$$\int_{x_1}^{x_2}\frac{\partial}{\partial t}\rho(t,x)\,dx = f(\rho(t,x_1)) - f(\rho(t,x_2)) \tag{2.2}$$

Equation (2.2) measures the flow of vehicles entering the road segment at x_1 and leaving the segment at x_2. In other words, the quantity ρ is neither created nor destroyed. Thus the total amount of ρ contained inside any given interval $[x_1, x_2]$ can be changed only due to the flow of ρ across boundary points. But $f(\rho(t,x)) = \rho(t,x)v(t,x)$ where $v(t,x)$ is the average velocity of vehicles. Integrat-

ing both sides of equation (2.2) on $[t_1, t_2]$ yields

$$\int_{t_1}^{t_2}\int_{x_1}^{x_2}\frac{\partial}{\partial t}\rho(t,x)\,dxdt = \int_{t_1}^{t_2} f(\rho(t,x_1)) - f(\rho(t,x_2))\,dt \tag{2.3}$$

For continuously differentiable functions ρ and $f(\rho)$ this equation is the same as

$$\int_{t_1}^{t_2}\int_{x_1}^{x_2}\frac{\partial}{\partial t}\rho(t,x)\,dxdt = -\int_{t_1}^{t_2}\left[f(\rho(t,x_2)) - f(\rho(t,x_1))\right]dt = -\int_{t_1}^{t_2}\int_{x_1}^{x_2}\frac{\partial}{\partial x}f(\rho(t,x))\,dxdt \tag{2.4}$$

Rearranging and simplifying equation (2.4) gives

$$\int_{t_1}^{t_2}\int_{x_1}^{x_2}\left[\frac{\partial}{\partial t}\rho(t,x) + \frac{\partial}{\partial x}f(\rho(t,x))\right]dxdt = 0 \tag{2.5}$$

Since this equation holds for arbitrary limits of integration, the integrand must be zero. Consequently equation (2.5) holds for all x_1 and x_2, which leads to the conservation law

$$\frac{\partial}{\partial t}\rho + \frac{\partial}{\partial x}f(\rho) = 0 \tag{2.6}$$

where ρ is the conserved physical quantity and f is the flux function.

In the case of smooth initial data we can not expect that there are continuous solutions for equation (2.6) that exist globally in time. To see such cases we have the following example.

Example 2.1. Consider the problem

$$\begin{cases}\rho_t + \rho\rho_x = 0\\ \rho(0,x) = \rho_0(x) = \dfrac{1}{1+x^2}.\end{cases} \tag{2.7}$$

For small $t > 0$, the solution can be found by the method of characteristics as follows:

$$\begin{cases}\frac{dx}{dt} = \rho,\\ \frac{d\rho}{dt} = 0\end{cases} \tag{2.8}$$

Solving this system of ordinary differential equation we have
$\rho(t,x) = c_1$ and $x(t) = c_1 t + c_2$, where c_1 and c_2 are arbitrary constants. Applying initial condition one can obtain that

$$x(t) = x + \frac{t}{1+x^2}.$$

The function $\rho(t,x)$ is constant along the characteristic lines in the x-t plane. Now the main goal is to find the positive time t_s(breaking time) and the location x_s of the first appearance of the shock. To achieve this we consider, $f(\rho) = \frac{\rho^2}{2}$, $f'(\rho) = \rho$, $f''(\rho) = 1$, and $\rho_0(\xi) = \frac{1}{1+\xi^2}$, where $\rho_0'(\xi) = \frac{-2\xi}{(1+\xi^2)^2}$.
The non-negative function

$$z(\xi) = -f''(\rho_0(\xi))\rho_0'(\xi) = \frac{2\xi}{(1+\xi^2)^2}$$

has a maximum at ξ_M, where $z'(\xi_M) = 0$ which on solving gives $\xi_M = \frac{1}{\sqrt{3}}$ and $z(\xi_M) = \frac{\sqrt{27}}{8}$. Thus, the breaking time t_s and the location of the first appearance of the shock is at

$$x_s = f'(\rho(\xi_M))t + \xi_M = \sqrt{3}.$$

For t sufficiently small $0 \le t < \frac{8}{\sqrt{27}}$, the characteristic lines do not intersect each other and the solution is unique. The solution to our Cauchy problem is thus given implicitly by

$$\rho(x + \frac{t}{1+x^2}, t) = \frac{1}{1+x^2}.$$

On the other hand, when $t > \frac{8}{\sqrt{27}}$, the characteristic lines start to intersect each other. As a result, the map

$$x \longmapsto x + \frac{t}{1+x^2}$$

is not one-to-one and the map $(x + \frac{t}{1+x^2}, t) = \frac{1}{1+x^2}$ no longer defines a single valued solution of our Cauchy problem. This example lead us to the idea of weak solution.

2.2 Weak Solution

Smooth solutions of hyperbolic conservation law can blow up (develop discontinuities or singularities) in finite time. In such a case one could not follow the practice of accepting the solution of a differential equation even when the equation itself failed to make sense because closed form solutions of the nonlinear problems could not be computed. In order to compute discontinuous solutions, we needed to extend the notion of solution itself. Thus, to construct solutions global in time, we are forced to work in a space of discontinuous functions, and

interpret the conservation equations in their distributional sense as in equation (2.10). Now we give the definition of weak solution [8].

Definition 2.1. Let $f : \mathbb{R}^n \to \mathbb{R}^n$ be a smooth vector field. A measurable function $\rho : \mathbb{R} \times [0,\infty) \to \mathbb{R}^n$ is a weak solution of the system of conservation laws

$$\begin{cases} \rho_t + (f(\rho))_x = 0 \\ \rho(0,x) = \phi(x) \end{cases} \tag{2.9}$$

if

$$\int_0^\infty \int_{-\infty}^\infty (\rho\varphi_t + f(\rho)\varphi_x)dxdt + \int_{-\infty}^\infty \rho(0,x)\varphi(0,x)dx = 0 \tag{2.10}$$

for all smooth function $\varphi : \Omega \longrightarrow \mathbb{R}^n$ with compact support.

Remark 2.1. In the above definition no continuity assumption is made on ρ. We only need ρ and $f(\rho)$ to be locally integrable in Ω. We also notice that weak solutions are defined up to L^1 equivalence.

The proof of the following theorem can be found in [8, 26].

Theorem 2.1. *Suppose $\rho^-, \rho^+ \in \mathbb{R}^n$ and $\lambda \in \mathbb{R}$. If the function*

$$\rho(t,x) = \begin{cases} \rho^+ & \text{if } x > \lambda t \\ \rho^- & \text{if } x < \lambda t \end{cases} \tag{2.11}$$

is a weak solution of the system of conservation laws (2.9), then

$$\lambda(\rho^+ - \rho^-) = f(\rho^+) - f(\rho^-). \tag{2.12}$$

Proof. Let $\varphi = \varphi(t,x)$ be any continuously differentiable function with compact support $supp\varphi \subset \Omega$. Let Γ be a smooth curve that divides Ω into two parts. $\Omega^- := \Omega \cap \{x < \lambda t\}, \quad \Omega^+ := \Omega \cap \{x > \lambda t\}$. Let $\vec{n} = (n_1, n_2)$ be the unit normal to the curve Γ pointing from Ω^- to Ω^+ and $\vec{n^-} = -\vec{n^+}$. Suppose that the curve Γ is represented parametrically as $\{(t,x) : x = s(t) = \lambda t\}$ for some smooth function $s : [0,\infty) \to \mathbb{R}$.

Then $n^+ = (n_1^+, n_2^+) = \dfrac{1}{\sqrt{1+(\dot{s}(t))^2}}(1, -\dot{s}(t))$ where $\dot{s}(t) = \dfrac{d}{dt}\lambda t = \lambda$. Substituting we get $\quad n^+ = \dfrac{1}{\sqrt{1+\lambda^2}}(1, -\lambda)$.

Define the vector field $g := (\rho(t,x) \cdot \varphi(t,x), f(\rho(t,x)) \cdot \varphi(t,x))$. From definition of weak solution we know that

$$\iint_\Omega (\rho\varphi_t + f(\rho)\varphi_x)dxdt = 0 \tag{2.13}$$

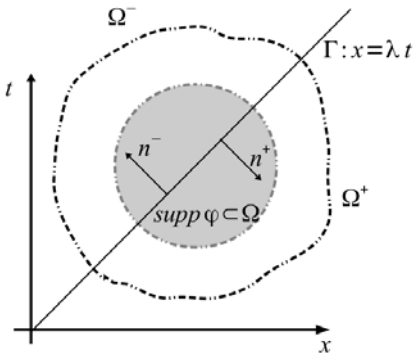

Fig. 2.1: Region where the divergence theorem is applied

Equation(2.13) can be written as

$$0 = \iint_{\Omega^+ \cup \Omega^-} divg \quad dxdt = \int_{\partial\Omega^-} (n^- \cdot g)ds + \int_{\partial\Omega^+} (n^+ \cdot g)ds \tag{2.14}$$

where ds denotes the differential of the arc length along the curve Γ. Since $supp\varphi \subset \Omega$, then $\varphi = 0$ on the boundary $\partial\Omega$. That is

$$\iint_{\Omega} (\rho\varphi_t + f(\rho)\varphi_x)dxdt = \iint_{\Omega^-} (\rho\varphi_t + f(\rho)\varphi_x)dxdt + \iint_{\Omega^+} (\rho\varphi_t + f(\rho)\varphi_x)dxdt = 0 \tag{2.15}$$

Applying integration by parts on Ω^- we get

$$\begin{aligned} \iint_{\Omega^-} (\rho\varphi_t + f(\rho)\varphi_x)dxdt &= -\iint_{\Omega^-} (\rho_t + f(\rho)_x)\varphi dxdt + \int_{\Gamma=\partial\Omega^-} g \cdot \vec{n}^- ds \\ &= -\int_{\partial\Omega^-} n^- \cdot g ds = -\int_{\partial\Omega^-} (\rho^- \cdot n_2 + f(\rho^-) \cdot n_1)\varphi ds \end{aligned} \tag{2.16}$$

Similarly, applying integration by parts on Ω^+ with n^+ gives

$$\iint_{\Omega^+} (\rho\varphi_t + f(\rho)\varphi_x)dxdt = \int_{\partial\Omega^+} (\rho^+ n_2 + f(\rho^+)n_1)\varphi ds \tag{2.17}$$

Adding equation(2.16) and (2.17) and comparing with equation (2.14) we obtain

$$-\int_{\Gamma} (\rho^- n_2 + f(\rho^- n_1))\varphi ds + \int_{\Gamma} (\rho^+ n_2 + f(\rho^+ n_1))\varphi ds = 0 \tag{2.18}$$

or which on rearranging gives

$$-\int_{\Gamma} ((\rho^+ - \rho^-)n_2 + (f(\rho^+) - f(\rho^-)n_1))\varphi ds = 0 \tag{2.19}$$

Since $\varphi \in C_c^1(\Omega)$ is arbitrary, we must have

$$(\rho^+ - \rho^-)n_2 + (f(\rho^+) - f(\rho^-))n_1 = 0. \tag{2.20}$$

After rearranging and simplifying equation (2.20) we obtain the famous Rankine-Hugoniot jump condition

$$\lambda(\rho^+ - \rho^-) = f(\rho^+) - f(\rho^-). \tag{2.21}$$

Here we observe that equation (2.21) form a set of n scalar equations relating the right and left states of $\rho^-, \rho^+ \in \mathbb{R}^n$ and the speed λ of the discontinuity.

Remark 2.2. In the scalar case, one can arbitrarily assign the left and right states $\rho^-, \rho^+ \in \mathbb{R}$ and determine the shock speed as

$$\lambda = \frac{f(\rho^+) - f(\rho^-)}{\rho^+ - \rho^-} \tag{2.22}$$

Geometrically this can be interpreted as the slop of the secant line through the points $(\rho^-, f(\rho^-))$ and $(\rho^+, f(\rho^+))$ on the graph of the flux function f.

Example 2.2. Consider the problem

$$\begin{cases} \rho_t + \rho\rho_x &= 0 \qquad t \geq 0 \\ \rho(0,x) &= \begin{cases} 0 & \text{if } x < 0 \\ 1 & \text{if } x > 0 \end{cases} \end{cases}$$

The solution ρ is constant along the characteristic curves. We have a region on which we do not have enough information. There are many possibilities to define our solution in this region.

As first possibility take

$$\rho_1(t,x) = \begin{cases} 0 & \text{for } x < \dfrac{t}{2} \\ 1 & \text{for } x > \dfrac{t}{2} \end{cases}$$

One can easily see that $\rho_1(t,x)$ is a classical solution on the either side of the curve of discontinuity $x = \dfrac{t}{2}$. Also $\rho_1(t,x)$ satisfies the Rankine-Hugoniot condition along the curve of discontinuity.

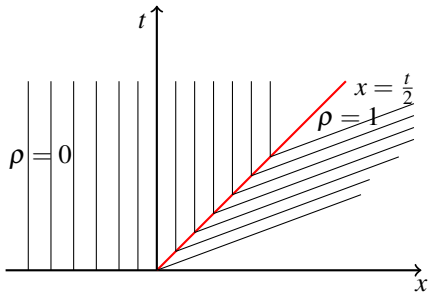

Fig. 2.2: Non physical solution

Therefore, $\rho_1(t,x)$ is a weak solution to the initial value problem. This is not the only possible solution. As a second possibility consider

$$\rho_2(t,x) = \begin{cases} 0 & \text{for } x \leq 0 \\ \dfrac{x}{t} & \text{for } 0 \leq x \leq t \\ 1 & \text{for } x \geq t \end{cases}$$

$\rho_2(t,x)$ is a continuous solution of the given problem.

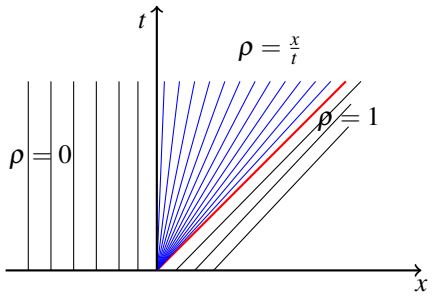

Fig. 2.3: Physically Acceptable solution

This types of a solution which 'fans' the wedge $0 < x < t$ is called a rarefaction wave. $\rho_1(t,x)$ is not physically realistic but $\rho_2(t,x)$ is considered to be the more physically realistic solution and we consider this as our solution. In general, for every $0 < \alpha < 1$, the function $\rho_\alpha : [0,+\infty) \times \mathbb{R} \to \mathbb{R}$ defined by

$$\rho_\alpha(t,x) := \begin{cases} 0 & \text{if } x < \dfrac{\alpha}{2}t; \\ \alpha & \text{if } \dfrac{\alpha}{2}t \leq x \leq \dfrac{(1+\alpha)}{2}t; \\ 1 & \text{if } x \geq \dfrac{(1+\alpha)}{2}t \end{cases}$$

is also a weak solution.

The piece-wise constant function ρ_α satisfies the equation outside the jumps. Moreover, the Rankine-Hugoniot conditions hold along the two lines of discontinuities $x = \frac{\alpha}{2}t$ and $x = \frac{(1+\alpha)}{2}t$ for all $t > 0$. From this example it is clear that weak solution must be supplemented with further admissibility conditions in order to get physically acceptable solution. Thus we have the following entropy condition.

For the discussion of the following concepts and results we mainly rely on the references [8, 19, 26, 45].

2.3 Entropy Admissible Solutions

In the previous section, we have seen that the weak formulation is not enough to guarantee uniqueness of the solution for initial value problems. In this section we shall see how to guarantee unique solution by supplementing the weak formulation with admissibility condition. One way is using the entropy condition. The entropy acts as an indicator of discontinuities, and can be used to isolate a unique solution. This leads to the following definition.

Definition 2.2. A C^1 function $\eta : \mathbb{R}^n \to \mathbb{R}$ is an entropy for (2.6) if it is convex and there exists a C^1 function $q : \mathbb{R}^n \to \mathbb{R}$ such that

$$D\eta(\rho) \cdot Df(\rho) = Dq(\rho) \tag{2.23}$$

for every $\rho \in \mathbb{R}^n$. The function q is said to be an entropy flux for η. The pair (η, q) is called entropy-entropy flux pair for (2.6).

Definition 2.3. A weak solution $\rho = \rho(t,x)$ to the Cauchy problem

$$\begin{cases} \rho_t + f(\rho)_x & = 0 \\ \rho(0,x) & = \rho_0 \end{cases} \tag{2.24}$$

is said to be entropy admissible if, for every C^1 function $\varphi \geq 0$ with compact support in $[0,T] \times \mathbb{R}$ and for every entropy-entropy flux pair (η, q), it holds

$$\int_0^T \int_{\mathbb{R}} (\eta(\rho)\varphi_t + q(\rho)\varphi_x) dx dt \geq 0. \tag{2.25}$$

Let $\Omega \subseteq \mathbb{R}^n$ be an open set and $f : \Omega \to \mathbb{R}^n$ be a smooth flux function. Suppose that the system of conservation laws

$$\rho_t + f(\rho)_x = 0 \tag{2.26}$$

is strictly hyperbolic.

Remark 2.3 (Lax condition). A weak solution $\rho = \rho(t,x)$ of (2.24) is admissible if at every point (τ,ξ) of approximate jump, the left and the right state ρ^-,ρ^+ and the speed $\lambda = \lambda(\rho^-,\rho^+)$ of the jump satisfy

$$\lambda(\rho^-) \geq \lambda \geq \lambda(\rho^+).$$

Example 2.3 (Traffic Light Problem). Consider the evolution of traffic at signalized intersection. Suppose that a bumper-to-bumper traffic is standing at a red light placed at position $x = 0$, while the road ahead stay empty. Then, we can express the given problem as

$$\begin{cases} \rho_t + f(\rho)_x = 0 \\ \rho_0 = \begin{cases} \rho_{max}, & \text{if } x \leq 0; \\ 0, & \text{if } x > 0. \end{cases} \end{cases} \tag{2.27}$$

Assume that at time $t = 0$, the traffic light turns green and the cars start to pass through the junction. At the beginning, only cars nearer to the light start moving while most remain standing. To see the real situation of the dynamics, we solve the given problem by the method of characteristics.
The characteristic equation becomes

$$\frac{dx}{dt} = f'(\rho), \quad \frac{d\rho}{dt} = 0$$

which after solving gives $x(t) = f'(\rho(x(0)))t + x(0)$ and $\rho =$ constant. The characteristics are straight lines $x(0) = x(t) - f'(\rho)t$ with slop $f'(\rho(x(0)))$. $f'(\rho(x(0)))$ is the local wave speed.
If $x \leq 0$, then $x(0) = x(t) - f'(\rho_{max})t \leq 0$ and this implies $x(t) \leq f'(\rho_{max})t$. If $x > 0$, then $x(0) = x(t) - f'(0)t > 0$ and this implies that $x(t) > f'(0)t$. Thus,

$$\rho(t,x) = \begin{cases} \rho_{max}, & \text{if } x \leq f'(\rho_{max})t; \\ ?, & \text{if } f'(\rho_{max})t < x < f'(0)t; \\ 0 & \text{if } x(t) > f'(0)t. \end{cases}$$

At point of discontinuity, $x(t) = x(0) + f'(\rho(x))t$ which implies that $x(t) = f'(\rho(x))t$ since $x(0) = 0$. In the middle region, where the characteristics satisfy $x(t) = f'(\rho(x))t$ one can easily obtain that $\rho(x) = (f')^{-1}\left(\frac{x}{t}\right)$. Therefore,

$$\rho(t,x) = \begin{cases} \rho_{max}, & \text{if } x \leq f'(\rho_{max})t; \\ (f')^{-1}\left(\frac{x}{t}\right), & \text{if } f'(\rho_{max})t < x \leq f'(0)t; \\ 0 & \text{if } x(t) > f'(0)t. \end{cases} \tag{2.28}$$

Next using the relation $f(\rho) = v_{max}\left(\rho - \frac{\rho^2}{\rho_{max}}\right)$ and its derivative one can easily obtain the following expression

$$x = v_{max}\left(1 - \frac{2\rho}{\rho_{max}}\right)t.$$

Again solving for ρ we get

$$\rho = \frac{\rho_{max}}{2}\left(1 - \frac{x}{v_{max}t}\right).$$

Note that other choice of the flux function is also possible.

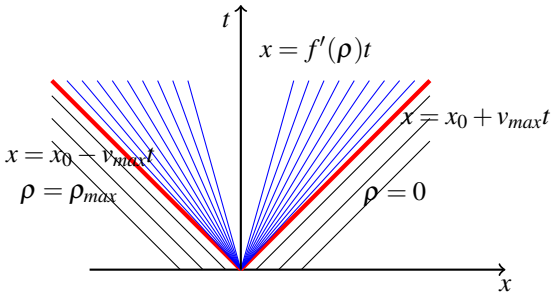

Fig. 2.4: The evolution in the case of traffic light, when the red light turns green

After solving for $f'(\rho_{max})$ in terms of v_{max} and substituting the obtained expression in equation (2.28), the density at any time t becomes

$$\rho(t,x) = \begin{cases} \rho_{max}, & \text{if } x \leq -v_{max}t; \\ \frac{\rho_{max}}{2}\left(1 - \frac{x}{v_{max}t}\right), & \text{if } -v_{max}t < x \leq v_{max}t; \\ 0 & \text{if } x(t) > v_{max}t. \end{cases}$$

For a fixed time $t > 0$, the density is equal to ρ_{max} to the left of the point $x = x(0) - v_{max}t$; hence there is a queue to the left of this point. In the middle the density $\rho = (f')^{-1}\left(\frac{x}{t}\right)$ i.e there is a decreasing in density which is the effect of progressive accumulation of cars at the green light. The density vanishes to the right of the point $x = x(0) + v_{max}t$, hence no car reached yet this point. The flow is maximal at the traffic light when $\rho(t,0) = \frac{\rho_{max}}{2}$ and we observe that after the light turn green the density in the middle thins out.

Thus, from the initial data and maximum density we have $\rho^+ < \rho_c < \rho^-$. Hence, the speed of the characteristics can be ordered as $f'(\rho^+) > 0 > f'(\rho^-)$. This tell us that the characteristics on the left move left, and the characteristics

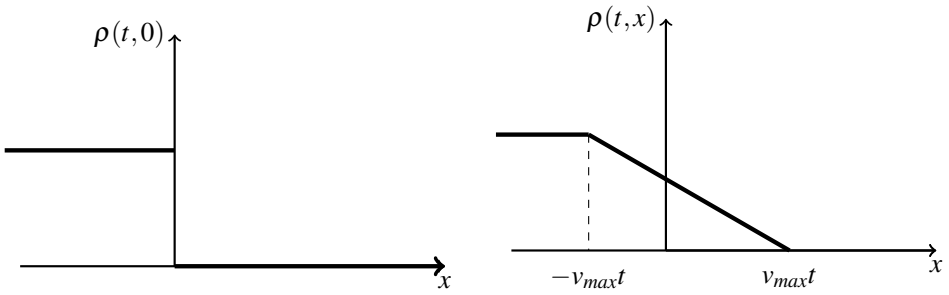

(a) Initial density (b) Density at ant time t

Fig. 2.5: The initial density at $t = 0$ and the density at time $t > 0$

on the right side move right and envelope appears through which no characteristic curves emanating from the initial condition pass through. Since the entropy condition prevents the formation of the shock, a rarefaction wave would be formed as shown in the Figure 2.4. Note that, the rarefaction wave move forward and back.

Now consider the velocity of a single car located initially at the position $x = -x_0$. Then the car starts moving when $-v_{max}t_0 = x_0$, so $t_0 = -\frac{x_0}{v_{max}}$. The velocity of the car becomes $v(t,x) = v_{max}\left(1 - \frac{\rho}{\rho_{max}}\right)$. To obtain an equation for $x(t)$ we plug in $v(t,x) = \frac{dx}{dt}$ and the expression for $\rho(t,x)$ in the middle region:

$$\frac{dx}{dt} = v_{max}\left[1 - \frac{1}{2}\left(1 - \frac{x}{v_{max}t}\right)\right] = \frac{v_{max}}{2} + \frac{x}{2t}.$$

Using the method of integrating factor we obtain $x(t) = v_{max}t + C\sqrt{t}$. From initial condition we know that $x\left(\frac{x_0}{v_{max}}\right) = -x_0$. Using this we obtain that $C = -2\sqrt{x_0 v_{max}}$. Hence,

$$x(t) = v_{max}t - 2\sqrt{x_0 v_{max}t}.$$

If the light turns red again before the queue has dissipated, the shock does not get through, the flow never comes free and the traffic jam develops. Some times the car at the back of the queue during the first red period may encounter the queue in the second times when the light turn red again. On the other hand, if the flow rate towards the traffic light is greater than that of away from the traffic light, the queue has never-ending growth.

Note that similar condition may experienced at incident sites, merging areas and behind a slow-moving vehicles.

Example 2.4 (Traffic jam ahead). Consider the following equation of scalar conservation law:

$$\begin{cases} \rho_t + f(\rho)_x = 0 \\ \rho_0 = \begin{cases} \frac{1}{8}\rho_{max}, & \text{if } x < 0; \\ \rho_{max}, & \text{if } x > 0. \end{cases} \end{cases} \tag{2.29}$$

For $x > 0$, the density is maximal and the traffic is bumper-to-bumper. The cars on the left moves with speed $v = \frac{7}{8}v_{max}$ so that we expect congestion propagating back into the traffic. When ρ is small, it is reasonable to assume that the average speed v is more or less equal to the maximal velocity v_{max} given by the speed limit.

As discussed above, $v(\rho) = v_{max}\left(1 - \frac{\rho}{\rho_{max}}\right)$. Then, equation(2.29) becomes

$$\rho_t + v_{max}\left(1 - \frac{2\rho}{\rho_{max}}\right)\rho_x = 0$$

subjected to

$$\rho(x_0) = \begin{cases} \frac{1}{8}\rho_{max}, & \text{if } x < 0; \\ \rho_{max}, & \text{if } x > 0. \end{cases}$$

When $x < 0$,

Applying the given initial datum and flux function we get

$$f(\rho) = v_{max} \times \frac{1}{8}\rho_{max}\left(1 - \frac{\frac{1}{8}\rho_{max}}{\rho_{max}}\right) = \frac{v_{max}\rho_{max}}{64}$$

and the maximal flow attain at $\rho = \frac{\rho_{max}}{2}$.

When $x > 0$, there is no flow. Since the wave on the left move right, and the wave on the right move left, they intersect and a shock wave would be formed as shown in the Figure (2.6). We compute the shock speed using Rankine-

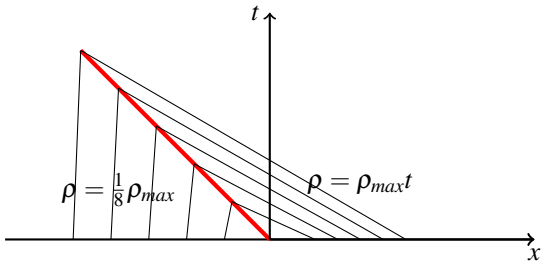

Fig. 2.6: Evolution of characteristic curve for shock wave

Hugoniot condition

$$\lambda = \frac{f(\rho^+) - f(\rho^-)}{\rho^+ - \rho^-} = \frac{-1}{8} v_{max}.$$

This indicates that, the shock propagates back with speed $\frac{-1}{8} v_{max}$ as it revealed by the braking of the cars slowing down because of traffic jam ahead. Moreover, since $f'(\rho^-) = \frac{3}{4} v_{max} > \lambda > f'(\rho^+) = -v_{max}$ the shock is entropy admissible. Therefore, the unique solution is

$$\rho(t,x) = \begin{cases} \frac{1}{8}\rho_{max}, & \text{if } x < \frac{-1}{8} v_{max} t; \\ \rho_{max}, & \text{if } x > \frac{-1}{8} v_{max} t. \end{cases}$$

The two constant states are connected by shock curve.

Definition 2.4. A weak solution $\rho = \rho(t,x)$ to the scalar Cauchy problem (2.24) satisfies the Kruzkov entropy admissibility condition if

$$\int_0^T \int_{\mathbb{R}} \{|\rho - k|\varphi_t + sgn(\rho - k)(f(\rho) - f(k))\varphi_x\}\, dxdt \geq 0$$

for every $k \in \mathbb{R}$ and every C^1 function $\varphi \geq 0$ with compact support in $[0,T] \times \mathbb{R}$.

Now we have the following theorem.

Theorem 2.2. *Let $\rho = \rho(t,x)$ be a piecewise C^1 solution to the scalar equation (2.24). Then ρ satisfies the Kruzkov entropy admissible condition if and only if along every line of jump $x = \xi(t)$ the following condition holds. For every $\alpha \in [0,1]$*

$$\begin{cases} f(\alpha\rho^+ + (1-\alpha)\rho^-) \geq \alpha f(\rho^+) + (1-\alpha) f(\rho^-), & \text{if } \rho^- < \rho^+ \\ f(\alpha\rho^+ + (1-\alpha)\rho^-) \leq \alpha f(\rho^+) + (1-\alpha) f(\rho^-), & \text{if } \rho^- > \rho^+ \end{cases} \tag{2.30}$$

where $\rho^- := \rho(t, \xi(t)-)$ and $\rho^+ := \rho(t, \xi(t)+)$

Geometrically, condition (2.30) implies that, the graph of f remains above the segment connecting $(\rho^-, f(\rho^-))$ to $(\rho^+, f(\rho^+))$ if $\rho^- < \rho^+$. If $\rho^- > \rho^+$, the graph of f remains below the segment connecting $(\rho^-, f(\rho^-))$ to $(\rho^+, f(\rho^+))$. For detail explanation and proof of this theorem see [8] page 87.

Definition 2.5. A Riemann problem for the system(2.26) is the Cauchy problem for the initial datum

$$\rho_0(x) := \begin{cases} \rho^- & \text{if } x < 0, \\ \rho^+ & \text{if } x > 0, \end{cases} \tag{2.31}$$

where $\rho^-, \rho^+ \in \Omega$.

The existence of solution to the Cauchy problem was proved in [8] by employing the method of wave-front tracking. The method of wave-front tracking is a set of techniques for constructing approximate solution to hyperbolic conservation laws in one space dimensions. The idea of the method is that the initial data is approximated with a piece-wise constant function and each Riemann problem is solved approximately within the class of piece-wise constant function. If the exact solution contains a centered rarefaction, this must be approximated by a rarefaction fan containing several small jumps. At the first time t_1 where two fronts interact, the new Riemann problem is again approximately solved by piece-wise constant functions. The solution is then prolonged up to the second interaction time t_2, where the new Riemann problem is solved and so on.

The other important feature is that, in a solution constructed by wave front tracking method, the locations of the jumps and of interaction points depend on the solution itself. For detail technical analysis such as wave front tracking, uniqueness and continuously dependence on the initial data we refer to [8, 19, 45]. If the flux function is continuous and piece-wise linear, all discontinuities in the solution are referred as fronts. A discontinuity that satisfies the entropy condition is referred as a shock wave and the continuous part of the solution of the Riemann problem are called rarefaction waves. These terminology as well as the term entropy condition comes from gas dynamics.

The global existence of entropy weak solutions within a class of functions with bounded variation is already proved in the classical sense using different approach. To recall we state the following theorem.

Theorem 2.3. *Let f be locally Lipschitz continuous and let $\rho_0 \in \mathbf{L^1}$ have bounded variation. Then the Cauchy problem*

$$\begin{aligned} &\partial_t \rho + \partial_x f(\rho) = 0, \\ &\rho(0,x) = \rho_{,0}(x), \end{aligned}$$

admits an entropy weak solution $\rho = \rho(t,x)$ defined for all $t \geq 0$, with

$$Tot.Var.\{\rho(t,.)\} \leq Tot.var\{\rho_0\}, \quad \|\rho(t,.)\|_{L^\infty} \leq \|\rho_0\|_{L^\infty} \quad \forall t \geq 0.$$

This theorem is proved in detail in [8] section 6.

Theorem 2.4. *For f uniformly convex, there exists a unique weak admissible solution to Riemann problem (2.26) and (2.31).*

(1) If $\rho^- > \rho^+$, then the admissible solution has a shock curve of speed λ and the solution is given by

$$\rho(t,x) = \begin{cases} \rho^- & \text{if } \frac{x}{t} < \lambda, \\ \rho^+ & \text{if } \frac{x}{t} > \lambda \end{cases} \tag{2.32}$$

where $\lambda = \frac{[f(\rho)]}{[\rho]}$

(2) If $\rho^- < \rho^+$*, then the solution has a rarefaction wave and the solution is given by*

$$\rho(t,x) = \begin{cases} \rho^- & \text{if } \frac{x}{t} < f'(\rho^-), \\ G\left(\frac{x}{t}\right) & \text{if } f'(\rho^-) < \frac{x}{t} < f'(\rho^+), \\ \rho^+ & \text{if } \frac{x}{t} > f'(\rho^+) \end{cases} \tag{2.33}$$

where $G \equiv (f')^{-1}$

For the proof we refer the reader to see Lawrence C. Evans [26] chapter three. A curve of discontinuity is a shock curve for a solution ρ if the curve satisfies the Rankine-Hugoniot jump condition and the entropy condition for that solution ρ.

Chapter 3
Traffic Flow Optimization on Roundabouts

3.1 Introduction

In this chapter, we focus on traffic flow optimization on roundabouts. Roundabouts can be seen as particular road networks and they can be modelled as a concatenation of junctions. At each junction we will consider the model introduced in [25], suitably modified to adapt it to the roundabout structure.

The chapter is structured as follows. In Section 3.2 we describe the junction model and the roundabout model in general. In Section 3.3, we give detail construction and the solution of the Riemann problem. Section 3.4 is devoted to the description of the numerical scheme. In Section 3.5 we describe the cost functionals and compute local optimal priority parameters and finally we close the chapter by discussing simulation results.

3.2 Mathematical Model for Roundabout

In this section, we first describe a roundabouts with three entrances and three exits. Then we present traffic flow modelling on the road network of a roundabout. Next we generalize to a roundabout with arbitrary m incoming and m outgoing roads, $m \in \mathbb{N}$, that can be modelled as a concatenation of m 2×2 junctions with two incoming and two outgoing roads. In particular, in both cases each junction has one incoming main lane, one outgoing main lane and a third link with incoming and outgoing fluxes. We model the third road with a buffer of infinite capacity for the entering flux and with an infinite sink for the exiting one.

3.2.1 Roundabout with three Entrances and three Exits

In this subsection, we shall introduce traffic flow models on road networks of a roundabout. For this, we start the section by describing a junction which is the basic concept in the network. Junction can represent an intersection of different roads such as a merging or a diverging or T-intersection. If a road network is viewed as a graph where each arc is a road segment, then the junctions correspond to the nodes (vertices). The origin or end vertices are also the particular forms of a junction. These vertices are actually used to represent the real beginning of a road or, to demarcate the part of the physical road network. The other form of junctions are just the combinations of these basic ones. For instance, a junction with an n-incoming and m-outgoing road is a combination of multiple merging and diverging. In this chapter, we shall restrict ourselves to a junction of two incoming and two outgoing type to study traffic flow phenomena on the roundabout.

Consider a roundabout joining three roads as illustrated in Figure 3.1.

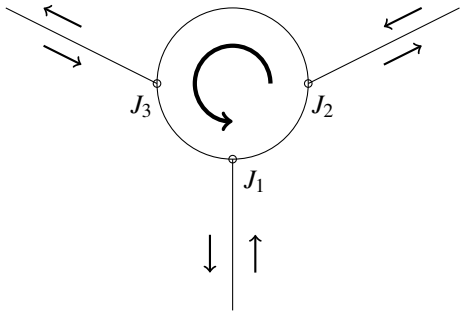

Fig. 3.1: Sketch of the roundabout considered in the section.

A roundabout can be seen as a periodic sequence of junctions and it can be represented by an oriented graph, in which roads are described by arcs and junctions by vertices. Each link forming the roundabout is modelled by an interval $\mathscr{I}_i = [a_i, b_i] \subset \mathbb{R}$, $i = 1,2,3$, $a_i < b_i$. In particular, each junction can be modelled as a 2×2 junction, see Figure 3.2. To recover the behavior of the roundabout, periodic boundary conditions are introduced on the main lane such that $b_i = a_{i+1}$, $i = 1,2,3$ and $b_3 = a_1$. At each junction we will consider the model introduced in [25], suitably modified to adapt it to the roundabout structure. The evolution of the traffic flow in the main lane segments is described by a scalar hyperbolic conservation law

$$\partial_t \rho_i + \partial_x f(\rho_i) = 0, \quad (t,x) \in \mathbb{R}^+ \times \mathscr{I}_i \quad i = 1,2,3, \tag{3.1}$$

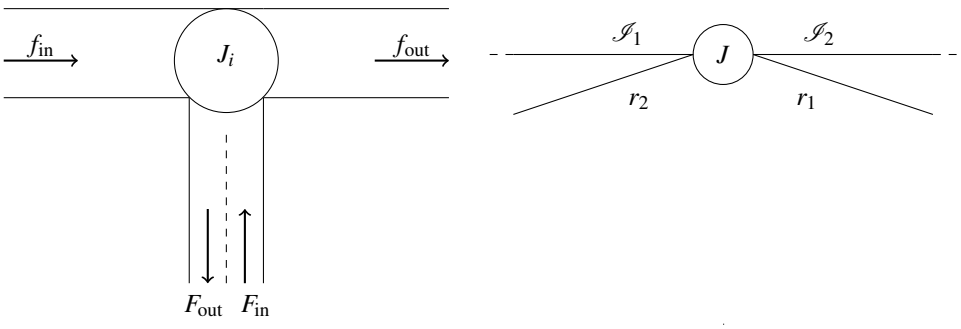

(a) Part of the roundabout. (b) Corresponded junction.

Fig. 3.2: Detail of the network modelled in the section

where $\rho_i = \rho_i(t,x) \in [0,\rho_{\max}]$ is the mean traffic density, $\rho_{\max}$ the maximal density allowed on the road. The flux function $f : [0,\rho_{\max}] \to \mathbb{R}^+$ is given by following flux-density relation

$$f(\rho) = \begin{cases} \rho v_{\text{f}} & \text{if } 0 \le \rho \le \rho_{\text{c}}, \\ \dfrac{f^{\max}}{\rho_{\max} - \rho_c}(\rho_{\max} - \rho) & \text{if } \rho_{\text{c}} \le \rho \le \rho_{\max}, \end{cases}$$

with v_{f} the maximal speed of the traffic, $\rho_{\text{c}} = \dfrac{f^{\max}}{v_{\text{f}}}$ the critical density at which the flow transitions from free to congested flow state. At ρ_{c} the traffic flow attains $f(\rho_{\text{c}}) = f^{\max}$, which is the maximal flow allowed on the road. For continuity of the flux at the critical density ρ_{c}, the relation $\rho v_f(\rho_{\max} - \rho_{\text{c}}) = f^{\max}(\rho_{\max} - \rho)$ must hold. When $\rho = 0$, there are no vehicle on the road and a driver is free to drive as fast as either the speed limit or as fast as she (he) feel comfortable. In reality different drivers have different maximum velocities as per their behavior. In this dissertation we do not treat drivers behavior. As the density of cars increases drivers start reducing their speed and we have $\frac{dv}{d\rho} \le 0$. If the cars are bamper-to- bamper, then cars should stop and $v = 0$. This time the density attains maximum value and we call it jam density so that $v(\rho_{jam}) = 0$. Hereafter, we will assume $\rho_{\max} = 1$ and $v_{\text{f}} = 1$ for simplicity. The law giving the flux as function of the density is commonly referred as fundamental diagram in the transportation literature. Nowadays, there are different types of fundamental diagram which are widely available in the literature, for example see [21, 30] and references therein. In this chapter we chose the fundamental diagram introduced in [21]. This is because triangular fundamental diagram is useful in converting rarefaction wave into standing wave compared to the others. Thus, it is helpful in minimizing the complexity of computation which might occur due to

rarefaction wave mainly in subsection 3.3.1 when we solve Riemann problem at junction using wave front tracking method. Figure 3.3 gives an example of flux function satisfying the previous hypotheses.

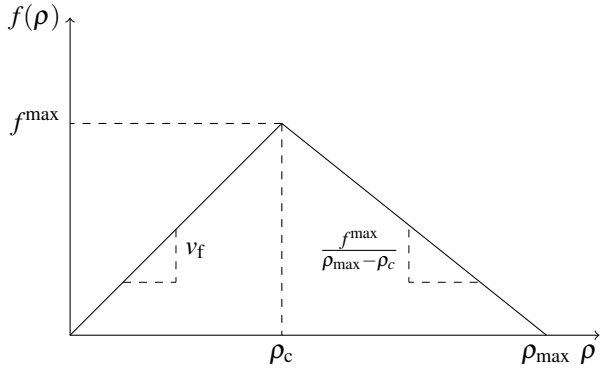

Fig. 3.3: Fundamental diagram considered throughout the chapter.

The incoming lanes of the secondary roads entering the junctions are modelled with a buffer of infinite size and capacity. This choice is made to avoid backward moving shocks at the boundary. In particular, the evolution of the queue length of each buffer is described by an ordinary differential equation (ODE)

$$\frac{dl_i(t)}{dt} = F^i_{\text{in}}(t) - \gamma_{\text{r1},i}(t), \quad t \in \mathbb{R}^+ \quad i = 1,2,3, \tag{3.2}$$

where $l_i(t) \in [0,+\infty[$ is the queue length, $F^i_{\text{in}}(t)$ the flux entering the lane and $\gamma_{\text{r1},i}(t)$ the flux exiting the lane into the roundabout. For simplicity, the outgoing lane is considered as a sink that accepts all the flux coming from the main lane. Moreover, no flux from the incoming lane is allowed entering on the outgoing stretch of the same road.
The Cauchy problem to solve can be expressed as

$$\begin{cases} \partial_t \rho_i + \partial_x f(\rho_i) = 0, & (t,x) \in \mathbb{R}^+ \times \mathscr{I}_i, \\ \dfrac{dl_i(t)}{dt} = F^i_{\text{in}}(t) - \gamma_{\text{r1},i}(t), & t \in \mathbb{R}^+, \\ \rho_i(0,x) = \rho_{i,0}(x), & \text{on } \mathscr{I}_i, \\ l_i(0) = l_{i,0} \end{cases} \tag{3.3}$$

for $i = 1,2,3$, where $\rho_{i,0}(x)$ are the initial traffic densities and $l_{i,0}$ the initial lengths of the buffers. This will be coupled with an optimization problem at the junctions that gives the distribution of traffic among the roads.

The existence and well-posedness of the solutions to Cauchy problem at node with buffer is proved in [29].

To treat the problem systematically, we start by the following definition.

Definition 3.1 (Demand and Supply function). The demand $d(F^i_{\text{in}}, l_i)$ of the entrance lane for the secondary roads, the demand function $\delta(\rho_i)$ on the incoming main lane segment, and the supply function $\sigma(\rho_i)$ on the outgoing main lane segment at each junction of the roundabout can be defined as

$$d(F^i_{\text{in}}, l_i) = \begin{cases} \gamma^{\max}_{\text{r1},i} & \text{if } l_i(t) > 0, \\ \min\left(F^i_{\text{in}}(t), \gamma^{\max}_{\text{r1},i}\right) & \text{if } l_i(t) = 0, \end{cases} \tag{3.4}$$

$$\delta(\rho_i) = \begin{cases} f(\rho_i) & \text{if } 0 \le \rho_i < \rho_{\text{c}}, \\ f^{\max} & \text{if } \rho_{\text{c}} \le \rho_i \le 1, \end{cases} \tag{3.5}$$

$$\sigma(\rho_i) = \begin{cases} f^{\max} & \text{if } 0 \le \rho_i \le \rho_{\text{c}}, \\ f(\rho_i) & \text{if } \rho_{\text{c}} < \rho_i \le 1, \end{cases} \tag{3.6}$$

for $i = 1, 2, 3$, where $\gamma^{\max}_{\text{r1},i}$ is the maximal flow on the incoming lane $r_{1,i}$.

Figure 3.4 depicts demand and supply function in the $(\rho, f(\rho))$ plane. From

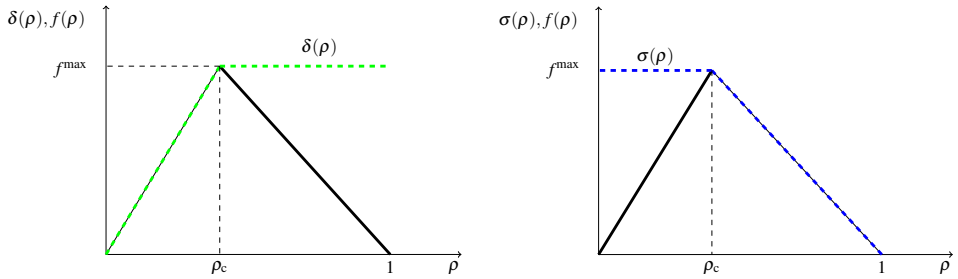

(a) Demand on the incoming Road (b) Supply on the outing Road

Fig. 3.4: Demand and supply function.

the figures one can easily see that for $0 < \rho < \rho_{\text{c}}$, the demand function is increasing while the supply capacity of the outgoing road remains constant. The demand function attains maximum value at critical density. But for $\rho_{\text{c}} < \rho < 1$, the supply function is decreasing due to traffic congestion on the road while the demand function remains constant. In [43] the authors proposed the LWR model for intersection using a description in terms of supply and demand functions by introducing a buffer of finite storage capacity at a junction.

Next we describe how a traffic coming from the incoming roads choose to distribute to the outgoing roads. To this aim, we introduce $\beta \in (0, 1)$, the split

ratio of the outgoing lane $r_{2,i}$, and its flux $\gamma_{r2,i}(t) = \beta f(\rho_i(t,0-)),\ i = 1,2,3$. More precisely, at each junction J, we consider a matrix describing the distribution of the traffic among outgoing roads. The formal definition for distribution rate at a junction with arbitrary number of incoming and outgoing roads is given as follows.

Definition 3.2 ([30]). Fix a junction J with n incoming roads, say $I_1,\dots,I_n$, and m outgoing roads, say $I_{n+1},\dots,I_{n+m}$. A traffic distribution matrix A is given by

$$A = \begin{pmatrix} \beta_{n+1,1}, & \cdots, & \beta_{n+1,n} \\ \vdots & \vdots & \vdots \\ \beta_{n+m,1}, & \cdots, & \beta_{n+m,n} \end{pmatrix} \tag{3.7}$$

where $0 \le \beta_{j,i} \le 1$ for every $i \in \{1,\dots,n\}$ and for every $j \in \{n+1,\dots,n+m\}$ and

$$\sum_{j=n+1}^{n+m} \beta_{j,i} = 1 \tag{3.8}$$

for every $i \in \{1,\dots,n\}$.

This definition illustrates that, given a junction J and an incoming road I_i, the $i-$th column of A describes how the traffic from incoming road I_i distributes in percentages to the outgoing roads. This means that if N is the total quantity of the traffic coming from road I_i, then $\beta_{j,i}N$ traffic moves towards roads I_j. This definition stresses maximizing traffic flux through a junction in contrary to our case which maximize flux on outgoing main road of the roundabout. That is, in the context of the present work, the distribution rate at a given junction can be written as

$$A = \begin{pmatrix} \beta & 0 \\ 1-\beta & 1 \end{pmatrix} \tag{3.9}$$

This is due to the fact that no flux from the entrance road is allowed entering on the adjacent outgoing road.

Remark 3.1. One may also assume that the matrix A is time dependent. For example in the case of car traffic on an urban road network, the preferences of drivers may change depending on the period of the day [30].

On the network, distribution rate alone can not sufficiently describe traffic flow at all junctions since some of them are merging and the others are diverging. For instance, for junction with two incoming and one outgoing roads. This is due to the fact that if not all cars can go through the junction, then there should be a yield rule between incoming roads that describe the percentage of cars crossing the junction. For this we have the following remark in the context of a roundabout.

Remark 3.2. A parameter $\mathrm{p} \in]0,1[$ is introduced as given in [30] to ensure uniqueness of the solution. More precisely, p is a right of way parameter that defines the amount of flux that enters the outgoing main lane from each incoming road. When the priority applies, $\mathrm{p}f(\rho_i(t,0+))$ is the flux allowed from the incoming main lane into the outgoing main lane, and $(1-\mathrm{p})f(\rho_{i+1}(t,0+))$ is the flux from the entrance of the roundabout.

In this remark we note that the role of the priority parameter is to force the priority to neither impose insufficient flows nor send excess vehicles than the capacity of the main outgoing road of the roundabout. Now we give the definitions of weak solutions at the junction.

Definition 3.3 (Weak solutions). Consider a roundabout with three roads $\mathscr{I}_i = [a_i, b_i] \subset \mathbb{R}$, $a_i < b_i$, for $i = 1,2,3$, with $b_3 = a_1$, three entrances $r_{1,i}\, i = 1,2,3$, and three exits $r_{2,i}\, i = 1,2,3$. A collection of functions $(\rho_i, l_i)_{i=1,2,3} \in \prod_{i=1}^{3} \mathscr{C}^0\left(\mathbb{R}^+; \mathbf{L^1} \cap \mathrm{BV}(\mathscr{I}_i)\right) \times \prod_{i=1}^{3} \mathbf{W^{1,\infty}}(\mathbb{R}^+;\mathbb{R}^+)$ is an admissible solution to (3.3) if

1. ρ_i is a weak solutions on $\mathscr{I}_i$, i.e., $\rho_i : [0,+\infty[\times\mathscr{I}_i \to [0,1]$, such that
$$\int_{\mathbb{R}^+}\int_{\mathscr{I}_i}\Big(\rho_i\partial_t\varphi_i + f(\rho_i)\partial_x\varphi_i\Big)dxdt + \int_{\mathscr{I}_i}\rho_{i,0}\varphi_{i,0}dx = 0, \tag{3.10}$$
for every $\varphi_i \in \mathscr{C}^1_c(\mathbb{R}^+ \times \mathscr{I}_i)$, $i = 1,2,3$.
2. ρ_i satisfies the Kružhkov entropy condition [50] on $(\mathbb{R}^+ \times \mathscr{I}_i)$, i.e.,
$$\int_{\mathbb{R}^+}\int_{\mathscr{I}_i}(|\rho_i - k|\partial_t\varphi_i + \mathrm{sgn}\,(\rho_i - k)(f(\rho_i) - f(k))\partial_x\varphi_i)dxdt + \int_{\mathscr{I}_i}\big|\rho_{i,0} - k\big|\varphi_i(0,x)dx \geq 0 \tag{3.11}$$
for every $k \in [0,1]$ and for all $\varphi_i \in \mathscr{C}^1_c(\mathbb{R} \times \mathscr{I}_i)$, $i = 1,2,3$.
3. At each junction J_i, $f(\rho_i(t,0-)) + \gamma_{\mathrm{r}1,i}(t) = f(\rho_{i+1}(t,0+)) + \gamma_{\mathrm{r}2,i}(t)$ for $i = 1,2,3$ (where we set $\rho_4 = \rho_1$).
4. At each junction J_i, the flux of the outgoing main lane $f(\rho_{i+1}(t,0+))$ is maximum provided that it satisfies the conditions
$$f(\rho_{i+1}(t,0+)) = \min\Big((1-\beta)\delta(\rho_i(t,0-)) + d(F_{\mathrm{in}}(t), l_i(t)), \sigma(\rho_{i+1}(t,0+))\Big), \tag{3.12}$$
for $i = 1,2,3$, and $\rho_4 = \rho_1$ and 3.
5. l_i is a solution of (3.2) for almost every $t \in \mathbb{R}^+$, $i = 1,2,3$.

Notice that, in this definition the linear optimization problem maximizes the flux on the outgoing main road of a roundabout rather than at the junction.

Condition (1) corresponds to conservation of cars.

3.2.2 Roundabout with Arbitrary m Entrances and m Exits

In this subsection we consider a roundabout joining m arbitrary incoming and outgoing roads, $m \in \mathbb{N}$, $m \geq 2$, as illustrated in Figure 3.5.

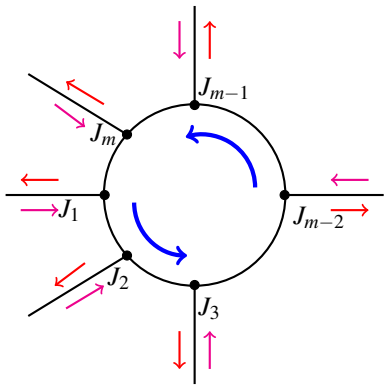

Fig. 3.5: Roundabout with arbitrary m incoming and m outgoing roads

As in Subsection 3.2.1, each link forming the roundabout is modelled by intervals $I_i = [x_{i-1}, x_i] \subset \mathbb{R}$, $x_{i-1} < x_i$, $i = 1, 2, \ldots, m$. Junction J_i is located at $x = x_i$ for $i = 1, 2, \ldots, m$.

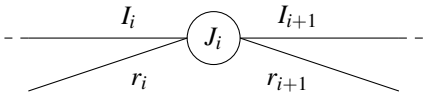

Fig. 3.6: Sketch of a roundabout junction.

To recover the behavior of the roundabout periodic boundary conditions are introduced on the main lane such that $x_m = x_0$. Each junction is composed of a main lane and by two links representing a lane with incoming flux (r_i) and a lane with outgoing flux (r_{i+1}), see Figure 3.6. The other formulation and evolution of the traffic flow on the main lane segments and on the incoming third road is exactly described as in the previous subsection.

The following two consecutive definitions are repeated only for notational purpose for later use in Subsection 3.3.2 through different approach.

Definition 3.4. The demand $d(F_i^{\text{in}}, l_i)$ of the incoming lane for the secondary road, the demand function $\delta(\rho_i)$ on the incoming road forming a roundabout at each junction, and the supply function $\sigma(\rho_i)$ on the outgoing main lane segment at each junction of the roundabout can be defined as

$$d(F_i^{\text{in}}, l_i) = \begin{cases} \gamma_{r_i}^{\max} & \text{if } l_i(t) > 0, \\ \min(F_i^{in}, \gamma_{r_i}^{\max}) & \text{if } l_i(t) = 0, \end{cases} \tag{3.13}$$

$$\delta(\rho_i) = \begin{cases} f(\rho_i) \text{ if } 0 \le \rho_i < \rho_c, \\ f^{\max} \text{ if } \rho_c \le \rho_i \le 1, \end{cases} \tag{3.14}$$

$$\sigma(\rho_i) = \begin{cases} f^{\max} \text{ if } 0 \le \rho_i \le \rho_c, \\ f(\rho_i) \text{ if } \rho_c < \rho_i \le 1, \end{cases} \tag{3.15}$$

for $i = 1, 2, \ldots, m$, where $\gamma_{r_i}^{\max}$ is the maximal flow on the incoming lane r_i, $i = 1, 2, \ldots, m$.

Definition 3.5. Consider a roundabout as in Figure 3.5. A $2m$-tuple

$$(\rho_i, l_i)_{i=1,\ldots,m} \in \prod_{i=1}^{m} \mathscr{C}^0\left(\mathbb{R}^+; \mathbf{L^1} \cap \mathrm{BV}(I_i)\right) \times \prod_{i=1}^{m} \mathbf{W^{1,\infty}}(\mathbb{R}^+; \mathbb{R}^+)$$

is an admissible solution to (3.3) if

1. ρ_i satisfies the Kružhkov entropy condition [50] on $(\mathbb{R}^+ \times I_i)$, that is, for every $k \in \mathbb{R}$ and for all $\varphi \in \mathscr{C}_c^1(\mathbb{R} \times I_i)$, $t > 0$,

$$\begin{aligned} &\int_{\mathbb{R}^+} \int_{I_i} (|\rho_i - k| \partial_t \varphi + \operatorname{sgn}(\rho_i - k)(f(\rho_i) - f(k)) \partial_x \varphi) dx dt \\ &\quad + \int_{I_i} \left|\rho_{i,0} - k\right| \varphi(0, x) dx \ge 0; \quad i = 1, 2, \ldots, m. \end{aligned} \tag{3.16}$$

2. $f(\rho_i(t, x_i-)) + \gamma_{r_i}(t) = f(\rho_{i+1}(t, x_i+)) + \gamma_{r_{i+1}}(t)$, $i = 1, 2, \ldots, m$.
3. The outgoing flux $f(\rho_{i+1}(t, x_i+))$ is maximum provided that it satisfies the conditions

$$f(\rho_{i+1}(t, x_i+)) = \min\left((1 - \beta_i)\delta(\rho_i(t, x_i-)) + d(F_i^{\text{in}}(t), l_i(t)), \sigma(\rho_{i+1}(t, x_i+))\right), \tag{3.17}$$

   and condition 2 above.
4. l_i solves (3.2) for almost every $t \in \mathbb{R}^+$, for all $i = 1, 2, \ldots, m$.

In the next section we give the construction of Riemann problem and some important results.

3.3 Riemann Problem at the Junction

In this section we treat the construction of Riemann solver at each junction of a roundabout under consideration. We shall employ wave-front tracking method to construct a solution for a Riemann problem at a junction of a roundabout with three incoming and three outgoing roads in Subsection 3.3.1. We repeatedly solve the problem until wave junction interaction terminate within the region. The absence of wave junction interaction indicates the smoothness of traffic evolution on the roundabout. In Subsection 3.3.2 we extend the construction of the Riemann solver at each junctions of a roundabout with arbitrary m entrances and m exiting road by formulating the problem in discrete form. For simplicity, we will focus on each single junction and drop the index i when not necessary.

3.3.1 For Roundabout with 3 Entrances and 3 Exits

In this subsection we describe the construction of the Riemann Solver at a junction and then we apply it to our particular case to recover the expressions of the cost functionals later on. The Riemann problem at J is the Cauchy problem (3.3) where the initial conditions are given by $\rho_{0,i}(x) \equiv \rho_{0,i}$ on $\mathscr{I}_i$ for $i = 1,2,3$. In the following, we will focus only on one junction J with two incoming roads and two outgoing ones. Then we fix constants $\rho_{1,0}, \rho_{2,0} \in [0,1]$, $l_0 \in [0,+\infty[$, $F_{\text{in}} \in]0,+\infty[$ and a priority factor $\text{p} \in (0,1)$. We define the Riemann Solver as in [25] at junction by means of a Riemann Solver $\mathscr{RS}_l : [0,1]^2 \to [0,1]^2$, which depends on the instantaneous load of the buffer l. For each l the Riemann Solver $\mathscr{RS}_l(\rho_{1,0}, \rho_{2,0}) = (\hat{\rho}_1, \hat{\rho}_2)$ is constructed in the following way.

1. Define $\Gamma_1 = f(\rho_1(t,0-))$, $\Gamma_2 = f(\rho_2(t,0+))$, $\Gamma_{\text{r1}} = \gamma_{\text{r1}}(t)$;
2. Consider the space $(\Gamma_1, \Gamma_{\text{r1}})$ and the sets $\mathscr{O}_1 = [0, \delta(\rho_{1,0})]$, $\mathscr{O}_{\text{r1}} = [0, d(F_{\text{in}}, l)]$;
3. Trace the lines $(1-\beta)\Gamma_1 + \Gamma_{\text{r1}} = \Gamma_2$; and $\Gamma_1 = \frac{\text{p}}{(1-\text{p})(1-\beta)}\Gamma_{\text{r1}}$;
4. Consider the region

$$\Omega = \Big\{(\Gamma_1, \Gamma_{\text{r1}}) \in \mathscr{O}_1 \times \mathscr{O}_{\text{r1}} : (1-\beta)\Gamma_1 + \Gamma_{\text{r1}} \in [0, \Gamma_2]\Big\}. \tag{3.18}$$

At this step two different situations can occur depending on the value of Γ_2. That is,

1. Demand-limited case: Γ_2=$(1-\beta)\delta(\rho_{1,0}) + d(F_{\text{in}}, l)$.
   In the absence of demanding traffic on the road the junction operate with

less traffic. In this case we set as a solution $\hat{\Gamma}_1 = \delta(\rho_{1,0})$, $\hat{\Gamma}_{r1} = d(F_{in}, l)$ and $\hat{\Gamma}_2 = (1-\beta)\delta(\rho_{1,0}) + d(F_{in}, l)$, as illustrated in Figure 3.7(a).

2. Supply-limited case: $\Gamma_2 = \sigma(\rho_{2,0})$.
Some times excess traffic may occur on the section of a road. This time the junction becomes congested unless drivers behaves in good manner in addition to the give way rule. In supply-limited case, we first calculate the intersection point of $(1-\beta)\Gamma_1 + \Gamma_{r1} = \Gamma_2$ and $\Gamma_1 = \frac{p}{(1-p)(1-\beta)}\Gamma_{r1}$ and denote it by Q. If $Q \in \Omega$, we set ($\hat{\Gamma}_1$,$\hat{\Gamma}_{r1}$)=Q and $\hat{\Gamma}_2 = \Gamma_2$, see Figure 3.7(b); if $Q \notin \Omega$, we set ($\hat{\Gamma}_1$,$\hat{\Gamma}_{r1}$)=S and $\hat{\Gamma}_2 = \Gamma_2$, where S is the point of the segment $\Omega \cap (\Gamma_1, \Gamma_{r1}) : (1-\beta)\Gamma_1 + \Gamma_{r1} = \Gamma_2$ closest to the line $\Gamma_1 = \frac{p}{(1-p)(1-\beta)}\Gamma_{r1}$ see Figure 3.7(c).

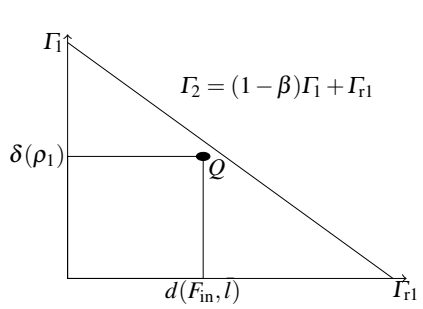

(a) Demand-limited case

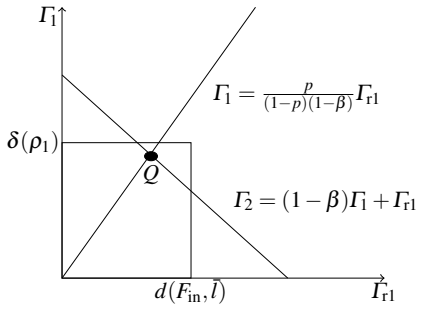

(b) Supply-limited case: intersection inside Ω

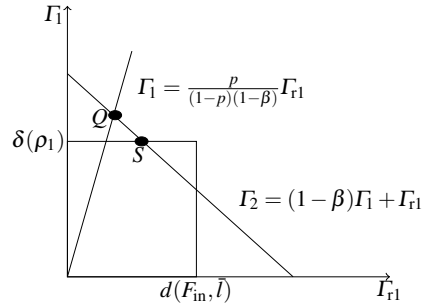

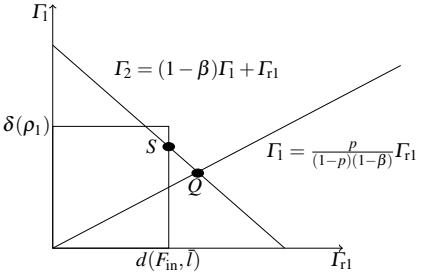

(c) Supply-limited case: intersection outside Ω

Fig. 3.7: Solutions of the Riemann Solver at the junction.

For later use we define the function τ as follows, for detail properties see [30, page 75].

Definition 3.6. Let $\tau : [0,1] \to [0,1]$ be the map such that:

1. $f(\tau(\rho)) = f(\rho)$ for every $\rho \in [0,1]$;
2. $\tau(\rho) \neq \rho$ for every $\rho \in [0,1] \setminus \{\rho_c\}$.

Remark 3.3. Compared to [25], the model presented in this chapter has a modified Riemann problem at junction. In particular, on roundabouts exits precede entrances. Therefore, the flow coming from the main lane and crossing the junction, interacting with the incoming flow is $(1-\beta)\Gamma_1$. This leads to consider the priority line as $\Gamma_1 = \frac{p}{(1-p)(1-\beta)}\Gamma_{r1}$ adding a factor of $\frac{1}{1-\beta}$ with respect to the other model. This takes into account the amount of cars that leave the roundabout before the entrance. All the results in [25] can be extended and adapted to fit this case.

Theorem 3.1. *Consider a junction J and fix a right of way parameter $p \in (0,1)$. For every $\rho_{1,0}, \rho_{2,0} \in [0,1]$ and $l_0 \in [0, +\infty[$ there exists a unique admissible solution $(\rho_1(t,x), \rho_2(t,x), l(t))$ in the sense of Definition 3.3, compatible with the Riemann Solver proposed in Section 3.3. More precisely, there exists a unique couple $(\hat{\rho}_1, \hat{\rho}_2) \in [0,1]^2$ such that $\mathscr{RS}_l(\rho_{1,0}, \rho_{2,0}) = (\hat{\rho}_1, \hat{\rho}_2)$:*

$$\hat{\rho}_1 \in \begin{cases} \{\rho_{1,0}\} \cup]\tau(\rho_{1,0}), 1] & \text{if } 0 \leq \rho_{1,0} \leq \rho_c, \\ [\rho_c, 1] & \text{if } \rho_c \leq \rho_{1,0} \leq 1, \end{cases} \qquad f(\hat{\rho}_1) = \hat{\Gamma}_1, \tag{3.19}$$

and

$$\hat{\rho}_2 \in \begin{cases} [0, \rho_c] & \text{if } 0 \leq \rho_{2,0} \leq \rho_c, \\ \{\rho_{2,0}\} \cup [0, \tau(\rho_{2,0})[& \text{if } \rho_c \leq \rho_{2,0} \leq 1, \end{cases} \qquad f(\hat{\rho}_2) = \hat{\Gamma}_2. \tag{3.20}$$

For the incoming road the solution is given by the wave $(\rho_{1,0}, \hat{\rho}_1)$, while for the outgoing road the solution is given by the wave $(\hat{\rho}_2, \rho_{2,0})$. Furthermore, for a.e. $t > 0$, it holds

$$(\rho_1(t,0-), \rho_2(t,0+)) = \mathscr{RS}_{l(t)}(\rho_1(t,0-), \rho_2(t,0+)).$$

Proof. Existence and uniqueness follow directly by construction of the Riemann Solver presented under subsection 3.3.1. In the following we will show the proof of the consistency of $\mathscr{RS}_{l(t)}$. Fix any $t = t_0 \geq 0$. If $(\rho_1(t_0,0-), \rho_2(t_0,0+))$ is a solution of the Riemann Solver, corresponding to the same buffer value $l(t_0)$ we need to show that

$$\mathscr{RS}_{l(t_0)}(\rho_1(t_0,0-), \rho_2(t_0,0+)) = (\rho_1(t_0,0-), \rho_2(t_0,0+))$$

Without loss of generality, we assume that $t_0 = 0$. Recall that the solution of the Riemann problem consists of a shock wave with a negative speed on the incom-

ing road and a shock wave with positive speed on the outgoing road. Having this in mind we detail each cases as follows.

On the incoming main road of the roundabout: if $0 \leq \rho_{1,0} \leq \rho_c$, then either $\hat{\rho}_1 = \rho_{1,0}$ or $\hat{\rho}_1 \in (\tau(\rho_{1,0}), 1]$. In the first case $\delta(\rho_{1,0}) = f(\rho_{1,0}) = f(\hat{\rho}_1) = \delta(\hat{\rho}_1)$, see Figure 3.10a. In the second case, $\delta(\rho_{1,0}) = f(\rho_{1,0}) \leq f^{max} = \delta(\hat{\rho}_1)$, as shown in Figure 3.10b. On the other hand if $\rho_c \leq \rho_{1,0} \leq 1$, we have that $\rho_c \leq \hat{\rho}_1 \leq 1$ and $\delta(\rho_{1,0}) = f^{max} = \delta(\hat{\rho}_1)$ as it can be seen from Figure 3.10c. Hence, we have

$$\delta(\rho_{1,0}) \leq \delta(\hat{\rho}_1) \tag{3.21}$$

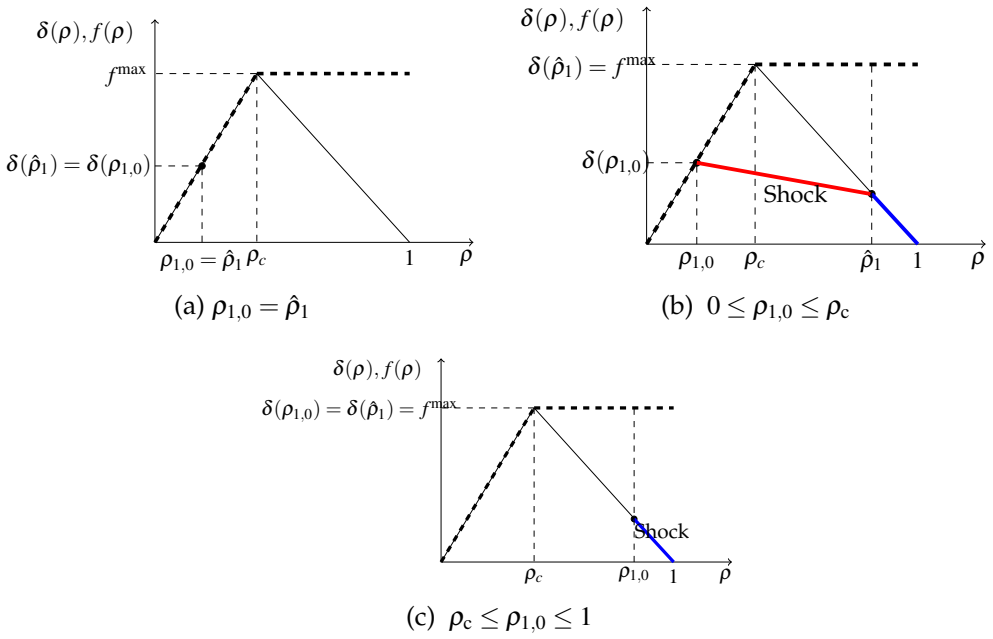

(a) $\rho_{1,0} = \hat{\rho}_1$ (b) $0 \leq \rho_{1,0} \leq \rho_c$

(c) $\rho_c \leq \rho_{1,0} \leq 1$

Fig. 3.8: Demand evolution in the Riemann problem(On incoming road).

On the outgoing main road of the roundabout: if $0 \leq \rho_{2,0} \leq \rho_c$, then $0 \leq \hat{\rho}_2 \leq \rho_c$ as well and the corresponding supply function becomes $\sigma(\rho_{2,0}) = f^{max} = \sigma(\hat{\rho}_2)$, see Figure 3.9c. For $\rho_c \leq \rho_{2,0} \leq 1$, then either $\hat{\rho}_2 = \rho_{2,0}$ or $\hat{\rho}_2 \in [0, \tau(\rho_{2,0}))$. In the first case $\sigma(\rho_{2,0}) = f(\rho_{2,0}) = f(\hat{\rho}_2)$ as shown in Figure 3.9a. In the second case $\sigma(\rho_{2,0}) = f(\rho_{2,0}) \leq f^{max} = \sigma(\hat{\rho}_2)$, as illustrated in Figure 3.9b.

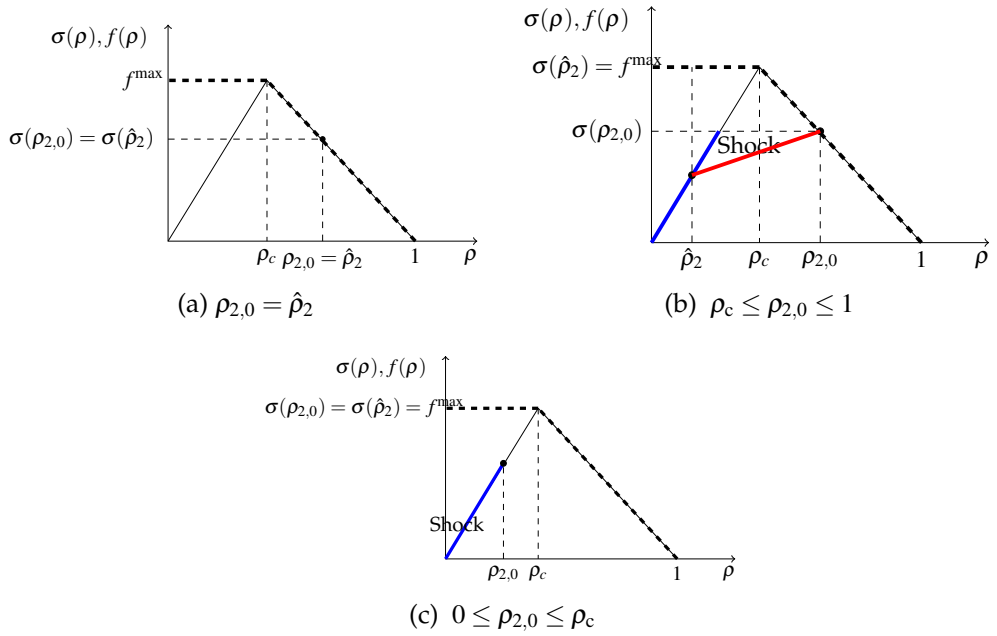

(a) $\rho_{2,0} = \hat{\rho}_2$ (b) $\rho_c \leq \rho_{2,0} \leq 1$

(c) $0 \leq \rho_{2,0} \leq \rho_c$

Fig. 3.9: Supply evolution in the Riemann problem(On outgoing road)

Hence, we can conclude that

$$\sigma(\rho_{2,0}) \leq \sigma(\hat{\rho}_2) \tag{3.22}$$

On the incoming entrance road of the roundabout we consider two different cases, when the buffer is initially empty and when it is not. In both cases different situations can occur.

Case: 1 Initially empty buffer: $l(0) = 0$. This implies that $d(F_{in}, l(0)) = \min(F_{in}, \gamma_{r1}^{\max})$
Case: 1.1 Buffer increases: $l(0+) > 0$. This implies $d(F_{in}, l(0+)) = \gamma_{r1}^{\max}$ by definition.

If $d(F_{in}, l(0)) = F_{in}$, then $d(F_{in}, l(0)) \leq d(F_{in}, l(0+))$. If $d(F_{in}, l(0)) = \gamma_{r1}^{\max}$, then $d(F_{in}, l(0)) = d(F_{in}, l(0+))$.

Case: 1.2 Buffer remains empty: $l(0+) = 0$. This implies that $d(F_{in}, l(0+)) = \min(F_{in}, \gamma_{r1}^{\max})$. Hence, $d(F_{in}, l(0)) = d(F_{in}, l(0+))$

Case: 2 Buffer initially not empty: $l(0) > 0$. This implies $d(F_{in}, l(0)) = \gamma_{r1}^{\max}$.
Case: 2.1 Buffer increases(decreases) linearly: $0 < l(0) < l(0+) (0 < l(0+) < l(0))$.

This implies $d(F_{in}, l(0+)) = \gamma_{r1}^{\max}$ by definition. Hence, $d(F_{in}, l(0)) = d(F_{in}, l(0+))$.
Hence, from these case we can deduce that

$$d(F_{in}, l(0)) \leq d(F_{in}, l(0+)) \tag{3.23}$$

Our aim is to show that the optimal point lies in the feasible set Ω as defined in (3.18), resulting from the Riemann Solver does not change. From equation (3.21) $-$ (3.23) it is straight forward to infer that the set Ω either increases between times t $= 0$ and t > 0 or does not change, as illustrated in Figure 3.10 and 3.11. In order to prove that the optimal point does not change, we shall treat the supply and the demand-limited cases separately in sequel as follows.

1. Supply-limited junction problem

We assume that the junction is supply-limited at t $= 0$. In this situation, by construction of the Riemann solver, it holds $\rho_{2,0} = \hat{\rho}_2$ and hence $\sigma(\rho_{2,0}) = \sigma(\hat{\rho}_2)$. Thus, the priority line is fixed, and the intersection point Q does not change.

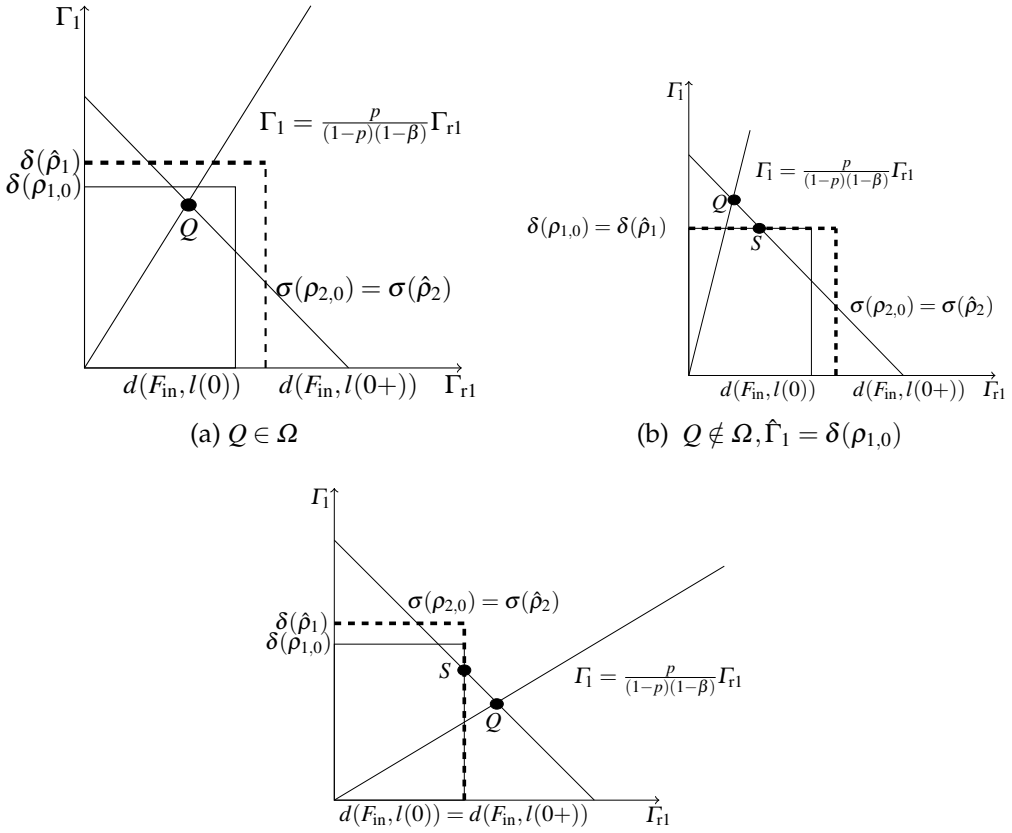

(a) $Q \in \Omega$

(b) $Q \notin \Omega, \hat{\Gamma}_1 = \delta(\rho_{1,0})$

(c) $Q \notin \Omega, \hat{\Gamma}_{r,1} = d(F_{\text{in}}, l(0))$

Fig. 3.10: Supply-limited junction problem.

(a) Feasible solution inside Ω

Since Q is determined by the intersection of the two lines and Ω can only increase $\delta(\rho_{1,0}) \leq \delta(\hat{\rho}_1)$ and $d(F_{in}, l(0)) \leq d(F_{in}, l(0+))$, we have

$$(\hat{\rho}_1, \hat{\rho}_2) = \mathscr{RS}_{l(0)}(\hat{\rho}_1, \hat{\rho}_2).$$

(b) Feasible solution on the border of Ω, $\hat{\Gamma}_1 = \delta(\rho_{1,0})$

We need to show that the point S in the figure does not change. point S is obtained by orthogonal projection on the convex set. By construction of the Riemann Solver it holds that $\rho_{1,0} = \hat{\rho}_1$. This implies $\delta(\rho_{1,0}) = \delta(\hat{\rho}_1)$ by case 1. Again from case 1 and case 2 we observe that $d(F_{in}, l(0))$ can only increase. Consequently we have,

$$(\hat{\rho}_1, \hat{\rho}_2) = \mathscr{RS}_{l(0)}(\hat{\rho}_1, \hat{\rho}_2).$$

(c) Feasible solution on the border of Ω, $\hat{\Gamma}_{r1} = d(F_{in}, l(0))$

On the incoming road towards the entrance of the roundabout, the only case where the demand can increase is the case 1.1. In this particular setting, if $d(F_{in}, l(0)) = F_{in}$ we have that $\gamma_{r1}(0) = F_{in}$ and $F_{in} \leq \gamma_{r1}^{\max}$. When the buffer start increasing we have $\gamma_{r1}(0+) = d(F_{in}, l(0+)) = \gamma_{r1}^{\max}$, which implies $\gamma_{r1}^{\max} \leq F_{in}$. Hence $\gamma_{r1}^{\max} = F_{in}$ and $d(F_{in}, l(0)) = d(F_{in}, l(0+))$. The demand on the main road of the roundabout can only increase. Hence,

$$(\hat{\rho}_1, \hat{\rho}_2) = \mathscr{RS}_{l(0)}(\hat{\rho}_1, \hat{\rho}_2)$$

2. Demand-limited junction problem

In this case $\rho_{1,0} = \hat{\rho}_1$ and on the external incoming road of the roundabout $\gamma_{r1}^{\max} = F_{in}$ and this implies $\delta(\rho_{1,0}) = \delta(\hat{\rho}_1)$ and $d(F_{in}, l(0)) = d(F_{in}, l(0+))$ by case 1 and 2 above. The supply can only increase by (3.22). Hence,

$$(\hat{\rho}_1, \hat{\rho}_2) = \mathscr{RS}_{l(0)}(\hat{\rho}_1, \hat{\rho}_2)$$

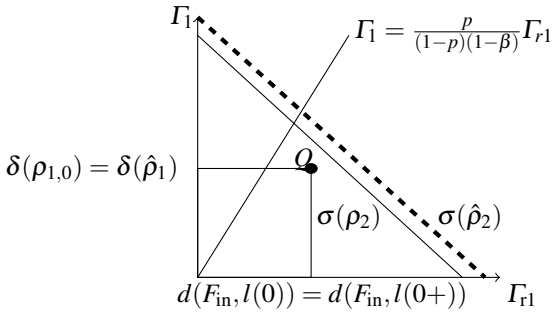

Fig. 3.11: Demand-limited junction problem.

Moreover, the limiting side of Ω does not change, i.e, it is not possible to pass from a demand-limited junction problem to a supply-limited one and vice versa. This follows from the fact that $\sigma(\rho_{2,0}) = \sigma(\hat{\rho}_2)$ when we have a supply-limited junction problem, Figure 3.10 and $d(F_{in}, l(0)) = d(F_{in}, l(0+))$, $\delta(\rho_{1,0}) = \delta(\hat{\rho}_1)$ when we have a demand-limited junction problem, Figure 3.11. This conclude the proof of the theorem.

We suppose that the network and the buffer are empty at $t = 0$ and we assume that the following boundary data are given: f^{in} the inflow on the incoming main lane, f^{out} the outflow on the outgoing main lane and F_{in} the incoming flux of the secondary road. Moreover, to reduce the number of cases to be studied, we assume $F_{\text{in}} \leq f^{\max} = \gamma_{\text{r1}}^{\max}$ and $f^{\text{out}} \leq f^{\max}$. Now, we can solve the corresponding initial-boundary value problem at a junction using Definition 3.3.

The first step is to compute the demand and supply functions of the roads. We have $\delta(\rho_{1,0}) = 0$, $d(F_{\text{in}}, l) = \min(F_{\text{in}}, \gamma_{\text{r1}}^{\max}) = F_{\text{in}}$ and $\sigma(\rho_{2,0}) = f^{\max}$. Then we can compute Γ_2 using Definition 3.3 as follows

$$\Gamma_2 = \min\Big((1-\beta)\delta(\rho_{1,0}) + d(F_{\text{in}}, l), \sigma(\rho_{2,0})\Big) = F_{\text{in}}.$$

It is straightforward to see that the problem is demand limited, hence the optimal point is the point at maximal demands. Thus it follows $\hat{\Gamma}_1 = 0$, $\hat{\Gamma}_2 = F_{\text{in}}$ and $\hat{\Gamma}_{\text{r1}} = F_{\text{in}}$, from which we uniquely derive $\rho_{1,0} = 0$ and $\hat{\rho}_2 = F_{\text{in}} < \rho_{\text{c}}$. Since we are demand limited we also have $l(t) = 0$. The solution in the x-t plane looks as in Figure 3.12. The wave produced by the junction problem interacts with the right boundary $x = 1$ at time $t_1 = 1$. Moreover at $x = -1$, the boundary condition enforces the creation of an additional wave at $t = 0$ with speed equal to 1. This gives a density $\hat{\rho}_1 = f^{\text{in}} < \rho_{\text{c}}$, which reaches the junction at the same time $t_1 = 1$, see Figure 3.12.

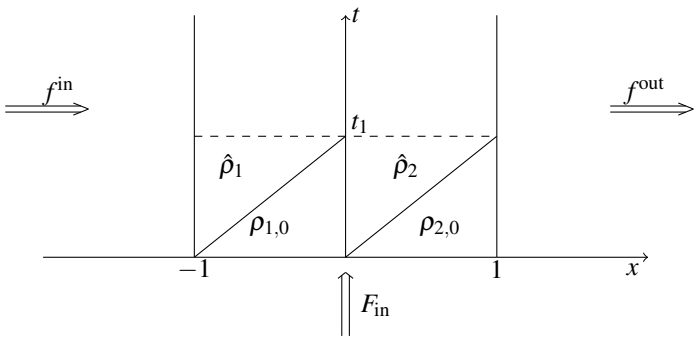

Fig. 3.12: Solution of the initial-boundary value problem for $t \in [0, t_1]$.

At $t_1 = 1$ we solve a new Riemann problem at the junction with initial densities

$$\rho(1,x) = \begin{cases} \hat{\rho}_1 \text{ if } x < 0, \\ \hat{\rho}_2 \text{ if } x > 0. \end{cases}$$

We assume that the splitting ratio $\beta \in (0,1)$ is the same for all roads and fixed. Also note that $0 \leq \hat{\rho}_1 < \rho_c$ and $0 \leq \hat{\rho}_2 < \rho_c$. The demand and supply functions on the respective roads are $\delta(\hat{\rho}_1) = f^{\text{in}}$, $d(F_{\text{in}}, l_0) = \min(F_{\text{in}}, \gamma_{r1}^{\max}) = F_{\text{in}}$, $\sigma(\hat{\rho}_2) = f^{\max}$. Computing Γ_2 from these values we obtain

$$\Gamma_2 = \min\Big((1-\beta)\delta(\hat{\rho}_1) + d(F_{\text{in}}, l), \sigma(\hat{\rho}_2)\Big)$$

Now two cases can occur at this point according to the value of Γ_2. These are

A. Demand-limited case: $\Gamma_2 = (1-\beta)\delta(\hat{\rho}_1) + d(F_{\text{in}}, l)$

In this case the Riemann problem at t_1 is demand limited. No wave is created in the incoming link, and a wave with speed 1 emanates from the junction on the outgoing road with a density $\rho_2 = (1-\beta)f^{\text{in}} + F_{\text{in}}$. The buffer remains empty. At this point we have two different situations according to:

- $F_{\text{in}} < f^{\text{out}}$,
- $f^{\text{out}} < F_{\text{in}}$.

In the first case ($F_{\text{in}} < f^{\text{out}}$) the wave from the junction interacts with the boundary $x = 1$ at $t_2 = 2$, generating a wave with negative speed and a density $\rho_3 = \dfrac{f^{\max} - (1-f^{\max})f^{\text{out}}}{f^{\max}} \in [\rho_c, 1]$ which reaches the junction at $t_3 = \dfrac{2\lambda(\rho_2,\rho_3) - 1}{\lambda(\rho_2,\rho_3)}$ as shown in Figure 3.14.

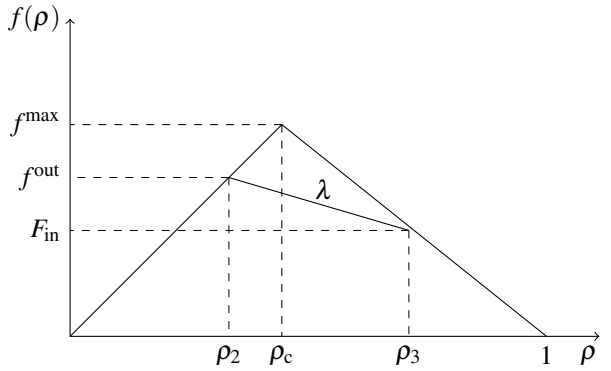

Fig. 3.13: Wave created at the right boundary.

In the discussion above, $\lambda(\rho_2,\rho_3) = \dfrac{((1-\beta)f^{\text{in}} + F_{\text{in}} - f^{\text{out}})f^{\max}}{(1-\beta)f^{\text{in}}f^{\max} + F_{\text{in}}f^{\max} - f^{\max} + (1-f^{\max})f^{\text{out}}}$ is given by the Rankine-Hugoniot jump condition. Notice that if the flux function is continuous and piecewise linear, the Rankine-Hugoniot condition can be used to calculate the speed of any front.

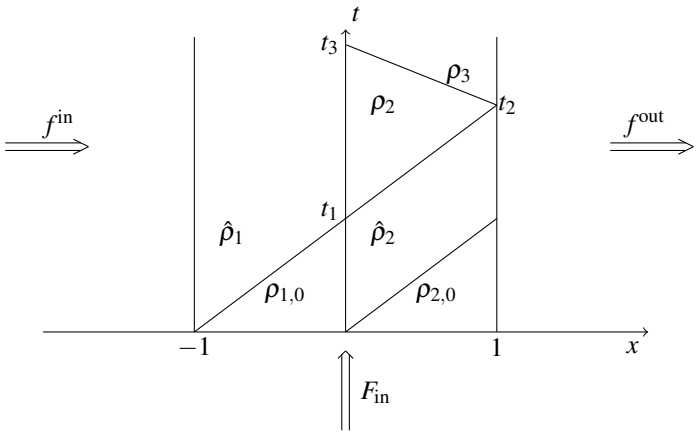

Fig. 3.14: Solution of the junction problem for $t \in [0, t_3]$

In the second case ($f^{\text{out}} < F_{\text{in}}$) at time t_1 the wave that interacts with the boundary $x = 1$ produces a wave with negative speed and the same density ρ_3 as above. This wave intersect the wave that comes out from the junction at time t_1 inside the region [0, 1] at point O generating an additional wave with negative speed.

Computing the coordinates of the intersection point O = (t_o, x_o) we get

$$t_o = \frac{\lambda(\hat{\rho}_2,\rho_3) - 2}{\lambda(\hat{\rho}_2,\rho_3) - 1} \quad \text{and} \quad x_o = \frac{1}{1-\lambda(\hat{\rho}_2,\rho_3)} \tag{3.24}$$

Now we can solve the following classical Riemann problem at O

$$\begin{aligned} &\partial_t \rho + \partial_x f(\rho) = 0 \\ &\rho(t,x) = \begin{cases} (1-\beta)f^{\text{in}} + F_{\text{in}} & \text{if } x < x_o, \\ \rho_3 & \text{if } x > x_o, \end{cases} \end{aligned} \tag{3.25}$$

where x_o is given by (3.24). Since $(1-\beta)f^{\text{in}} + F_{\text{in}} < \rho_{\text{c}} < \rho_3$, from the Rankine-Hugoniot condition we can compute the characteristic speed of the wave emanating from the point O

$$\lambda(\rho_2,\rho_3)=\frac{f^{\text{out}}-(1-\beta)f^{\text{in}}-F_{\text{in}}}{\rho_3-\bar{\rho}_2}=\frac{\Big(f^{\text{out}}-(1-\beta)f^{\text{in}}-F_{\text{in}}\Big)f^{\max}}{f^{\max}\Big(1+f^{\text{out}}-(1-\beta)f^{\text{in}}-F_{\text{in}}\Big)-f^{\text{out}}}<0. \tag{3.26}$$

The solution of the classical Riemann problem at O reads

$$\rho(t,x)=\begin{cases}(1-\beta)f^{\text{in}}+F_{\text{in}} & \text{if } x<\lambda(t-t_o)+x_o,\\ \rho_3 & \text{if } x>\lambda(t-t_o)+x_o,\end{cases} \tag{3.27}$$

where t_o and λ are respectively as in (3.24) and (3.26). The wave with speed λ reaches the junction at time $t_3=t_o-\dfrac{1}{\lambda(\rho_2,\rho_3)}$ as shown in Figure 3.15.

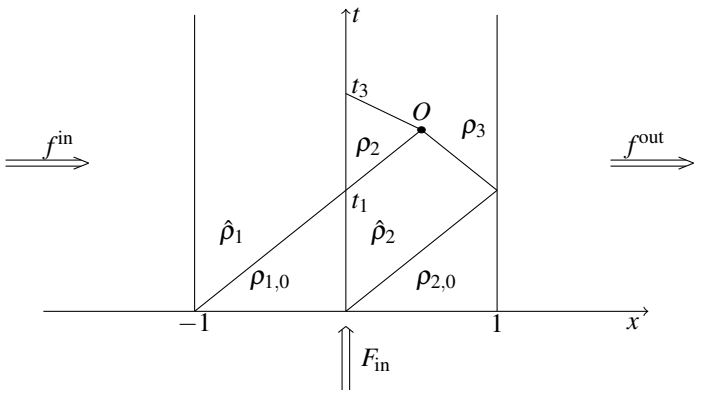

Fig. 3.15: Solution of the junction problem for $t\in[0,t_3]$ when the wave interact inside the region [0, 1].

This time we solve the following Riemann problem at the junction.

$$\begin{aligned} &d(F_{\text{in}},l)=F_{\text{in}},\\ &\delta(\hat{\rho}_1)=f^{\text{in}}, &(3.28)\\ &\sigma(\rho_3)=f^{\text{out}}. &(3.29)\end{aligned}$$

with

$$\rho(t_3,x)=\begin{cases}\hat{\rho}_1 \text{ if } x<0,\\ \rho_3 \text{ if } x>0.\end{cases} \tag{3.30}$$

In both cases at t_3

$$f^{\text{out}}\le(1-\beta)f^{\text{in}}+F_{\text{in}}.$$

Clearly, at time t_3 the junction problem is supply limited resulting in the following fluxes $\Gamma_2 = f^{\text{out}}$, $\Gamma_1 = \dfrac{\mathrm{p}}{1-\beta} f^{\text{out}}$ and $\Gamma_{\text{r1}} = (1-\mathrm{p}) f^{\text{out}}$. Moreover, let us introduce the following values

- $\mathrm{p}_1 = \dfrac{f^{\text{out}} - F_{\text{in}}}{f^{\text{out}}}$,
- $\mathrm{p}_2 = \dfrac{(1-\beta) f^{\text{in}}}{f^{\text{out}}}$.

Observe that

$$\mathrm{p}_2 - \mathrm{p}_1 = \frac{(1-\beta) f^{\text{in}}}{f^{\text{out}}} - \frac{f^{\text{out}} - F_{\text{in}}}{f^{\text{out}}} = \frac{(1-\beta) f^{\text{in}} + F_{\text{in}} - f^{\text{out}}}{f^{\text{out}}} \geq 0, \tag{3.31}$$

which implies $\mathrm{p}_1 \leq \mathrm{p}_2$, see Figure 3.16

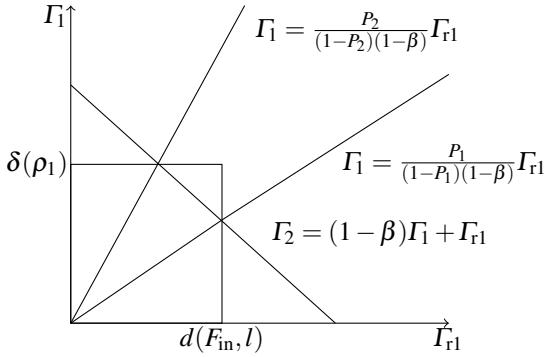

Fig. 3.16: Relationship between p_1 and p_2

The solutions of the Riemann problem at the junction are given by:

(1a) If $\max(0, \mathrm{p}_1) \leq \mathrm{p} \leq \min(\mathrm{p}_2, 1)$, then $\left(\dfrac{\mathrm{p}}{1-\beta} f^{\text{out}}, (1-\mathrm{p}) f^{\text{out}}, f^{\text{out}} \right)$ is the solution of the Riemann problem.

(2a) If $1 \geq \mathrm{p} > \min(\mathrm{p}_2, 1)$, then $\left(f^{\text{in}}, f^{\text{out}} - (1-\beta) f^{\text{in}}, f^{\text{out}} \right)$ is the solution.

(3a) If $0 \leq \mathrm{p} < \max(0, \mathrm{p}_1)$, then $\left(\dfrac{f^{\text{out}} - F_{\text{in}}}{1-\beta}, F_{\text{in}}, f^{\text{out}} \right)$ is the solution.

According to the different values of p, different cases can occur. For this reason, in the following we give detail computation of the solution case by case.

1. The case: $\max(0,\mathrm{p}_1) \leq \mathrm{p} \leq \min(\mathrm{p}_2,1)$

We solve the Riemann problem at t_3. The solution of the Riemann problem is given by (1a). From this it follows

$$\rho_1 = \frac{(1-\beta)f^{\max} - (1-f^{\max})\mathrm{p}f^{\mathrm{out}}}{(1-\beta)f^{\max}} \tag{3.32}$$

and the wave speed $\lambda(\hat{\rho}_1,\rho_1)$ is

$$\lambda(\hat{\rho}_1,\rho_1) = \frac{\left(f^{\mathrm{in}}(1-\beta) - \mathrm{p}f^{\mathrm{out}}\right)f^{\max}}{(1-\beta)(f^{\mathrm{in}}-1)f^{\max} + (1-f^{\max})\mathrm{p}f^{\mathrm{out}}} \tag{3.33}$$

The characteristic $x = \lambda(\hat{\rho}_1,\rho_1)(t-t_3)$ crosses the boundary $x=-1$ at

$$t_4 = t_3 - \frac{1}{\lambda(\hat{\rho}_1,\rho_1)} \tag{3.34}$$

On the outgoing road there is no new wave created since $\hat{\Gamma}_2 = f^{\mathrm{out}} = f(\rho_3)$ which can be seen in Figure 3.17.

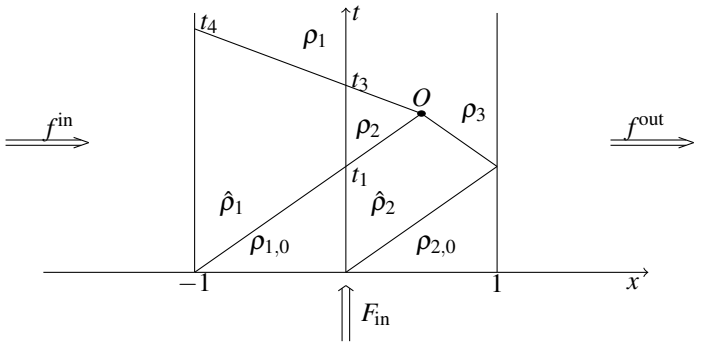

Fig. 3.17: Solution for $t \in [0,t_4]$.

The value of the flux from the buffer at this time is $\Gamma_{r1} = (1-\mathrm{p})f^{\mathrm{out}}$. Then we have

$$\dot{l} = F_{\mathrm{in}} - \Gamma_{r1} = F_{\mathrm{in}} - (1-\mathrm{p})f^{\mathrm{out}} > 0.$$

Solving the buffer length is given by

$$l(t) = (F_{\mathrm{in}} - (1-\mathrm{p})f^{\mathrm{out}})(t-t_3) > 0, \quad \text{for } t > t_3. \tag{3.35}$$

Clearly, the length of the buffer start increasing. The cases $F_{\text{in}} < f^{\text{out}}$ also treated exactly in the same way. Moreover, at t_4 there is no additional wave on the incoming road since $(1-\text{p})f^{\text{out}} < f^{\text{in}}$.

2. The case: $\min(\text{p}_2, 1) < \text{p} \leq 1$

In this case the solution of the Riemann problem is given by (2a). On the incoming main road there is no wave with negative speed exiting the junction. Similarly, on the outgoing main road there is no wave since $\hat{\Gamma}_2 = f^{\text{out}}$. The solution is shown in Figure 3.18. The buffer increases since $l(t) = (F_{\text{in}} + (1-\beta)f^{\text{in}} - f^{\text{out}})(t-t_3) > 0$.

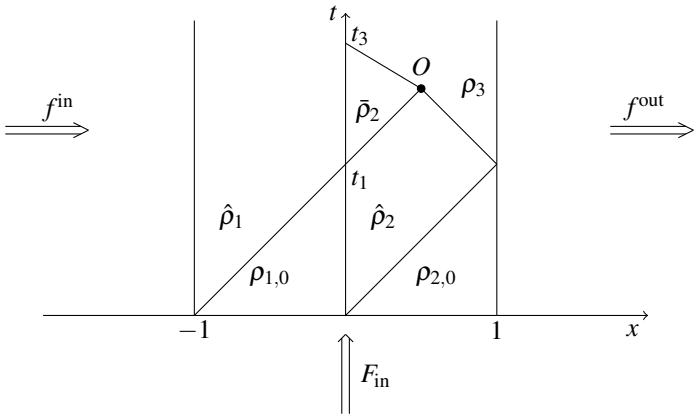

Fig. 3.18: Solution for $t \in [0, t_3]$ in the case $\min(\text{p}_2, 1) \leq \text{p} < 1$.

3. The Case: $0 \leq \text{p} < \max(0, \text{p}_1)$

The solution of the Riemann problem is given by (3a). This implies that $\dfrac{f^{\text{out}} - F_{\text{in}}}{1-\beta} = \dfrac{1-\check{\rho}_1}{1-\rho_{\text{c}}} f^{\max}$ which yields

$$\check{\rho}_1 = \frac{f^{\max}(1-\beta+f^{\text{out}}-F_{\text{in}}) + F_{\text{in}} - f^{\text{out}}}{(1-\beta)f^{\max}}. \tag{3.36}$$

Note that on the incoming main road of a roundabout $0 \leq \hat{\rho}_1 \leq \rho_{\text{c}}$ and hence $\rho_{\text{c}} \leq \check{\rho}_1 \leq 1$. The wave with characteristic speed

$$\lambda(\hat{\rho}_1, \check{\rho}_1) = \frac{f^{\text{in}} - \hat{\Gamma}_1}{\hat{\rho}_1 - \check{\rho}_1} = \frac{\Big((1-\beta)f^{\text{in}} + F_{\text{in}} - f^{\text{out}}\Big) f^{\max}}{(1-\beta)f^{\text{in}} f^{\max} - f^{\max}(1-\beta+f^{\text{out}}-F_{\text{in}}) + F_{\text{in}} - f^{\text{out}}} \tag{3.37}$$

emanating from the junction crosses the boundary $x = -1$ at time $t = t_4$ expressed as:

$$t_4 = t_3 - \frac{1}{\lambda(\hat{\rho}_1, \check{\rho}_1)} \tag{3.38}$$

Since $\dfrac{f^{\text{out}} - F_{\text{in}}}{1-\beta} < \delta(\hat{\rho}_1) = f^{\text{in}}$, there is no wave produced by the interaction with the boundary $x = -1$ at time t_4. Also, on the outgoing main lane there is no new wave. The complete solution at t_4 is depicted in Figure 3.19.

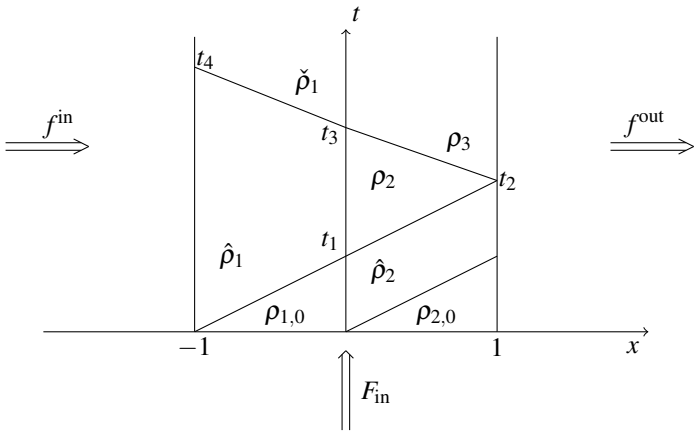

Fig. 3.19: Complete solution for $t \in [0, t_4]$.

From the value of $\hat{\Gamma}_{r1}$ we can solve the ODE (3.2) and find $l(t) = 0$. This concludes the analysis of this subsection.

In this subsection we presented the situation in which the junction is initially demand limited and gradually end up with supply constrained case. In the next subsections we focus only on the supply constrained cases.

B. Supply-limited case: $\Gamma_2 = \sigma(\hat{\rho}_2)$

Some times the amount of traffic demanding form the incoming road to access the junction may be greater than the capacity of the outgoing road from the junction. In this case we have

$$f^{\max} \leq (1-\beta) f^{\text{in}} + F_{\text{in}} \tag{3.39}$$

and hence, it is straightforward to compute the value of $\Gamma_2 = f^{\max}$, $\Gamma_1 = \dfrac{\mathrm{p}}{1-\beta} f^{\max}$ and $\Gamma_{\mathrm{r}1} = (1-\mathrm{p}) f^{\max}$.
Moreover, we introduce the following as in the previous case

- $\mathrm{p}_1 = \dfrac{f^{\max} - F_{\text{in}}}{f^{\max}}$,
- $\mathrm{p}_2 = \dfrac{(1-\beta) f^{\text{in}}}{f^{\max}}$.

Observe that also in this case it holds

$$\mathrm{p}_2 - \mathrm{p}_1 = \frac{(1-\beta) f^{\text{in}}}{f^{\max}} - \frac{f^{\max} - F_{\text{in}}}{f^{\max}} = \frac{(1-\beta) f^{\text{in}} + F_{\text{in}} - f^{\max}}{f^{\max}} \geq 0 \tag{3.40}$$

because of (3.39), which implies $\mathrm{p}_1 \leq \mathrm{p}_2$, see Figure 3.20. Then the solutions of the Riemann problem at the junction are given by

(1b) If $\mathrm{p}_1 \leq \mathrm{p} \leq \mathrm{p}_2$, then $\left(\dfrac{\mathrm{p}}{1-\beta} f^{\max}, (1-\mathrm{p}) f^{\max}, f^{\max} \right)$ is the solution of the Riemann problem.

(2b) If $\mathrm{p} \geq \mathrm{p}_2$, then $\left(f^{\text{in}}, f^{\max} - (1-\beta) f^{\text{in}}, f^{\max} \right)$ is the solution.

(3b) If $\mathrm{p} \leq \mathrm{p}_1$, then $\left(\dfrac{f^{\max} - F_{\text{in}}}{1-\beta}, F_{\text{in}}, f^{\max} \right)$ is the solution.

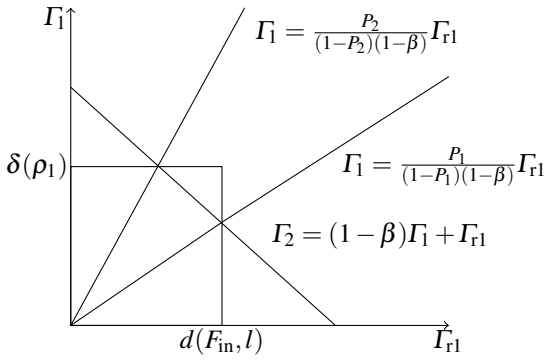

Fig. 3.20: Relationship between p_1 and p_2

In this case also, depending on the values of p different cases can occur. Exactly similar to the previous procedure we compute the solution at the junctions in detail.

1. The Case: $p_1 \leq p \leq p_2$

We solve now the Riemann problem at the junction at t_1. Since we assume that we are supply limited and that $p_1 \leq p \leq p_2$ it is straightforward to have the following fluxes at the junction: $\Gamma_1 = \frac{p}{1-\beta} f^{max}, \Gamma_{r1} = (1-p) f^{max}$ and $\Gamma_2 = f^{max}$. It follows that

$$\rho_1 = 1 - \frac{(1-f^{max})p}{1-\beta} \tag{3.41}$$

and that from Rankine- Hugoniot condition the wave speed λ is

$$\lambda(\hat{\rho}_1, \rho_1) = \frac{f^{in}(1-\beta) - p f^{max}}{(1-\beta)(f^{in}-1) + (1-f^{max})p} \tag{3.42}$$

The characteristic $x = \lambda(t-1)$ crosses the boundary $x = -1$ at

$$\begin{aligned} t_2 &= \frac{\lambda}{1-\lambda} = 1 - \frac{(1-\beta)(f^{in}-1) + (1-f^{max})p}{f^{in}(1-\beta) - p f^{max}} \\ &= \frac{1-\beta-p}{f^{in}(1-\beta) - p f^{max}} \end{aligned} \tag{3.43}$$

In the outgoing road $\rho_2 = \rho_c$ which produces a wave with positive speed 1 as can be seen in Figure 3.21

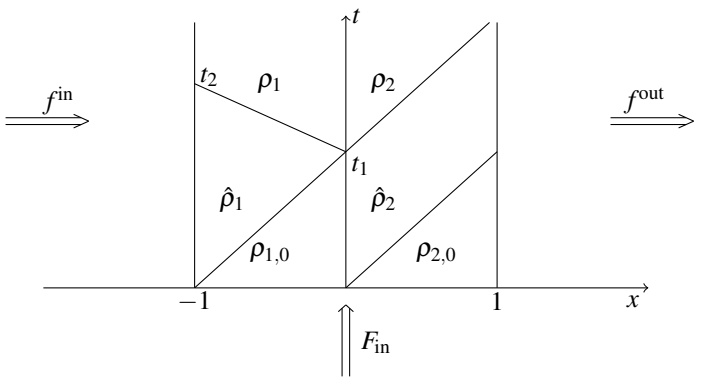

Fig. 3.21: Junction problem at t_1.

The value of the corresponding flux from the buffer is $\Gamma_{r1} = (1-p) f^{max}$. For all β and $p \in]0,1[$ we have $1-p < 1$, so the length of the buffer satisfies

$$\dot{l} = F_{in} - \Gamma_{r1} = F_{in} - (1-p) f^{max} > 0$$

Since $F_{\text{in}} > (1-\text{p})f^{\max}$ or $\text{p}f^{\max} > f^{\max} - F_{\text{in}}$ then $\text{p} > \dfrac{f^{\max} - F_{\text{in}}}{f^{\max}} = \text{p}_1$. Therefore,

$$l(t) = (F_{\text{in}} - (1-\text{p})f^{\max})(t-1) > 0. \tag{3.44}$$

That means, the length of the buffer increases linearly.

In this case, at time t_1 the interaction between the wave in the outgoing road and the boundary at $x = 1$ can generate an additional wave if $F_{\text{in}} > f^{\text{out}}$. When this is the case, in fact, there is a wave with negative speed which can interact with other waves between $[0,1]$. We make the following assumption:

$$F_{\text{in}} > f^{\text{out}}. \tag{3.45}$$

When (3.45) is satisfied there is a wave with negative speed created at $(t_1, 1)$. This new wave creates a density

$$\rho_3 = 1 - \frac{f^{\text{out}}(1-f^{\max})}{f^{\max}}, \tag{3.46}$$

and has a wave speed $\lambda(\hat{\rho}_2, \rho_3)$, given by

$$\lambda(\hat{\rho}_2, \rho_3) = \frac{F_{\text{in}} - f^{\text{out}}}{\hat{\rho}_2 - \rho_3} = \frac{F_{\text{in}} - f^{\text{out}}}{F_{\text{in}} - 1 + \frac{f^{\text{out}}(1-f^{\max})}{f^{\max}}} = \frac{f^{\max}(F_{\text{in}} - f^{\text{out}})}{(F_{\text{in}} - 1)f^{\max} + (1-f^{\max})f^{\text{out}}}. \tag{3.47}$$

This wave with equation $x = \lambda(t-1) + 1$ intersect the characteristic line $x = t - 1$ at a point S as in Figure 3.22.

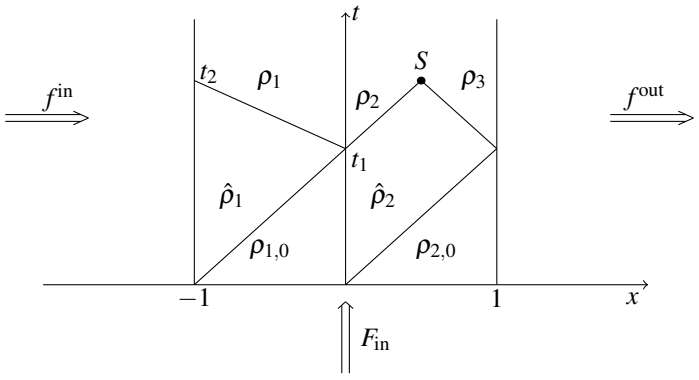

Fig. 3.22: Solution at t_1.

Solving the system we get the coordinates of the point $S = (t_S, x_S)$:

$$t_S = t_3 = \frac{\lambda - 2}{\lambda - 1} = \frac{f^{\max}(F_{\text{in}} - f^{\text{out}}) - 2((F_{\text{in}} - 1)f^{\max} + (1 - f^{\max})f^{\text{out}})}{f^{\max}(F_{\text{in}} - f^{\text{out}}) - ((F_{\text{in}} - 1)f^{\max} + (1 - f^{\max})f^{\text{out}})} = \\ = \frac{f^{\max}F_{\text{in}} - 2f^{\max} + 2f^{\text{out}} - f^{\max}f^{\text{out}}}{f^{\text{out}} - f^{\max}} \tag{3.48}$$

$$x_S = \frac{1}{1 - \lambda} = \frac{(F_{\text{in}} - 1)f^{\max} + (1 - f^{\max})f^{\text{out}}}{(F_{\text{in}} - 1)f^{\max} + (1 - f^{\max})f^{\text{out}} - f^{\max}(F_{\text{in}} - f^{\text{out}})} = \\ = \frac{f^{\max}f^{\text{out}} + f^{\max} - f^{\max}F_{\text{in}} - f^{\text{out}}}{f^{\max} - f^{\text{out}}}. \tag{3.49}$$

Once we have determined the coordinates of S, we can solve the classical Riemann problem at S:

$$\partial_t \rho + \partial_x f(\rho) = 0 \\ \rho(t,x) = \begin{cases} \rho_{\text{c}} \text{ if } x < x_S, \\ \rho_3 \text{ if } x > x_S, \end{cases} \tag{3.50}$$

where x_S is given by (3.49). Note that $\rho_{\text{c}} < \rho_3$, hence, from the Rankine-Hugoniot jump condition we can compute the characteristic speed of the wave emanating from the point S as:

$$\lambda(\rho_{\text{c}}, \rho_3) = \frac{f(\rho_3) - f(\rho_{\text{c}})}{\rho_3 - \rho_{\text{c}}} = \frac{f^{\max}}{f^{\max} - 1}. \tag{3.51}$$

The solution of the classical Riemann problem at S is, then

$$\rho(t,x) = \begin{cases} \rho_{\text{c}} \text{ if } x < \lambda(t - t_S) + x_S, \\ \rho_3 \text{ if } x > \lambda(t - t_S) + x_S, \end{cases} \tag{3.52}$$

where λ and t_S are respectively as in (3.51) and (3.48). The characteristic line with speed λ starting from S interacts with the junction at $x = 0$. This line intercepts the t-axis at

$$t_4 = t_S - \frac{1}{\lambda}x_S = t_S + \frac{1 - f^{\max}}{f^{\max}}x_S = \frac{(f^{\max})^2 - f^{\max}F_{\text{in}} + f^{\max} - f^{\text{out}}}{f^{\max}(f^{\max} - f^{\text{out}})}. \tag{3.53}$$

The situation at $t = t_4$ looks as in Figure 3.23

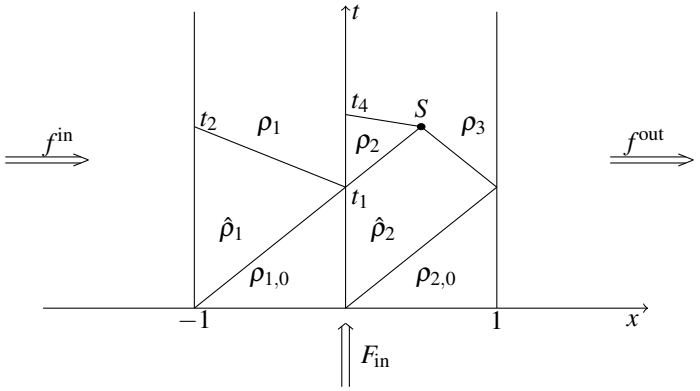

Fig. 3.23: Solution at time $t = t_4$.

We can then, solve at t_4 another Riemann problem at the junction:

$$\rho(t_4, x) = \begin{cases} \rho_1 \text{ if } x < 0, \\ \rho_3 \text{ if } x > 0. \end{cases} \tag{3.54}$$

To do so, we compute:

$$d(F_{\text{in}}, l) = \gamma_{\text{r1}}^{\max}, \tag{3.55}$$
$$\delta(\rho_1) = f^{\max}, \tag{3.56}$$
$$\sigma(\rho_3) = f^{\text{out}}. \tag{3.57}$$

In order to limit the complexity of the computation we fix $\gamma_{\text{r1}}^{\max} = f^{\max}$. Then it follows that $\Gamma_2 = \min((1-\beta)\delta(\rho_1) + d(F_{\text{in}}, l), \sigma(\rho_3)) = \min((1-\beta)f^{\max} + f^{\max}, f^{\text{out}}) = f^{\text{out}}$, $\hat{\Gamma}_1 = \dfrac{\text{p}}{1-\beta} f^{\text{out}}$ and $\hat{\Gamma}_{\text{r1}} = (1-\text{p}) f^{\text{out}}$. Since, by assumption, it holds that $f^{\text{out}} < f^{\max}$ the solution of the Riemann problem at the junction lies inside the feasible region as shown in Figure 3.24.

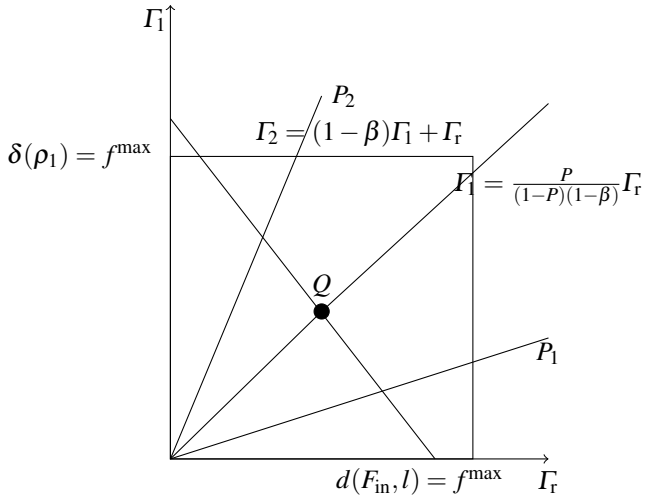

Fig. 3.24: Solution of the Riemann problem at the junction at t_4.

Since $\mathrm{p} \in [\mathrm{p}_1, \mathrm{p}_2]$, the solution of the Riemann problem at the junction is given by

$$(\hat{\Gamma}_1, \hat{\Gamma}_{\mathrm{r}1}, \hat{\Gamma}_2) = \left(\frac{\mathrm{p}}{1-\beta} f^{\mathrm{out}}, (1-\mathrm{p}) f^{\mathrm{out}}, f^{\mathrm{out}} \right)$$

From this we can uniquely recover the corresponding values of the queue length and of the densities of the mainline. Since the flux exiting the secondary road is $\hat{\Gamma}_{\mathrm{r}1} = (1-\mathrm{p}) f^{\mathrm{out}}$ then the queue length is

$$l(t) = l(t_4) + \left(F_{\mathrm{in}} - (1-\mathrm{p}) f^{\mathrm{out}} \right) (t - t_4) > 0. \tag{3.58}$$

Thus, the length of the buffer increases linearly.
On the outgoing mainline there is no new wave created since $\hat{\Gamma}_2 = f^{\mathrm{out}} = f(\rho_3)$. And on the incoming mainline we have $\hat{\Gamma}_1 = \frac{\mathrm{p}}{1-\beta} f^{\mathrm{out}} \Rightarrow \frac{\mathrm{p}}{1-\beta} f^{\mathrm{out}} = \frac{1-\check{\rho}_1}{1-\rho_{\mathrm{c}}} f^{\max}$ which gives

$$\check{\rho}_1 = 1 - \frac{(1-f^{\max})\mathrm{p} f^{\mathrm{out}}}{(1-\beta) f^{\max}}. \tag{3.59}$$

On the incoming main road of a roundabout $\rho_{\mathrm{c}} \leq \rho_1 \leq 1$ so $\rho_{\mathrm{c}} \leq \check{\rho}_1 \leq 1$, and the pair $(\rho_1, \check{\rho}_1)$ produces a wave with negative speed on the incoming road of the roundabout, with the speed given by $\lambda(\rho_1, \check{\rho}_1) = \frac{f^{\max}}{f^{\max} - 1}$. This characteristic line crosses the left boundary $x = -1$ at a time $t = t_5$ given by

$$t_5 = t_4 - \frac{1}{\lambda} = t_S + \frac{1-f^{\max}}{f^{\max}} (x_S + 1) = \frac{f^{\max} F_{\mathrm{in}} - f^{\max} f^{\mathrm{out}} - 2 f^{\max} + 2 f^{\mathrm{out}}}{f^{\max}(f^{\mathrm{out}} - f^{\max})}. \tag{3.60}$$

Moreover, since $\frac{\mathrm{p}}{1-\beta} f^{\text{out}} < f^{\text{in}}$, there is no wave produced by the interaction with the boundary $x = -1$ at time t_5. The solution at t_5 looks like as in Figure 3.25

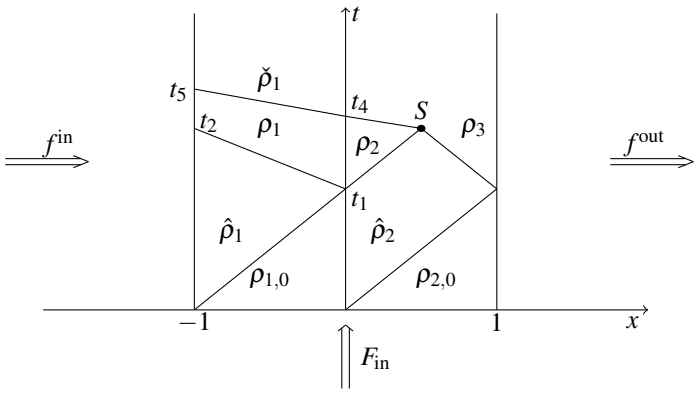

Fig. 3.25: Solution of the problem in $[0, t_5]$

In this case, depending on the priority parameter p, the waves emanating from the junction at t_1 and t_4 can collide within the region $-1 < x < 0$. This, in particular, occurs for the value of the priority parameter $\mathrm{p} = \bar{\mathrm{p}}$, given by

$$\bar{\mathrm{p}} = \frac{(1-\beta)\Big((f^{\max})^2 + f^{\max}(2f^{\text{in}} - f^{\text{out}} - f^{\text{in}}F_{\text{in}} + f^{\text{out}}f^{\text{in}}) + 2f^{\text{out}}f^{\text{in}}\Big)}{f^{\max}(F_{\text{in}}f^{\max} - f^{\max} + f^{\text{out}} - f^{\text{out}}f^{\max})} \tag{3.61}$$

where $\bar{\mathrm{p}}$ is the value at which the waves interact in the region [-1, 0]. We can, then, distinguish two additional cases $\mathrm{p}_1 \leq \mathrm{p} < \bar{\mathrm{p}}$ and $\bar{\mathrm{p}} \leq \mathrm{p} \leq \mathrm{p}_2$.

1. $\mathrm{p}_1 \leq \mathrm{p} < \bar{\mathrm{p}}$. In this case, the waves do not interact in the region $-1 < x < 0$ and no new waves are created. Hence, the study is concluded and the solution is depicted in Figure 3.25.
2. $\bar{\mathrm{p}} \leq \mathrm{p} \leq \mathrm{p}_2$. In this case there is a collision between the waves emanating from the junction at t_1 and t_4 on the incoming link and the final solution is shown in Figure 3.27.

   As described above, the pair $(\rho_1, \check{\rho}_1)$ produces a wave with negative speed $\lambda = \frac{f^{\max}}{f^{\max} - 1}$ on the incoming main road of the roundabout. This wave interacts with the wave exiting from $(t_1, 0)$ at point Q as in Figure 3.26

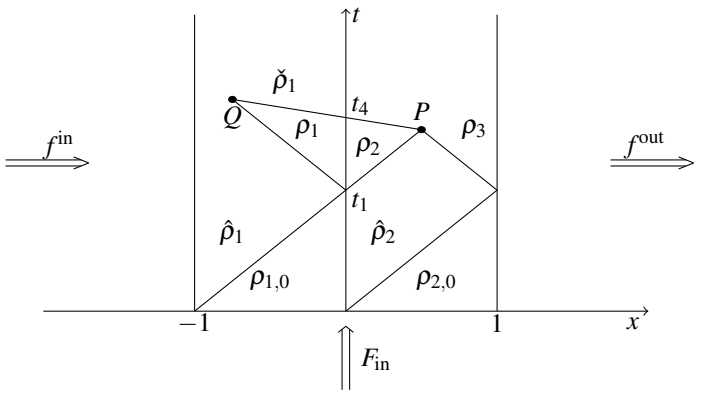

Fig. 3.26: Solution in the case $\bar{\mathrm{p}} \leq \mathrm{p} < \mathrm{p}_2$.

The coordinates of the point Q are then

$$t_Q = \frac{(f^{\max}-1)\Big((1-\beta)f^{\text{in}} - \mathrm{p}f^{\max}\Big) + t_4 f^{\max}\Big((1-\beta)(1-f^{\text{in}}) + \mathrm{p}(1-f^{\max})\Big)}{(1-\beta)(f^{\max}-f^{\text{in}})} \tag{3.62}$$

and

$$x_Q = \frac{f^{\max}}{f^{\max}-1}(t_Q - t_4) \tag{3.63}$$

Once we have determined the coordinates of point Q, we can solve the classical Riemann problem at Q

$$\partial_t \rho + \partial_x f(\rho) = 0 \tag{3.64}$$

$$\rho(t,x) = \begin{cases} \hat{\rho}_1 \text{ if } x < x_Q, \\ \check{\rho}_1 \text{ if } x > x_Q, \end{cases} \tag{3.65}$$

where Q is given by (3.63). By Rankine-Hugoniot jump condition we can derive

$$\begin{aligned} \lambda(\hat{\rho}_1, \check{\rho}_1) = \frac{f(\hat{\rho}_1) - f(\check{\rho}_1)}{\hat{\rho}_1 - \check{\rho}_1} = \frac{f^{\text{in}} - \hat{\Gamma}_1}{\hat{\rho}_1 - \check{\rho}_1} = \frac{f^{\text{in}} - \dfrac{\mathrm{p}}{1-\beta} f^{\text{out}}}{f^{\text{in}} - \left(1 - \frac{(1-f^{\max})\mathrm{p}f^{\text{out}}}{(1-\beta)f^{\max}}\right)} = \\ = \frac{\left(f^{\text{in}}(1-\beta) - \mathrm{p}f^{\text{out}}\right) f^{\max}}{(1-\beta)f^{\max}(f^{\text{in}}-1) - (1-f^{\max})\mathrm{p}f^{\text{out}}} \end{aligned} \tag{3.66}$$

where λ is the characteristic speed of the wave emanating from the intersection point Q. The solution of the classical Riemann problem at Q is

$$\rho(t,x) = \begin{cases} \hat{\rho}_1 \text{ if } x < \lambda(t-t_Q)+x_Q, \\ \check{\rho}_1 \text{ if } x > \lambda(t-t_Q)+x_Q, \end{cases} \tag{3.67}$$

where λ and t_Q are respectively as in (3.66) and (3.62). The wave with speed λ starting from Q crosses the left boundary $x = -1$ at

$$t_5 = t_Q - \frac{1+x_Q}{\lambda} \tag{3.68}$$

The complete solution can be seen in Figure 3.27

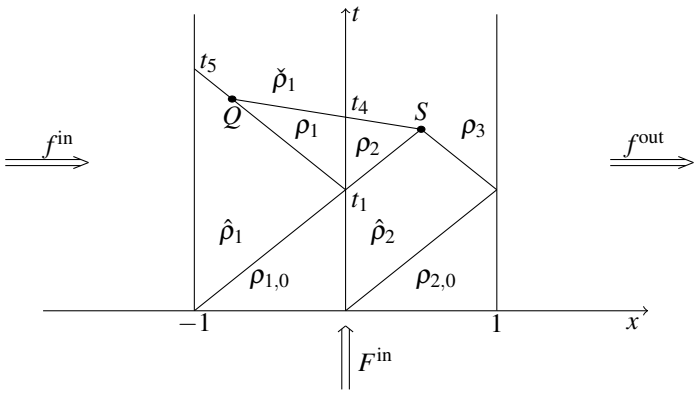

Fig. 3.27: Solution for $t \in [0, t_5]$ with $\bar{\mathrm{p}} \leq \mathrm{p} \leq \mathrm{p}_2$.

For all cases for $t \geq t_4$ the buffer length increases linearly with a value

$$l(t) = l(t_4) + \left(F_{\text{in}} - (1-\mathrm{p}) f^{\text{out}}\right)(t-t_4) > 0. \tag{3.69}$$

This concludes the analysis of the case $\mathrm{p}_1 \leq \mathrm{p} \leq \mathrm{p}_2$.

2. The Case: $\mathrm{p} > \mathrm{P}_2$

In this situation the priority rule is not respected due to limited traffic demand entering the junction from the main road of the roundabout. The solution of the Riemann problem is given by (2b). In this case, $\rho_1 = \hat{\rho}_1$ and no wave is created in the incoming main lane. On the outgoing link we have $\rho_2 = \rho_{\mathrm{c}}$, which generates a wave with speed equal to 1. The buffer length increases since $l(t) = (F_{\text{in}} + (1-\beta) f^{\text{in}} - f^{\max})(t-1) > 0$. The wave with positive speed $v_f = 1$ generated at $(t_1, 0)$ interacts with the wave generated from right boundary at point $S = (t_S, x_S)$ at time $t = t_S$ under assumption (3.45), see Figure 3.28. At the right boundary $f^{out} = \dfrac{1-\rho_3}{1-f^{max}} f^{max}$, hence we obtain that

$$\rho_3 = 1 - \frac{f^{\text{out}}(1-f^{\max})}{f^{\max}}. \tag{3.70}$$

Up to time t_4 the analysis is exactly the same as in the previous case. We will solve directly the Riemann problem at t_4 with the new assumption.

Again we solve the Riemann problem at the junction having density

$$\rho(t_4,x) = \begin{cases} \hat{\rho}_1 \text{ if } x < 0, \\ \rho_3 \text{ if } x > 0, \end{cases}$$

coupled with the following demand and supply functions

$$d(F_{\text{in}}, l) = \gamma_{\text{r1}}^{\max} = f^{\max}, \tag{3.71}$$

$$\delta(\hat{\rho}_1) = f^{\text{in}}, \tag{3.72}$$

$$\sigma(\rho_3) = f^{\text{out}}. \tag{3.73}$$

We can now compute

$$\Gamma_2 = \min\Big((1-\beta)\delta(\hat{\rho}_1) + d(F_{\text{in}}, l), \sigma(\rho_3)\Big) = \min\Big((1-\beta)f^{\text{in}} + f^{\max}, f^{\text{out}}\Big) = f^{\text{out}}$$

and

$$\hat{\Gamma}_1 = \frac{\mathrm{p}}{1-\beta} f^{\text{out}}.$$

Two cases can occur at this point. If $(1-\beta)f^{\text{in}} < f^{\text{out}}$ the solution of the Riemann problem at the junction is given by $(\hat{\Gamma}_1, \hat{\Gamma}_{\text{r1}}, \hat{\Gamma}_2) = (f^{\text{in}}, f^{\text{out}} - (1-\beta)f^{\text{in}}, f^{\text{out}})$ for all values of $\mathrm{p} > \bar{\mathrm{p}} = (1-\beta)\dfrac{f^{\text{in}}}{f^{\text{out}}}$. From this it is straightforward to see that $\hat{\rho}_1 = \rho_1$ since $f^{\text{in}} = \hat{\rho}_1$ for $v_{\text{f}} = 1$. No new waves are created.

For $\mathrm{p}_2 < \mathrm{p} < \bar{\mathrm{p}}$ we have $(\hat{\Gamma}_1, \hat{\Gamma}_{\text{r1}}, \hat{\Gamma}_2) = \left(\dfrac{\mathrm{p}}{1-\beta} f^{\text{out}}, (1-\mathrm{p})f^{\text{out}}, f^{\text{out}}\right)$. The solution of the problem in this case is similar to the case $(1-\beta)f^{\text{in}} > f^{\text{out}}$ hence, we obtain its description in the following. If $(1-\beta)f^{\text{in}} > f^{\text{out}}$ the solution of the Riemann problem at the junction becomes

$$(\hat{\Gamma}_1, \hat{\Gamma}_{\text{r1}}, \hat{\Gamma}_2) = \left(\frac{\mathrm{p}}{1-\beta} f^{\text{out}}, (1-\mathrm{p})f^{\text{out}}, f^{\text{out}}\right).$$

From this we can uniquely recover the corresponding values of the densities. The solution looks as in Figure 3.28.

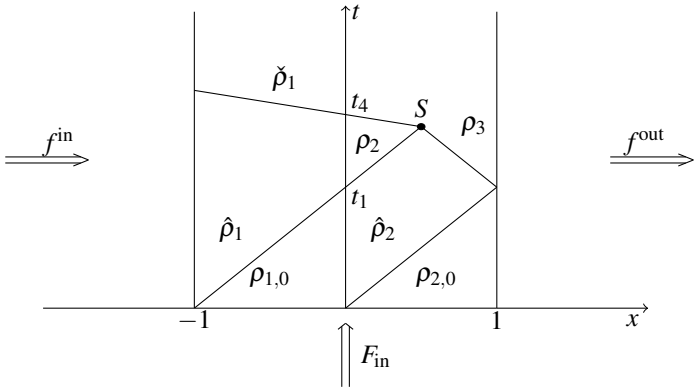

Fig. 3.28: Solution in the case $\mathrm{p} \geq \mathrm{p}_2$

Solving the ODE we observe that the buffer increases linearly and its expression is given by

$$l(t) = l(t_4) + \left(F_{\text{in}} - (1-\mathrm{p}) f^{\text{out}}\right)(t - t_4) > 0. \tag{3.74}$$

This completes the analysis for this case.

3. The case: $0 \leq \mathrm{p} \leq \mathrm{p}_1$

By similar argument as in the previous case the priority rule is not respected due to limited traffic demand entering the junction from entrance road of the roundabout. The solution of the Riemann problem is given by (3b). In this case, the computations are similar to those of Section 3.3.1. The solution is sketched in Figure 3.29. To be noted here that the point of intersection N in this case does not depend on the value of p but on the value of the other parameters.

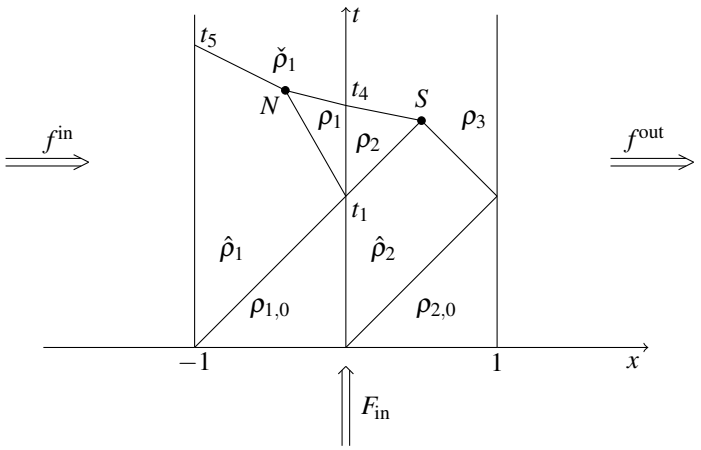

Fig. 3.29: Solution in the case $\mathrm{p} \leq \mathrm{p}_1$

Finally, we compute the queue length at t_4 which is given by

$$l(t) = l(t_4) + \left(F_{\text{in}} - (1-\mathrm{p}) f^{\text{out}}\right)(t - t_4) > 0. \tag{3.75}$$

With this, we conclude our discussion of solving the Riemann problem using wave front tracking method. After this time step, there is no wave junction interaction. Note that what we calculated in the above cases are not an approximation to the entropy weak solution but the exact solution. In the next section we shall extend the construction of the Riemann problem to a roundabout with arbitrary m entrances and m exiting roads. We also, note that the generalization of the study to a roundabout with an arbitrary number of roads being straightforward.

3.3.2 For Roundabout with Arbitrary m Entrances and m Exits

In this section, we extend the construction of the Riemann solver at each junctions of a roundabout with arbitrary m entrances and m exiting roads. In this case, we do not apply wave front tracking as in the previous section. Instead we formulate the problem in discrete form. The procedure is exactly similar to the previous case except the usage of indexes for later use. To recall, we define the Riemann Solver at junction by means of a Riemann Solver $\mathscr{RS}_l : [0,1]^2 \to [0,1]^2$, which depends on the instantaneous load of the buffer $l(t)$. For each l, the Riemann Solver $\mathscr{RS}_l(\rho_i, \rho_{i+1}) = (\hat{\rho}_i, \hat{\rho}_{i+1})$ is constructed in the following way. For each $i = 1, \ldots, m$, we fix the priority parameter $p_i \in (0,1)$ and proceed as follows.

1. Define $\Gamma_i = f(\rho_i(t,x_i-))$, $\Gamma_{i+1} = f(\rho_{i+1}(t,x_i+))$, $\Gamma_{r_i} = \gamma_{r_i}(t)$;
2. Consider the space (Γ_i, Γ_{r_i}) and the sets $\mathscr{O}_i = [0, \delta(\rho_i)]$, $\mathscr{O}_{r_i} = [0, d(F_i^{\text{in}}, l)]$;
3. Trace the lines $(1-\beta_i)\Gamma_i + \Gamma_{r_i} = \Gamma_{i+1}$; and $\Gamma_i = \dfrac{p_i}{(1-p_i)(1-\beta_i)}\Gamma_{r_i}$;
4. Consider the region

$$\Omega_i = \Big\{(\Gamma_i, \Gamma_{r_i}) \in \mathscr{O}_i \times \mathscr{O}_{r_i} : (1-\beta_i)\Gamma_i + \Gamma_{r_i} \in [0, \Gamma_{i+1}]\Big\}. \tag{3.76}$$

Similar to the discussion in the previous section different situations can occur depending on the values of Γ_{i+1}. That is, it can be either demand or supply-limited.

Demand-limited case: $\Gamma_{i+1}=(1-\beta_i)\delta(\rho_i) + d(F_i^{\text{in}}, l)$

In the demand limited case the solution of the Riemann problem at each junction can be calculated as $\hat{\Gamma}_i = \delta(\rho_i)$, $\hat{\Gamma}_{r_i} = d(F_i^{\text{in}}, l)$ and $\hat{\Gamma}_{i+1} = (1-\beta_i)\delta(\rho_i) + d(F_i^{\text{in}}, l)$, as illustrated in Figure 3.7(a).

Supply-limited case: $\Gamma_{i+1} = \sigma(\rho_{i+1})$

At each junction we solve the linear equation $(1-\beta_i)\Gamma_i + \Gamma_{r_i} = \Gamma_{i+1}$ and $\Gamma_i = \dfrac{p_i}{(1-p_i)(1-\beta_i)}\Gamma_{r_i}$ and denote the intersection point by Q. If $Q \in \Omega_i$, we set $(\hat{\Gamma}_i, \hat{\Gamma}_{r_i}) = Q$ and $\hat{\Gamma}_{i+1} = \Gamma_{i+1}$, see Figure 3.7(c); if $Q \notin \Omega_i$, we set $(\hat{\Gamma}_i, \hat{\Gamma}_{r_i})$=$S$ and $\hat{\Gamma}_{i+1} = \Gamma_{i+1}$, where S is the point of the segment $\Omega_i \cap (\Gamma_i, \Gamma_{r_i}) : (1-\beta_i)\Gamma_i + \Gamma_{r_i} = \Gamma_{i+1}$ closest to the line $\Gamma_i = \dfrac{p_i}{(1-p_i)(1-\beta_i)}\Gamma_{r_i}$ see Figure 3.7(c).

We can extend Theorem 3.1 to a junction of a roundabout with arbitrary m entrances and m existing roads as follow.

Theorem 3.2. *Consider a junction J_i and fix a priority parameter $p_i \in]0,1[$. For every $\rho_i^0, \rho_{i+1}^0 \in [0,1]$ and $l_i^0 \in [0, +\infty[$ there exists a unique admissible solution $(\rho_i(t,x), \rho_{i+1}(t,x), l_i(t))$ in the sense of Definition 3.5, compatible with the Riemann Solver proposed in subsection 3.3.2. Moreover, there exists a unique couple $(\hat{\rho}_i, \hat{\rho}_{i+1}) \in [0,1]^2$ such that*

$$\hat{\rho}_i \in \begin{cases} \{\rho_i^0\} \cup]\tau(\rho_i^0), 1] & \text{if } 0 \le \rho_i^0 \le \rho_c, \\ [\rho_c, 1] & \text{if } \rho_c \le \rho_i^0 \le 1, \end{cases} \qquad f(\hat{\rho}_i) = \hat{\Gamma}_i, \tag{3.77}$$

and

$$\hat{\rho}_{i+1} \in \begin{cases} [0,\rho_c] & \text{if } 0 \le \rho^0_{i+1} \le \rho_c, \\ \{\rho^0_{i+1}\} \cup [0,\tau(\rho^0_{i+1})[& \text{if } \rho_c \le \rho^0_{i+1} \le 1, \end{cases} \qquad f(\hat{\rho}_{i+1}) = \hat{\Gamma}_{i+1}. \tag{3.78}$$

For the incoming road the solution is given by the wave $(\rho^0_i, \hat{\rho}_i)$*, while for the outgoing road the solution is given by the wave* $(\hat{\rho}_{i+1}, \rho^0_{i+1})$*. Furthermore, for almost every* $t > 0$*, it holds*

$$(\rho_i(t,x_i-), \rho_{i+1}(t,x_i+)) = \mathscr{RS}_{l_i(t)}(\rho_i(t,x_i-), \rho_{i+1}(t,x_i+)).$$

The proof is exactly similar except considering every case per each junction.

A. Demand-limited case at junction J_i: $(1-\beta_i)\delta(\rho^n_i) + d(F^{\text{in}}_i, l^n_i) \le \sigma(\rho^n_{i+1})$

When the situation becomes demand-limited we set $\hat{\Gamma}_i = \delta(\rho_{i-1})$ and $\gamma_{r_i} = d(F^{\text{in}}_i, l_i)$. From this it is evident that those who demand to enter the junction can access it without restriction. Hence,

$$F^{n,+}_i = (1-\beta)\delta(\rho^n_i) + d(F^{\text{in}}_i, l^n_i) \tag{3.79}$$

and at the instant time t^n, the flux at the left side of the junction reads as

$$F^{n,-}_i = \delta(\rho^n_i). \tag{3.80}$$

where

$$\begin{array}{l} F^{n,-}_i = F^{n,-}_i\left(\rho^n_i, \rho^n_{i+1}, p_i, l_i, F^{\text{in}}_i\right) \\ F^{n,+}_{i-1} = F^{n,+}_{i-1}\left(\rho^n_{i-1}, \rho^n_i, p_{i-1}, l_{i-1}, F^{\text{in}}_{i-1}\right), \end{array} \qquad i = 1,2,\ldots,m. \tag{3.81}$$

The fluxes $F^{n,+}_{i-1}$ and $F^{n,-}_i$ stand respectively for inflow $\hat{\Gamma}_i$ and outflow $\hat{\Gamma}_{i+1}$ at junctions J_{i-1} and J_i on the main road of the roundabout.

Besides, the dynamics of the buffer length at the entrance of the roundabout at junction J_i is governed by

$$\frac{d}{dt}\, l^n_i(t) = F^{\text{in}}_i - d(F^{\text{in}}_i, l^n_i),$$

which gives after integration:

$$l^{n+1}_i = l^n_i + \left(F^{\text{in}}_i - d(F^{\text{in}}_i, l^n_i)\right)\Delta t. \tag{3.82}$$

B. Supply-limited case at Junction J_i: $(1-\beta_i)\delta(\rho^n_i) + d(F^{\text{in}}_i, l^n_i) > \sigma(\rho^n_{i+1})$

We calculate the flux at the right hand side of the junction as

$$F^{n,+}_i = \sigma(\rho^n_{i+1}), \tag{3.83}$$

while on the left side it becomes

$$F_i^{n,-} = \begin{cases} \delta(\rho_i^n) & \text{if } 1 \geq p_i > \min\{1, P_2^i\}, \\ \dfrac{p_i}{1-\beta_i}\sigma(\rho_{i+1}^n) & \text{if } \max\{0, P_1^i\} \leq p_i \leq \min\{1, P_2^i\}, \\ \dfrac{\sigma(\rho_{i+1}^n) - d(F_i^{\text{in}}, l_i^n)}{1-\beta_i} & \text{if } 0 \leq p_i < \max\{0, P_1^i\}, \end{cases} \tag{3.84}$$

where

$$P_1^i = \frac{\sigma(\rho_{i+1}^n) - d\left(F_i^{\text{in}}, l_i^n\right)}{\sigma(\rho_{i+1}^n)} \quad \text{and} \quad P_2^i = \frac{(1-\beta_i)\delta(\rho_i^n)}{\sigma(\rho_{i+1}^n)}. \tag{3.85}$$

As in the demand-limited case the dynamics of the corresponding buffer length is governed by

$$\frac{d}{dt} l_i^n = \begin{cases} F_i^{\text{in}} - (\sigma(\rho_i^n) - (1-\beta_i)\delta(\rho_i^n)) & \text{if } 1 \geq p_i > \min\{1, P_2^i\}, \\ F_i^{\text{in}} - (1-p_i)\sigma(\rho_{i+1}^n) & \text{if } \max\{0, P_1^i\} \leq p_i \leq \min\{1, P_2^i\}, \\ F_i^{\text{in}} - d(F_i^{\text{in}}, l_i^n) & \text{if } 0 \leq p_i < \max\{0, P_1^i\}, \end{cases}$$

which yields after integration:

$$l_i^{n+1} = \begin{cases} l_i^n + \left(F_i^{\text{in}} - \left(\sigma(\rho_{i+1}^n) - (1-\beta_i)\delta(\rho_i^n)\right)\right)\Delta t & \text{if } 1 \geq p_i > \min\{1, P_2^i\}, \\ l_i^n + \left(F_i^{\text{in}} - (1-p_i)\sigma(\rho_{i+1}^n)\right)\Delta t & \text{if } \max\{0, P_1^i\} \leq p_i \leq \min\{1, P_2^i\}, \\ l_i^n + \left(F_i^{\text{in}} - d(F_i^{\text{in}}, l_i^n)\right)\Delta t & \text{if } 0 \leq p_i < \max\{0, P_1^i\}. \end{cases} \tag{3.86}$$

In the next section we will briefly present numerical scheme used in this chapter.

3.4 Numerical Scheme

In this section we consider the traffic regulation problem for a network as the one in Figure 3.1 and Figure 3.5. Then we treat the numerical scheme used to study the evolution of traffic in both cases in the sequel.

Network Topology for Roundabout with 3 Entrances and 3 Exits

The roundabout can be modelled by

- 4 roads from the roundabout: $\mathscr{I}_1, \mathscr{I}_2, \mathscr{I}_3, \mathscr{I}_4$ with $\mathscr{I}_1$ and $\mathscr{I}_4$ linked with periodic boundary conditions;
- 3 roads connecting the roundabout with the rest of the network: 3 incoming lanes and 3 outgoing ones.

From the topology, it can be noted that all the junctions in the roundabout can be represented by 2x2 junctions for which it might be necessary to define a right of way parameter p.

3.4.1 Godunov Scheme

The Godunov scheme as introduced in [46] is based on exact solutions to Riemann problems. The main idea of this method is to approximate the initial datum by a piecewise constant function, then the corresponding Riemann problems are solved exactly and a global solution is simply obtained by lamenting them together. Finally, one takes the mean on the cell and proceeds by induction.

In the process of numerical investigation, the first step is to discretize the junction model. To this aim, we define a numerical grid in $(0,T)\times\mathbb{R}$ using the following notation.

- Δx is the fixed space grid size;
- Δt^n is the grid size, given by the CFL condition;
- $(t^n, x_j) = (t^{n-1} + \Delta t^n, j\Delta x)$ for $n \in \mathbb{N}$ and $j \in \mathbb{Z}$ are the grid points.

Each road is divided in N + 1 cells numbered from 0 to N. Under the CFL condition

$$\Delta t^n \max_{j\in\mathbb{Z}} \left|\lambda^n_{j+\frac{1}{2}}\right| \leq \frac{1}{2}\Delta x, \tag{3.87}$$

the waves generated by different Riemann problems do not interact. In the above inequality, $\lambda^n_{j+\frac{1}{2}}$ is the wave speed of the Riemann problem solution at the interface $x_{j+\frac{1}{2}}$ at time t^n. Under condition (3.87) the scheme can be written as

$$\rho^{n+1}_j = \rho^n_j - \frac{\Delta t^n}{\Delta x}(g(\rho^n_j, \rho^n_{j+1}) - g(\rho^n_{j-1}, \rho^n_j)), \tag{3.88}$$

where the numerical flux g takes in general the following expression:

$$g(u,v) = \begin{cases} \min_{z\in[u,v]} f(z) \text{ if } u \leq v, \\ \max_{z\in[v,u]} f(z) \text{ if } v \leq u. \end{cases} \tag{3.89}$$

Conditions at the Junction.

For the incoming main lane, that is connected at the junction at the right endpoint, we set

$$\rho_N^{n+1} = \rho_N^n - \frac{\Delta t^n}{\Delta x}(\hat{\Gamma}_1 - g(\rho_{N-1}^n, \rho_N^n)),$$

while for the outgoing one, connected at the junction at the left endpoint, we have

$$\rho_0^{n+1} = \rho_0^n - \frac{\Delta t^n}{\Delta x}(g(\rho_0^n, \rho_1^n) - \hat{\Gamma}_2),$$

where $\hat{\Gamma}_1$ and $\hat{\Gamma}_2$ are the maximized fluxes computed in Section 3.3.

ODE Treatment

Let us consider now the buffer modelled by the ODE (3.2). At each time step $t^n = t^{n-1} + \Delta t^n$ we compute the new value of the queue length with explicit Euler first order integration:

1. If $F_{\text{in}}(t^n) < \hat{\Gamma}_{\text{r1}}$

$$l^{n+1} = \begin{cases} l^n + (F_{\text{in}}(t^n) - \hat{\Gamma}_{\text{r1}})\Delta t^n & \text{for } t^{n+1} < \bar{t}, \\ 0 & \text{otherwise .} \end{cases}$$

2. If $F_{\text{in}}(t^n) \geq \hat{\Gamma}_{\text{r1}}$

$$l^{n+1} = l^n + (F_{\text{in}}(t^n) - \hat{\Gamma}_{\text{r1}})\Delta t^n.$$

For more details on the numerical scheme for the junction model we refer the reader to [25].

Network Topology for Roundabout with m Entrances and m Exits

In this subsection we can describe the topology of the roundabout under consideration (see Figure 3.5) in the following way.

- m + 1 roads forming the roundabout: $I_1, I_2, I_3, \ldots, I_{\text{m}+1}$, with I_1 and $I_{\text{m}+1}$ linked with periodic boundary conditions;
- m roads connecting the roundabout with the rest of the road network: m incoming and m outgoing lanes.

To compute approximate solutions, we adapt the classical Godunov scheme to our problem with some adjustment due to the presence of buffers on the entrance roads of the roundabout. We use the following notation to define a numerical grid in $(0,T)\times[x_0,x_m]$.

- x_i, $i=0,\dots,m$, are the cell interfaces;
- $L_i = x_i - x_{i-1}$ represents the length of each segment of the roundabout and Δt is the time step, to be defined according to the CLF stability condition below;
- $t^n = t^{n-1} + \Delta t$, $n \in \mathbb{N}$ are the time grid points.

3.4.2 Adapted Godunov Scheme at Junctions

In this subsection we consider the distance between two adjacent junctions of a roundabout as the fixed space grid size of the Godunov discretization and junctions as cell interfaces. This is because each link of the roundabout is reasonably short to fit the scheme discretization. In this setting, on the main road of the roundabout we set

$$\rho_i^{n+1} = \rho_i^n - \frac{\Delta t}{L_i}\left(F_i^{n,-} - F_{i-1}^{n,+}\right), \quad i = 1,2,\dots,m, \tag{3.90}$$

Under the Courant-Friedrichs-Lewy (CFL) condition [52]

$$\Delta t \leq \frac{\min_i L_i}{\lambda^{\max}} \tag{3.91}$$

where $\lambda^{\max} = \max\{v_f, w_f\}$. This condition ensures that waves origination at an interface do not cross other interfaces before Δt.

Computing Buffer Length From ODE

We consider the buffer evolution described by (3.2) to compute the queue length on the secondary road of a roundabout. At each time step $t^n = t^{n-1} + \Delta t$ we update the new value of the queue length as follows:

1. If $F_i^{\text{in}} \geq \gamma_{r_i}$, the buffer length is increasing and we set

$$l_i^{n+1} = l_i^n + \left(F_i^{\text{in}} - \gamma_{r_i}\right)\Delta t, \quad i = 1,2,\dots,m. \tag{3.92}$$

2. If $F_i^{\text{in}} < \gamma_{r_i}$, the buffer length is decreasing and we set

$$\tilde{t}_i = \frac{l_i^n}{\gamma_{\mathrm{r}_i} - F_i^{\mathrm{in}}} + t^n \tag{3.93}$$

the time at which the buffer empties.

i. if $t^{n+1} < \tilde{t}_i$

$$l_i^{n+1} = l_i^n + \Big(F_i^{\mathrm{in}} - \gamma_{\mathrm{r}i}\Big)\Delta t, \quad i = 1, 2, \ldots, m; \tag{3.94}$$

ii. if $\tilde{t}_i < t^{n+1}$, $\widetilde{\Delta t} = \tilde{t} - t^n$ and $l_i^{n+1} = 0$.

The above computation can be summarized as in the following algorithm.

Algorithm 1 State variable update procedure

1. Input: states at time t^n: $(\rho_i^n, l_i^n)_{i=1,\ldots,m}$.
2. Output: states at time t^{n+1}: $(\rho_i^{n+1}, l_i^{n+1})_{i=1,\ldots,m}$.
   (a) If $\tilde{t}_i > t^{n+1}$ or $\tilde{t}_i \leq t^n$ $\forall i$: set $t^{n+1} = t^n + \Delta t$ and update the density on roundabout with Godunov fluxes at junctions

$$\rho_i^{n+1} = \rho_i^n - \frac{\Delta t}{L_i}\Big(F_i^{n,-} - F_{i-1}^{n,+}\Big), \quad i = 1, 2, \ldots, m,$$

   and the buffer lengths at junction J_i of the roundabout with

$$l_i^{n+1} = l_i^n + \Delta t\Big(F_i^{\mathrm{in}} - \gamma_{\mathrm{r}_i}\Big), \quad i = 1, 2, \ldots, m.$$

   (b) If $t^n < \tilde{t}_i < t^{n+1}$, $\exists i \in \{1, 2, \ldots, m\}$: set $t^{n+1} = \tilde{t}_i$, and $\widetilde{\Delta t} = t^{n+1} - t^n$; then update the density on the roundabout with Godunov fluxes at junctions

$$\rho_i^{n+1} = \rho_i^n - \frac{\widetilde{\Delta t}}{L_i}\Big(F_i^{n,-} - F_{i-1}^{n,+}\Big), \quad i = 1, 2, \ldots, m,$$

   and the buffer lengths as

$$l_i^{n+1} = l_i^n + \Big(F_i^{\mathrm{in}} - \gamma_{\mathrm{r}_i}\Big)\widetilde{\Delta t}, \quad i = 1, 2, \ldots, m.$$

This Algorithm takes as inputs the states ρ_i^n, and l_i^n at time-step n for all roundabout links and on the incoming secondary roads and returns the states advanced by one time step.

3.5 Optimization on Networks

3.5.1 Minimal area approach

In this section we define the optimization problem, the cost functionals and derive their expressions. We introduce the Total Travel Time (TTT) on the road network and the Total Waiting Time (TWT) on the incoming lanes of the secondary roads, which are defined as follows:

$$TTT(T,\vec{\mathrm{p}}) = \sum_{i=1}^{3}\int_0^T \int_{\mathscr{I}_i} \rho(t,x)dxdt + \sum_{i=1}^{3}\int_0^T l_i(t)dt + T\cdot\sum_{i=1}^{3}\int_{\mathscr{I}_i}\rho(T,x)dx + T\cdot\sum_{i=1}^{3} l_i(T) \tag{3.95}$$

$$TWT(T,\vec{\mathrm{p}}) = \sum_{i=1}^{3}\int_0^T l_i(t)dt + T\cdot l_i(T) \tag{3.96}$$

for $T>0$ that we will take sufficiently large so that the solution is stabilized. In equation (3.95) the first and second term respectively equals to the time taken to travel on the main road of the roundabout and the waiting time on the buffer. Also, the third and fourth term respectively equals to the time taken to travel on the main road of the roundabout and the waiting time on the buffer at final time T.
Our aim is to optimize cost functionals (3.95), (3.96), that measure the Total Travel Time (TTT) and the Total Waiting Time (TWT) through a suitable choice of the right of way parameter p for incoming roads. To this end, we derive the explicit expression of the cost functionals locally at junctions to study their dependence on the right of way parameter p. We consider a single junction as in Figure 3.2(b) with $\mathscr{I}_1=[-1,0]$ and $\mathscr{I}_2=[0,1]$. We suppose that the network and the buffer are empty at $t=0$ and we assume that the following boundary data are given: f^{in} the inflow on the incoming main lane, f^{out} the outflow on the outgoing main lane and F_{in} the incoming flux of the secondary road. Note that, if initially the buffer is not empty, it can be fit to the problem without problem by constant translation. Moreover, to reduce the number of cases to be studied, we assume $F_{\text{in}} \le f^{\max} = \gamma_{\text{r1}}^{\max}$ and $f^{\text{out}} \le f^{\max}$.

The optimization problem is then

$$\min_{p\in[0,1]} \mathrm{TTT}(\mathrm{T},\mathrm{p}) \qquad \text{and} \quad \min_{p\in[0,1]} \mathrm{TWT}(\mathrm{T},\mathrm{p}) \tag{3.97}$$

The TTT and the TWT give an estimate of the time spent by drivers in the network sections or in the queues at the buffers, respectively. The cost functionals

are computed analytically on a single 2x2 junction. Then, the traffic behavior for the whole roundabout is studied numerically using local optima.

Local Total Waiting Time ($\mathrm{TWT_{loc}}$) and Total Travel Time ($\mathrm{TTT_{loc}}$)

We are now ready to compute the expressions for the Total Travel Time and the Total Waiting Time for each value of p. We treat the problem depending on the situation at the junction. It is either demand limited or supply limited. We detail the analytical computation for each case in the sequel.

A. Demand-limited Case

1. The case: $\max(\mathrm{p}_1, 0) \leq \mathrm{p} \leq \min(\mathrm{p}_2, 1)$

We calculate the TWT_{loc} as follows

$$TWT_{loc}(T,\mathrm{p}) = \int_{t_3}^{T} (F_{\mathrm{in}} - (1-\mathrm{p})f^{\mathrm{out}})(t-t_3)dt + T(F_{\mathrm{in}} - (1-\mathrm{p})f^{\mathrm{out}})(T-t_3). \tag{3.98}$$

while the $TTT_{loc}(T)$ is obtained by a constant term which does not depend on the priority parameter p plus a term depending on p, that we denote by $TTT_{loc}(T,\mathrm{p})$:

$$\begin{aligned} TTT_{loc}(T,\mathrm{p}) = &\iint_{A_1} \hat{\rho}_1 dtdx + \iint_{A_2} \rho_1(\mathrm{p})dtdx + T\int_{-1}^{1} (\rho_1(\mathrm{p}) + \rho_3)\,dx \\ &+ \int_{t_3}^{T} (F_{\mathrm{in}} - (1-\mathrm{p})f^{\mathrm{out}})(t-t_3)dt + T(F_{\mathrm{in}} - (1-\mathrm{p})f^{\mathrm{out}})(T-t_3), \end{aligned} \tag{3.99}$$

where the areas of the integration domains are defined by

$$A_1 = \frac{1}{2}(t_4(\mathrm{p}) - t_3) = A_2$$

as shown in Figure 3.30.

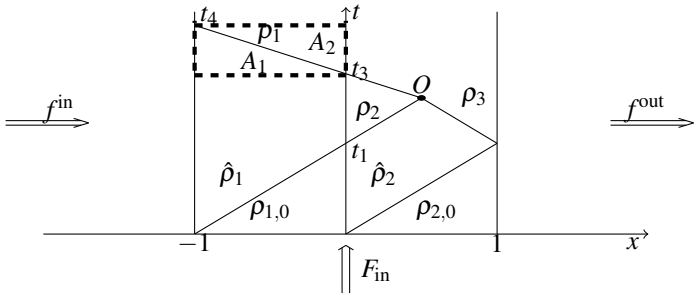

Fig. 3.30: Area of integration in the case: $\max(\mathrm{p}_1, 0) \leq \mathrm{p} \leq \min(\mathrm{p}_2, 1)$

2. The case: $\min(\mathrm{p}_2, 1) < \mathrm{p} \leq 1$

The $\mathrm{TWT}_{loc}(T, \mathrm{p})$ is computed as

$$\mathrm{TWT}_{loc}(T, \mathrm{p}) = \int_{t_3}^{T} (F_{\text{in}} + (1-\beta) f^{\text{in}} - f^{\text{out}})(t - t_3) dt + T(F_{\text{in}} + (1-\beta) f^{\text{in}} - f^{\text{out}})(T - t_3). \tag{3.100}$$

and the $\mathrm{TTT}_{loc}(T)$ is given by:

$$\mathrm{TTT}_{loc}(T, \mathrm{p}) = T \int_{-1}^{1} (\hat{\rho}_1 + \rho_3)\, dx + \int_{t_3}^{T} (F_{\text{in}} + (1-\beta) f^{\text{in}} - f^{\text{out}})(t - t_3) dt + T(F_{\text{in}} + (1-\beta) f^{\text{in}} - f^{\text{out}})(T - t_3). \tag{3.101}$$

3. The case: $0 \leq \mathrm{p} < \max(\mathrm{p}_1, 0)$

In this case $\mathrm{TWT}_{loc} = 0$ since the buffer is empty. The $\mathrm{TTT}_{loc}(T)$ is given by a constant term plus

$$\mathrm{TTT}_{loc}(T, \mathrm{p}) = T \int_{-1}^{1} (\check{\rho}_1 + \rho_3)\, dx. \tag{3.102}$$

B. Supply-limited Case

By similar argument we explicitly express the total travel time and the total waiting time locally case by case.

1. The case : $\mathrm{p}_1 \leq \mathrm{p} < \bar{\mathrm{p}}$

In this case both cost functionals depend on the variable p and can be expressed separately. We compute the TWT_{loc} as follows

$$\begin{aligned}\mathrm{TWT}_{loc}(T,\mathrm{p}) = &\int_{t_1}^{t_4} \left(\left(F_{\mathrm{in}} - (1-\mathrm{p}) f^{\max}\right)(t-1)\right) dt \\ &+ \int_{t_4}^{T} \left(l(t_4) + \left(F_{\mathrm{in}} - (1-\mathrm{p}) f^{\mathrm{out}}\right)(t-t_4)\right) dt + T l(t_4) \\ &+ T\left(F_{\mathrm{in}} - (1-\mathrm{p}) f^{\mathrm{out}}\right)(T-t_4). \end{aligned} \tag{3.103}$$

Concerning $\mathrm{TTT}_{loc}(T)$, it is given by the expression

$$\begin{aligned}\mathrm{TTT}_{loc}(T,\mathrm{p}) = &\iint_{A_1} \hat{\rho}_1 dt dx + \iint_{A_2} \rho_1(\mathrm{p}) dt dx + \iint_{A_3} \check{\rho}_1(\mathrm{p}) dt dx \\ &+ \int_{t_1}^{t_4} \left(\left(F_{\mathrm{in}} - (1-\mathrm{p}) f^{\max}\right)(t-1)\right) dt \\ &+ \int_{t_4}^{T} \left(l(t_4) + \left(F_{\mathrm{in}} - (1-\mathrm{p}) f^{\mathrm{out}}\right)(t-t_4)\right) dt \\ &+ T l(t_4) + T\left(F_{\mathrm{in}} - (1-\mathrm{p}) f^{\mathrm{out}}\right)(T-t_4) + T\int_{-1}^{1} (\check{\rho}_1(\mathrm{p}) + \rho_3)\, dx, \end{aligned} \tag{3.104}$$

where the areas of integration are defined by
$A_1 = \dfrac{1}{2}(t_2(\mathrm{p}) - 1)$, $A_2 = \dfrac{1}{2}(t_5(\mathrm{p}) + t_4 - t_2 - 1)$, $A_3 = \dfrac{1}{2}(t_5(\mathrm{p}) - t_4)$
and $T = t_5$, as in Figure 3.31.

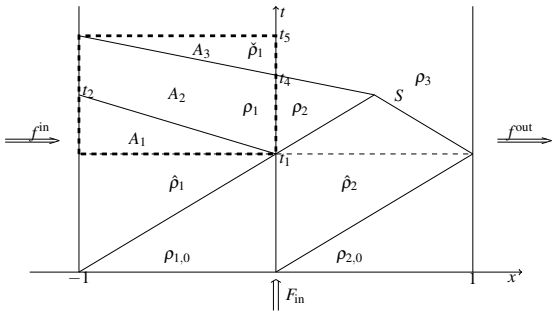

Fig. 3.31: Area of integration in the case $\mathrm{p}_1 \leq \mathrm{p} < \bar{\mathrm{p}}$

2. The case: $\bar{\mathrm{p}} \leq \mathrm{p} \leq \mathrm{p}_2$

The TWT_{loc} is as in (3.103), since it does not depend on the wave interactions but only on the queue length. The $\mathrm{TTT}_{loc}(T)$ can be expressed as

$$\begin{aligned}\mathrm{TTT}_{loc}(T,\mathrm{p}) = &\iint_{A_1+A_2+A_5} \hat{\rho}_1 dtdx + \iint_{A_3} \rho_1(\mathrm{p}) dtdx + \iint_{A_4+A_6+A_7} \check{\rho}_1(\mathrm{p}) dtdx \\ &+ \int_{t_1}^{t_4} ((F_{\mathrm{in}} - (1-\mathrm{p}) f^{\max}))(t-1))\, dt + T \int_{-1}^{1} (\check{\rho}_1(\mathrm{p}) + \rho_3)\, dx \\ &+ \int_{t_4}^{T} \left(l(t_4) + \left(F_{\mathrm{in}} - (1-\mathrm{p}) f^{\mathrm{out}}\right)(t-t_4)\right) dt \\ &+ T l(t_4) + T \left(F_{\mathrm{in}} - (1-\mathrm{p}) f^{\mathrm{out}}\right)(T-t_4). \end{aligned} \tag{3.105}$$

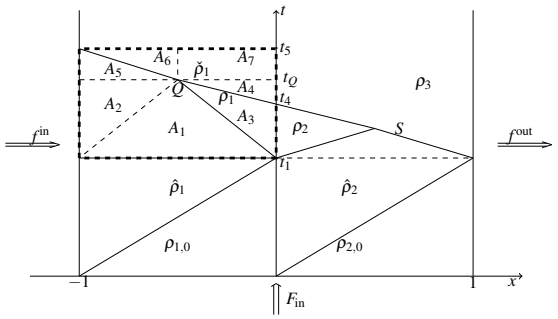

Fig. 3.32: Area of integration in the case $\bar{\mathrm{p}} \leq \mathrm{p} \leq \mathrm{p}_2$

The areas are defined by

$$\begin{aligned} A_1 &= \frac{1}{2}(t_Q(\mathrm{p}) - 1) & A_5 &= \frac{1}{2}(t_5(\mathrm{p}) - t_Q(\mathrm{p}))(x_Q(\mathrm{p}) + 1) \\ A_2 &= \frac{1}{2}(t_Q(\mathrm{p}) - 1)(x_Q(\mathrm{p}) + 1) & A_6 &= \frac{1}{2}(t_5(\mathrm{p}) - t_Q(\mathrm{p}))(x_Q(\mathrm{p}) + 1) \\ A_3 &= \frac{1}{2}(x_Q(\mathrm{p}) - x_Q(\mathrm{p})t_4) & A_7 &= (t_5(\mathrm{p}) - t_Q(\mathrm{p}))(-x_Q(\mathrm{p})) \\ A_4 &= \frac{1}{2}(t_Q(\mathrm{p}) - t_4)(-x_Q(\mathrm{p})) \end{aligned}$$

as in Figure 3.32.

3. The case: $\mathrm{p} > \mathrm{p}_2$

In this case we have to consider two different situations according to the value of p. If $\mathrm{p} > \bar{\bar{\mathrm{p}}} = (1-\beta)\dfrac{f^{\mathrm{in}}}{f^{\mathrm{out}}}$ and $(1-\beta)f^{\mathrm{in}} < f^{\mathrm{out}}$ then the functionals do not depend on p and hence, we skip it from our analysis. If $\mathrm{p}_2 < p < \bar{\bar{\mathrm{p}}}$ and p $(1-\beta)f^{\mathrm{in}} < f^{\mathrm{out}}$ or $(1-\beta)f^{\mathrm{in}} \geq f^{\mathrm{out}}$ then the TWT_{loc} is given by

$$\begin{aligned}\mathrm{TWT}_{loc}(T,\mathrm{p}) = &\int_{t_1}^{t_4}\Big(F_{\mathrm{in}} + (1-\beta)f^{\mathrm{in}} - f^{\max})(t-1)\Big)\,dt \\ &+ \int_{t_4}^{T}\Big((F_{\mathrm{in}} + (1-\beta)f^{\mathrm{in}} - f^{\max})(t_4-1) + \big(F_{\mathrm{in}} - (1-\mathrm{p})f^{\mathrm{out}}\big)(t-t_4)\Big)\,dt \\ &+ T(F_{\mathrm{in}} + (1-\beta)f^{\mathrm{in}} - f^{\max})(t_4-1) + T\big(F_{\mathrm{in}} - (1-\mathrm{p})f^{\mathrm{out}}\big)(T-t_4).\end{aligned} \tag{3.106}$$

The $\mathrm{TTT}_{loc}(T)$, as usual, is instead calculated by the constant term plus

$$\begin{aligned}\mathrm{TTT}_{loc}(T,\mathrm{p}) = &\int_{A_1}\hat{\rho}_1(\mathrm{p})\,dt\,dx + \int_{A_2}\check{\rho}_1(\mathrm{p})\,dt\,dx \\ &+ \int_{t_1}^{t_4}\Big(F_{\mathrm{in}} + (1-\beta)f^{\mathrm{in}} - f^{\max})(t-1)\Big)\,dt + T\int_{-1}^{1}(\check{\rho}_1(\mathrm{p}) + \rho_3)\,dx \\ &+ \int_{t_4}^{T}\Big((F_{\mathrm{in}} + (1-\beta)f^{\mathrm{in}} - f^{\max})(t_4-1) + \big(F_{\mathrm{in}} - (1-\mathrm{p})f^{\mathrm{out}}\big)(t-t_4)\Big)\,dt \\ &+ T(F_{\mathrm{in}} + (1-\beta)f^{\mathrm{in}} - f^{\max})(t_4-1) + T\big(F_{\mathrm{in}} - (1-\mathrm{p})f^{\mathrm{out}}\big)(T-t_4)\end{aligned} \tag{3.107}$$

and the areas for this case are $A_1 = \frac{1}{2}(t_5(\mathrm{p}) - t_4)$ and $A_2 = \frac{1}{2}(t_5(\mathrm{p}) - t_4)$ as shown in Figure 3.33.

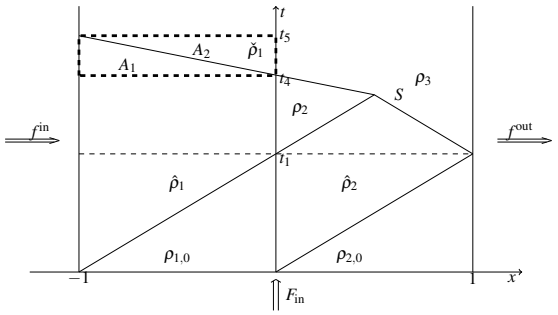

Fig. 3.33: Area of integration in the case $\mathrm{p} > \mathrm{p}_2$

4. The case: $0 \leq \mathrm{p} < \mathrm{p}_1$

We have two different situations which depend on the intersection of the waves as explained in Section 3.3.1. When the waves do not interact between $x = -1$ and $x = 0$ the TWT_{loc} is computed as

$$\mathrm{TWT}_{loc}(T,\mathrm{p}) = \int_{t_4}^{T} \left(F_{\mathrm{in}} - (1-\mathrm{p}) f^{\mathrm{out}}\right)(t-t_4)dt + T\left(F_{\mathrm{in}} - (1-\mathrm{p}) f^{\mathrm{out}}\right)(T-t_4), \tag{3.108}$$

while the $\mathrm{TTT}_{loc}(T,\mathrm{p})$ is given by

$$\begin{aligned}\mathrm{TTT}_{loc}(T,\mathrm{p}) = &\iint_{A_1} \rho_1 dtdx + \iint_{A_2} \check{\rho}_1(\mathrm{p})dtdx + \int_{t_4}^{T} \left(F_{\mathrm{in}} - (1-\mathrm{p}) f^{\mathrm{out}}\right)(t-t_4)dt \\ &+ T\left(F_{\mathrm{in}} - (1-\mathrm{p}) f^{\mathrm{out}}\right)(T-t_4) + T\int_{-1}^{1} (\check{\rho}_1(\mathrm{p}) + \rho_3)\, dx, \end{aligned} \tag{3.109}$$

where $A_1 = \frac{1}{2}(t_5 - t_4) = A_2$ as shown in Figure 3.34.

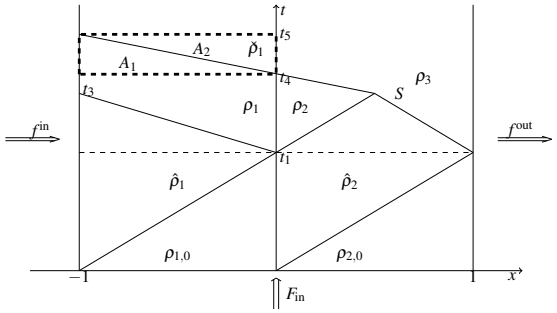

Fig. 3.34: Area of integration in the case $0 \leq \mathrm{p} < \mathrm{p}_1$

Whereas when the waves interact between $x = -1$ and $x = 0$, then the TWT remain the same and the $\mathrm{TTT}_{loc}(T,\mathrm{p})$ is computed as follows

$$\begin{aligned}\mathrm{TTT}_{loc}(T,\mathrm{p}) = &\iint_{A_1} \hat{\rho}_1 dtdx + \iint_{A_2+A_3+A_4} \check{\rho}_1(\mathrm{p})dtdx \\ &+ \int_{t_4}^{T} \left(F_{\mathrm{in}} - (1-\mathrm{p}) f^{\mathrm{out}}\right)(t-t_4)dt + T\left(F_{\mathrm{in}} - (1-\mathrm{p}) f^{\mathrm{out}}\right)(T-t_4) \\ &+ T\int_{-1}^{1} (\check{\rho}_1(\mathrm{p}) + \rho_3)\, dx. \end{aligned}$$

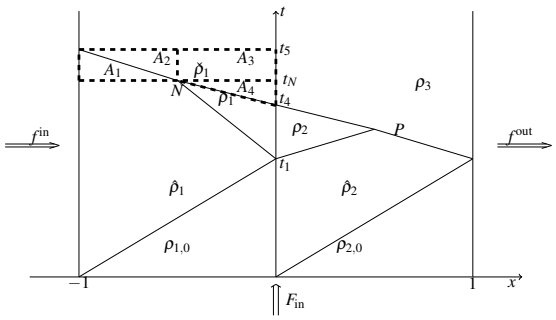

Fig. 3.35: Area of integration when the wave collide in the region [-1,0].

The areas of integration are defined by the following equations as shown in Figure 3.35.

$$A_1 = A_2 = \frac{1}{2}(t_5(\mathrm{p}) - t_N(\mathrm{p}))(x_N(\mathrm{p}) + 1), \qquad A_3 = (t_5 - t_N(\mathrm{p}))(-x_N(\mathrm{p})),$$
$$A_4 = \frac{1}{2}(t_N(\mathrm{p}) - t_4)(-x_N(\mathrm{p})).$$

Remark 3.4. We only consider the areas of integration for each case in which the cost functional depend on the priority parameter, p .

Note that the cost functionals are continuous w.r.t. $p \in [0,1]$, therefore they admits a minimum. However, due to the high number of parameters appearing, it is not possible to compute analytically the optimal solution. Hence, we compute the optimal priority parameter only numerically, as explained in the following subsection.

Numerical Simulations

In this section we show some simulation results corresponding to different choices of the right of way parameters. We consider approximations obtained by Godunov numerical method, with space step $\Delta x = 0.1$ and the time step determined by the CFL condition. The traffic flow on the road network is simulated in a time interval $[0,T]$, where $T = 50$. As for the initial condition on the roads of the network, we assume that at initial time $t = 0$ all the roads and the buffers are empty, $f^{\mathrm{in}} = f^{\mathrm{out}} = 0$ and we take $F_{\mathrm{in}} \neq 0$. We consider the following parameters for each link: $f^{\max} = 0.66$, $\rho_c = 0.66$ and $\gamma_{r1}^{\max} = 0.66$. Moreover, we distinguish different cases of simulations which vary according to the value of

$F_{\text{in}} \in \{0.1, 0.2, 0.3, 0.4, 0.5, 0.6\}$ and $\beta \in \{0.2, 0.3, 0.4, 0.5, 0.6, 0.7\}$. For each value of F_{in} and β we study different simulations cases.

Instantaneous right of way parameter

Due to the complicated expressions of the cost functionals it is difficult to use an analytical approach for the development of an optimized algorithm for the whole roundabout. For this reason, we consider at each junction and at each time step the optimal parameters to optimize the cost functionals TTT_{loc} and TWT_{loc} corresponding to the road densities near the junction. The technique for the simulation of the optimal case is based on the local optimization of every junction of 2×2 type, which form the roundabout.To compute the optimal value of the priority parameter, we take the minimum of the cost functionals computed in Section 3.5 over a grid of 100 points equidistributed in [0, 1]. The cost functionals are evaluated at each time step from the values of F_{in}, f^{out} and f^{in} given by

- $f^{\text{in}} = \delta(\rho_{inc})$
- $f^{\text{out}} = \sigma(\rho_{out})$
- $F_{\text{in}} = d(F_{\text{in}}, l^n)$

Fixed right of way parameter

We analyze the behavior of the cost functionals TTT_{loc} and TWT_{loc}, assuming that the priority parameter p is the same and kept fixed for each junction. This simulates, for instance, if the junction is regulated by a constant signalized system.

Simulation Results

In Figures 3.37 and 3.36 we show some of the simulation results for some representative cases. More precisely we show the value of the functionals TTT (3.95) and TWT (3.96) computed on the whole roundabout as a function of F_{in}. A legend for every picture indicates the different simulation cases. Moreover, the Tables 3.1– 3.6 depict the gain in percentage between the optimal case and the constant one for different values of p.

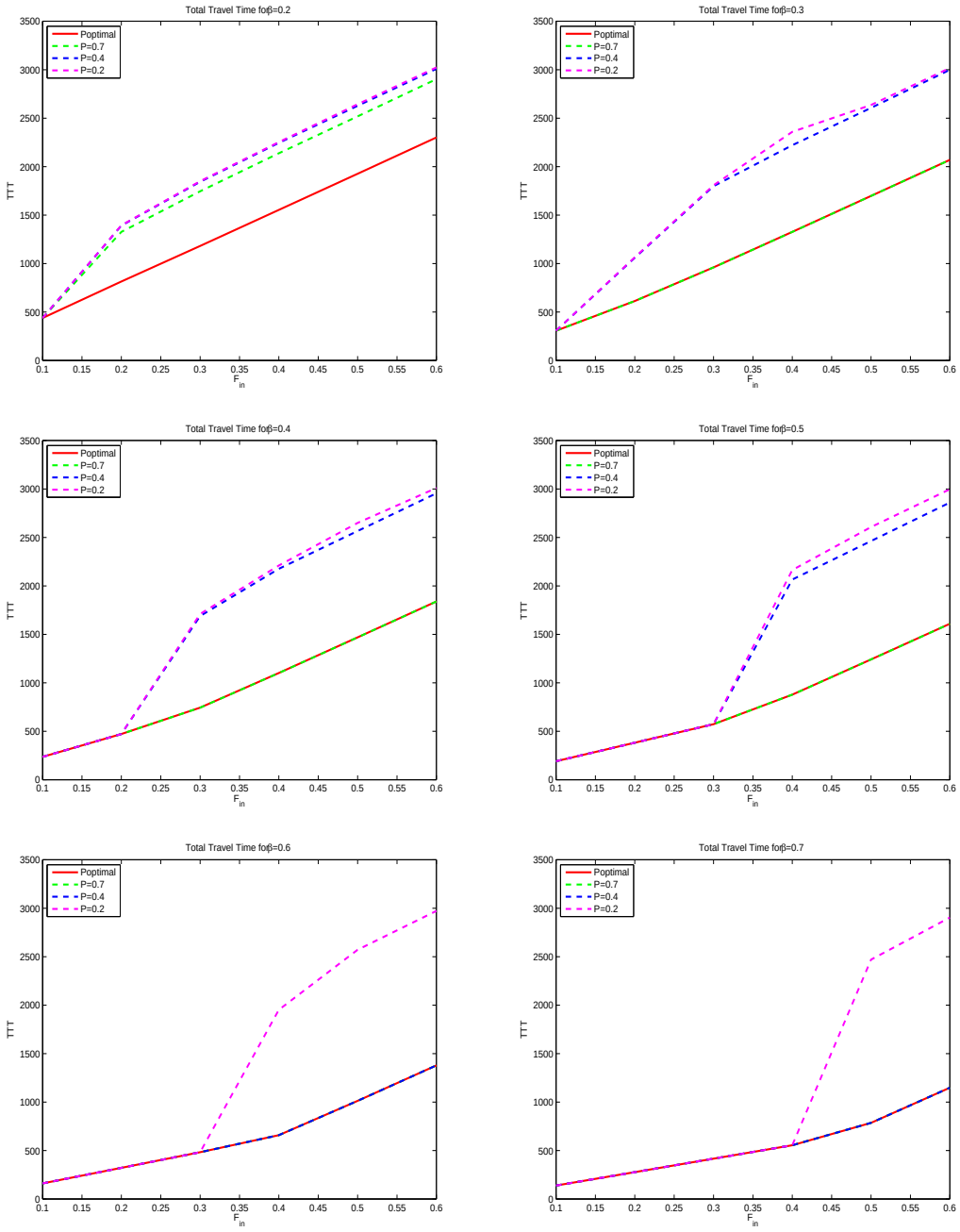

Fig. 3.36: TTT as a function of F_{in} computed for a time horizon $T = 50$.

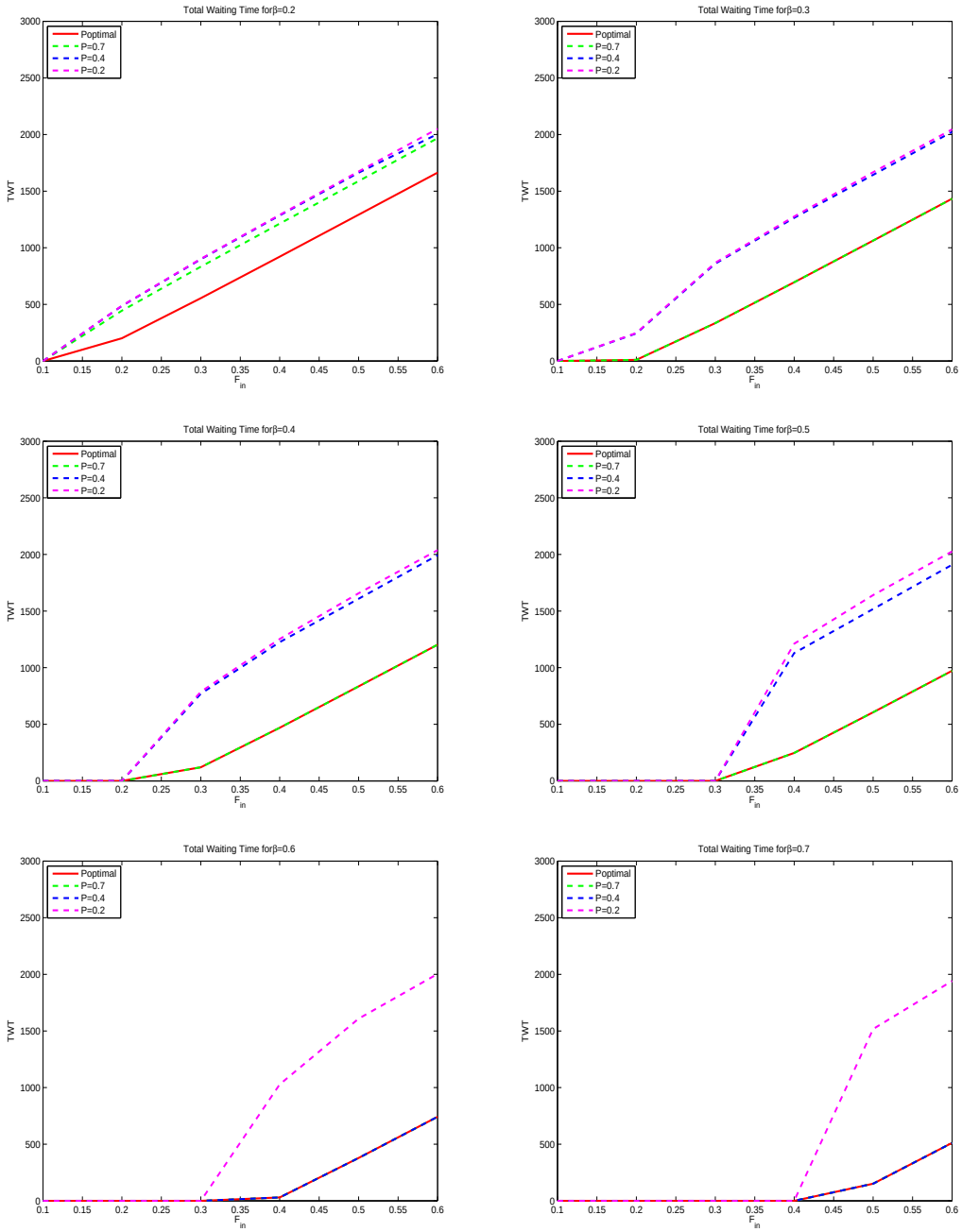

Fig. 3.37: TWT as a function of F_{in} computed for a time horizon $T = 50$.

F_{in} \ β	0.2	0.3	0.4	0.5	0.6	0.7
0.1	0.0000%	0.0000%	0.0000%	0.0000%	0.0000%	0.0000%
0.2	-23.9359%	0.0000%	0.0000%	0.0000%	0.0000%	0.0000%
0.3	-19.2538%	0.0000%	0.0000%	0.0000%	0.0000%	0.0000%
0.4	-15.8362%	0.0000%	0.0000%	0.0000%	0.0000%	0.0000%
0.5	-13.3060%	0.0000%	0.0000%	0.0000%	0.0000%	0.0000%
0.6	-11.5724%	0.0000%	0.0000%	0.0000%	0.0000%	0.0000%

Table 3.1: Gain in TTT computed with the optimal right of way parameter and a fixed one p = 0.7.

F_{in} \ β	0.2	0.3	0.4	0.5	0.6	0.7
0.1	0.0000%	0.0000%	0.0000%	0.0000%	0.0000%	0.0000%
0.2	-26.1638%	-26.7080%	0.0000%	0.0000%	0.0000%	0.0000%
0.3	-21.8880%	-30.3638%	-38.8852%	0.0000%	0.0000%	0.0000%
0.4	-18.2182%	-25.1910%	-32.8044%	-40.3677%	0.0000%	0.0000%
0.5	-15.3961%	-21.1096%	-27.1844%	-32.9931%	0.0000%	0.0000%
0.6	-13.3412%	-18.3294%	-23.2688%	-27.9928%	0.0000%	0.0000%

Table 3.2: Gain in TTT computed with the optimal right of way parameter and a fixed one p = 0.4.

F_{in} \ β	0.2	0.3	0.4	0.5	0.6	0.7
0.1	0.0000%	0.0000%	0.0000%	0.0000%	0.0000%	0.0000%
0.2	-26.2608%	-26.9396%	0.0000%	0.0000%	0.0000%	0.0000%
0.3	-22.0246%	-30.6028%	-39.4182%	0.0000%	0.0000%	0.0000%
0.4	-18.3772%	-28.0082%	-33.4924%	-42.2899%	-49.5546%	0.0000%
0.5	-15.6867%	-21.6484%	-28.6658%	-35.5027%	-43.4925%	-51.7438%
0.6	-13.5821%	-18.6328%	-24.1359%	-30.1316%	-36.6248%	-43.3260%

Table 3.3: Gain in TTT computed with the optimal right of way parameter and a fixed one p = 0.2.

F_{in} \ β	0.2	0.3	0.4	0.5	0.6	0.7
0.1	0.0000%	0.0000%	0.0000%	0.0000%	0.0000%	0.0000%
0.2	-37.7363%	0.0000%	0.0000%	0.0000%	0.0000%	0.0000%
0.3	-20.0221%	0.0000%	0.0000%	0.0000%	0.0000%	0.0000%
0.4	-13.6862%	0.0000%	0.0000%	0.0000%	0.0000%	0.0000%
0.5	-10.3010%	0.0000%	0.0000%	0.0000%	0.0000%	0.0000%
0.6	-8.3728%	0.0000%	0.0000%	0.0000%	0.0000%	0.0000%

Table 3.4: Gain in TWT computed with the optimal right of way parameter and a fixed one p = 0.7.

F_{in} \ β	0.2	0.3	0.4	0.5	0.6	0.7
0.1	0.0000%	0.0000%	0.0000%	0.0000%	0.0000%	0.0000%
0.2	-41.5096%	-92.2568%	0.0000%	0.0000%	0.0000%	0.0000%
0.3	-23.6510%	-43.9810%	-72.9952%	0.0000%	0.0000%	0.0000%
0.4	-16.5219%	-29.0594%	-44.6035%	-64.1409%	0.0000%	0.0000%
0.5	-12.5626%	-21.4584%	-31.6873%	-42.9263%	0.0000%	0.0000%
0.6	-9.2872%	-17.0847%	-24.7253%	-32.5150%	0.0000%	0.0000%

Table 3.5: Gain in TWT computed with the optimal right of way parameter and a fixed one p = 0.4.

F_{in} \ β	0.2	0.3	0.4	0.5	0.6	0.7
0.1	0.0000%	0.0000%	0.0000%	0.0000%	0.0000%	0.0000%
0.2	-41.6784%	-92.3688%	0.0000%	0.0000%	0.0000%	0.0000%
0.3	-23.8452%	-44.3239%	-73.5147%	0.0000%	0.0000%	0.0000%
0.4	-16.7143%	-29.4949%	-45.5005%	-66.1746%	-94.3553%	0.0000%
0.5	-12.8840%	-22.1229%	-33.0143%	-46.0431%	-61.9339%	-81.8636%
0.6	-10.4278%	-17.6115%	-25.7892%	-35.1576%	-45.9640%	-58.3022%

Table 3.6: Gain in TWT computed with the optimal right of way parameter and a fixed one p = 0.2.

In both cases, the cost functionals computed with a fixed right of way parameter or with the optimal ones have a different behavior only for those values of F_{in} for which the problem is supply limited. In both cases we have better re-

sults for the optimal case. We can see that even when optimizing the TWT, low values of the priority parameters that should favor the entrance with respect to the main lane are bad choices. In fact, for these values the roundabout tends to be overly congested blocking the entrances. From our analysis, it seems that in both cases the optimal priority parameters are the ones that favors the main lane compared to the entrances.

3.5.2 Instantaneous Optimization of ODE-PDE Constrained System

Hyperbolic conservation laws may be nonlinear and lead to non-convex or non-linear formulations of the corresponding optimization problem. In such cases fewer optimization techniques exist for the discretized version of the problems than for convex problems. One approach is to approximate the system with a relaxed version in order to use efficient linear programming techniques. The linearization approach was used in [34] for optimal ramp metering using Godunov discretization scheme.

In this subsection we are going to determine discrete instantaneous optimal priority parameters $p_i^n = p_i(t^n)$ in order to minimize total travel time on the roundabout on a fixed time interval $[0,T]$, expressed by the cost functional

$$J(\vec{p}) = \sum_{i=1}^{m} \int_0^T \int_{I_i} \rho(t,x)\, dxdt + \sum_{i=1}^{m} \int_0^T l_i(t)\, dt. \tag{3.110}$$

Here, $\vec{p} : [0,\mathrm{T}] \to [0,1]^m$ is the time dependent vector of control variables. We select instantaneous optimal control approach to minimize the total travel time on the networks of the roundabout under consideration. The idea of instantaneous control has been discussed in [42] for the optimization of traffic flow problems on road networks. The purpose is to minimize large storage requirements arising from the network structure and the strong coupling of adjoints and state equations by generating a sequence of optimal control problems of reduced dimension. In this subsection, rather than generating a sequence of sub-optimal control problems, we compute the gradient of the cost function at each time step t^n to obtain the optimal priority parameters. We apply the procedure to minimize the total travel time across a roundabout.

Given a time step Δt (to be replaced with $\widetilde{\Delta} t$ when needed) compatible with the CFL condition (3.91), we can introduce the instantaneous cost functional J^n at time t^n read as

$$\begin{aligned} J^n(\vec{p}) &= \Delta t \sum_{i=1}^{m} L_i \rho_i^{n+1} + \Delta t \sum_{i=1}^{m} l_i^{n+1} \\ &= \Delta t \sum_{i=1}^{m} \left[L_i \rho_i^n - \Delta t \left(F_i^{n,-} - F_{i-1}^{n,+} \right) \right] \\ &\quad + \Delta t \sum_{i=1}^{m} \left[l_i^n + \Delta t \left(F_i^{\text{in}} - \gamma_{r_i} \right) \right], \end{aligned} \tag{3.111}$$

where the dependencies of $F_i^{n,\pm}$ and γ_{r_i} on p_i are expressed by (3.79)-(3.82) in the demand-limited case and by (3.83)-(3.86) in the supply-limited situation. Within this framework, we treat both demand and supply-limited cases at junctions.

Nonlinear optimization techniques such as gradient descent method can be applied to the descretized system without any modification to the underlying dynamics. Gradient descent is a first-order optimization algorithm which gives no guarantee for finding a unique global minimum. In the computation of the gradient, we consider each cases based on the situation at the corresponding junction of the roundabout. The optimization problem thus writes

$$\min_{\vec{p} \in [0,1]^m} J^n(\vec{p}). \tag{3.112}$$

such that for each $\vec{p}$ equations (3.1) and (3.2) holds. Note that in our case the cost functional J^n is piece-wise linear with respect to p_i, $i = 1, \ldots, m$.

Theorem 3.3. *Consider junctions of a roundabout as in Figure 3.5 with two incoming and two outgoing roads at each junction. Suppose the instantaneous cost functional* J^n *at time* t^n *is given by equation* (3.111)*. Then the optimal priority parameter exists and it is obtained at* $\mathrm{P}_2^{\mathrm{i}}$ *which is given by equation* (3.85) *for* $i = 1, 2, \ldots m$ *and for each* n*.*

Proof. The cost functional J^n is piecewise linear and continuous with respect to the priority parameter p_i, $i = 1, 2, \ldots m$. Furthermore, it is non-convex. Straight forward computations with respect to p_i, $i = 1, 2, \ldots m$ gives

$$\frac{\partial}{\partial p_i^n} J^n(\vec{p}) = \begin{cases} \dfrac{\beta_i}{\beta_i - 1} \sigma(\rho_{i+1}^n) \Delta t^2 \leq 0 & \text{if } p_i \in [\max\{0, P_1^i\}, \min\{1, P_2^i\}] \\ 0 & \text{otherwise,} \end{cases} \tag{3.113}$$

where P_1^i, and P_2^i are as given by (3.85). This implies that J^n is decreasing on the interval $[\max\{0, P_1^i\}, \min\{1, P_2^i\}]$. Since J^n is piecewise continuous and decreasing on the compact set $[\max\{0, P_1^i\}, \min\{1, P_2^i\}]$, the optimal point exists by Weierstrass extreme value theorem. Consequently the values of optimal priority parameter is attained at P_2^i for each n and for $i = 1, 2, \ldots, m$. Therefore, any choice of $p_i \leq \min\{1, P_2^i\}$, $i = 1, \ldots, m$ solves (3.112), resulting in the same flow dynamics.

The optimal parameter values are used to update the priority variables p_i^n which is adjusted for each iteration n to produce local optimal solution that satisfies the given target.

Numerical Simulations

In this section we present the results obtained through numerical simulations for a roundabout modelled as a concatenation of four 2×2 junctions with two incoming and two outing roads at each junction using the gradient descent method. That is, we take m $= 4$ for the simulation purpose. Any other reasonably finite arbitrary choice of m is also possible.

We analyze the cost functional (3.110) introduced in Section 3.5.2. In particular, we want to compare the effectiveness of instantaneous optimal choices of the priority parameters given by $p_i = P_2^i$, $i = 1, \ldots, m$, with respect to fixed constant parameters. For this, we compute the corresponding value of the discretized functional

$$\tilde{J}(\vec{p}) = \Delta t \sum_{n=0}^{n_T} \sum_{i=1}^{m} L_i \rho_i^{n+1} + \Delta t \sum_{n=0}^{n_T} \sum_{i=1}^{m} l_i^{n+1}, \tag{3.114}$$

with $\vec{p} : [0,T] \to [0,1]^m$ is piecewise constant on $[t^n, t^{n+1}[$, $n = 0, \ldots, n_T$,where we set $t^0 = 0$ and $t^{n_T+1} = T$.

Below, we present the choice of simulation parameters. The numerical approximation of the hyperbolic conservation laws that describe the evolution of densities for each road of the roundabout is made using the adapted Godunov scheme described in Subsection 3.4.2. The time step is determined by the CFL stability condition (3.91) with coefficient equal to 0.5. Periodic boundary conditions are imposed on the left and on the right of the computational domain. The ODE is discretized using an explicit Euler first order integration method. The roundabout traffic evolution is simulated on a time interval $[0,T]$, with $T = 30$, long enough to attain a stabilized situation.

At initial time $t = 0$, we assume that all the links and the buffers are empty, and we impose $\mathrm{F_i}^{\mathrm{in}} \neq 0$ at each junctions. For the simulations, we consider $\rho_{max} = v_f = 1$, $f^{\max} = \rho_{\mathrm{c}} = 0.66$, $L_i = 1$ and $\gamma_{\mathrm{r}_i}^{\max} = 0.66$ for all $i = 1, \ldots, 4$. Finally, for each value of the fixed control parameters we study 6×6 simulation cases based on different values of the flux $\mathrm{F_i}^{\mathrm{in}}$ and β_i. For each of them we perform two simulations

1. **Instantaneous optimal priority parameters:** We use $p_i = P_2^i$, $i = 1, \ldots, 4$ in Algorithm 1 to compute the corresponding value of (3.114).
2. **Fixed optimal priority parameters:** In this case, the priority parameters p_i are kept fixed with the same constant values for all junctions in each simulation cases. Then, as in case 1, we apply Algorithm 1 to compute the state variables on each links of the roundabout and the buffer lengths and the corresponding total travel time on the roundabout.

Simulation Results

We run simulations for the values of F_i^{in} and β_i as given in Tables 1-6. Then we compute the difference between total travel time obtained with different fixed p_i and the optimal p_i^n. That is

$$\text{TTTD} = \frac{\text{TTTF} - \text{TTTO}}{\text{TTTF}}$$

where TTTF stands for the value of (3.114) corresponding to fixed p_i, TTTO represents total travel time with optimal p_i^n and TTTD for their difference. Tables 1-6 report the gain percentage in total travel times to compare the effectiveness of our approach.

β_i \ F_i^{in}	0.1	0.2	0.3	0.4	0.5	0.6
0.2	0%	47.42%	36.86%	29.44%	24.42%	20.66%
0.3	0%	0%	54.12%	43.42%	36.08%	30.52%
0.4	0%	0%	69.87%	57.42%	47.68%	40.36%
0.5	0%	0%	0%	71.07%	59.3%	50.11%
0.6	0%	0%	0%	0%	70.75%	59.76%
0.7	0%	0%	0%	0%	81.68%	68.92%

Table 3.7: Improvement in total travel time using instantaneous optimal parameters compared to fixed constant parameter $p_i = 0.2, i = 1, \ldots, 4$.

β_i \ F_i^{in}	0.1	0.2	0.3	0.4	0.5	0.6
0.2	0%	47.3%	36.76%	29.38%	24.15%	20.35%
0.3	0%	0%	54.04%	43.24%	35.72%	29.99%
0.4	0%	0%	69.72%	57.23%	47.19%	39.57%
0.5	0%	0%	0%	70.63%	58.4%	48.92%
0.6	0%	0%	0%	0%	69.01%	57.2%
0.7	0%	0%	0%	0%	0%	0%

Table 3.8: Percentage gained in total travel time using instantaneous optimal parameters compared to fixed constant parameter $p_i = 0.3, i = 1, \ldots, 4$.

β_i \ F_i^{in}	0.1	0.2	0.3	0.4	0.5	0.6
0.2	0%	47.19%	36.6%	29.14%	23.74%	19.94%
0.3	0%	0%	53.7%	42.95%	34.97%	29.32%
0.4	0%	0%	69.22%	56.51%	45.75%	38.29%
0.5	0%	0%	0%	69.11%	55.36%	45.86%
0.6	0%	0%	0%	0%	0%	0%
0.7	0%	0%	0%	0%	0%	0%

Table 3.9: Percentage gain in total travel time using instantaneous optimal parameters compared to fixed constant parameter $p_i = 0.4, i = 1, 2, \ldots, 4$.

.

β_i \ F_i^{in}	0.1	0.2	0.3	0.4	0.5	0.6
0.2	0%	46.94%	36.25%	28.36%	23.07%	19.38%
0.3	0%	0%	53.04%	41.49%	33.55%	28.02%
0.4	0%	0%	67.41%	52.97%	42.27%	35.03%
0.5	0%	0%	0%	0%	0%	0%
0.6	0%	0%	0%	0%	0%	0%
0.7	0%	0%	0%	0%	0%	0%

Table 3.10: Percentage gain in total travel time using instantaneous optimal parameters compared to fixed constant parameter $p_i = 0.5, i = 1, 2, \ldots, 4$.

.

β_i \ F_i^{in}	0.1	0.2	0.3	0.4	0.5	0.6
0.2	0%	46.22%	34.95%	27.02%	21.91%	18.33%
0.3	0%	0%	49.42%	37.67%	30.12%	24.96%
0.4	0%	0%	0%	0%	0%	0%
0.5	0%	0%	0%	0%	0%	0%
0.6	0%	0%	0%	0%	0%	0%
0.7	0%	0%	0%	0%	0%	0%

Table 3.11: Percentage gain in total travel time using instantaneous optimal parameters compared to fixed parameter $p_i = 0.6, i = 1,2,\ldots,4$.

.

β_i \ F_i^{in}	0.1	0.2	0.3	0.4	0.5	0.6
0.2	0%	43.23%	30.99%	23.7%	19.07%	15.87%
0.3	0%	0%	0%	0%	0%	10%
0.4	0%	0%	0%	0%	0%	0%
0.5	0%	0%	0%	0%	0%	0%
0.6	0%	0%	0%	0%	0%	0%
0.7	0%	0%	0%	0%	0%	0%

Table 3.12: Percentage gain in total travel time using instantaneous optimal parameters compared to fixed constant parameters $p_i = 0.7, i = 1,2,\ldots,4$.

As indicated in Tables 1-6, the percentage gain in total travel time is nul in the case of demand-limited and both approaches give the same value. However, as the traffic inflow increases on the incoming secondary road at the entrance of the roundabout, a sensible percentage gain is observable for different fixed constant p_i and optimal p_i, as illustrated in the above tables. These situation correspond to supply-limited cases on the main lane of the roundabout. This shows that, when a large population of vehicles remain on the main road of the roundabout, the instantaneous optimal choice of priority parameter increases the performance of the roundabout compared to different fixed values of p_i.

For the fixed priority parameters greater than P_2^i at each junction both approaches take the same values. This is due to the fact illustrated by Figure 3.7c in Section 3.3. That is, the junction solution is approximated by the point on

the feasible set. Furthermore, as the values of the fixed parameters p_i decreases, the instantaneous choice of optimal parameter shows better performance in increasing traffic throughput. Compared to small fixed priority parameters, larger fixed values are better in optimizing traffic flux on the network portion.

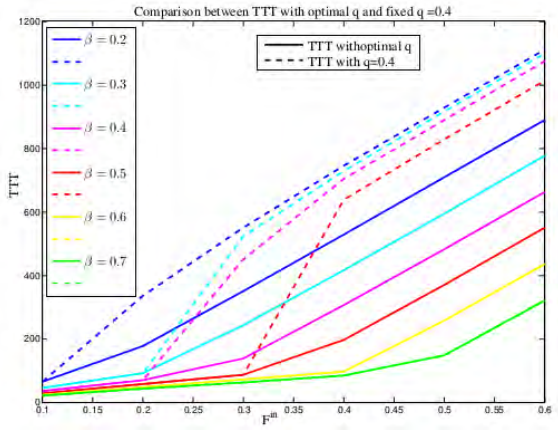

Fig. 3.38: Comparison between the total travel times obtained with optimal choice of p_i and fixed $p_i = 0.4$, for different values of incoming flux and splitting ratio.

In Figure 3.38 we plot the values of total travel time obtained by both approaches as a function of the incoming flux F_i^{in} for different values of splitting ratio β_i for the whole roundabout. The legend indicates different simulation cases.

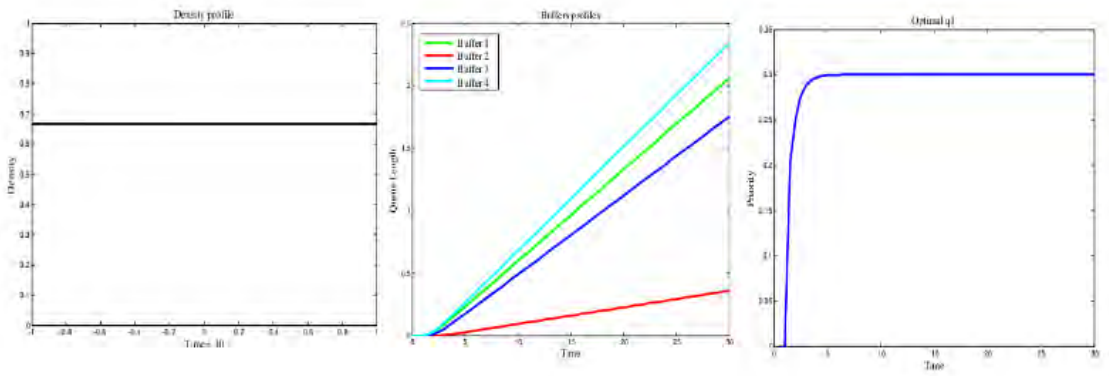

Fig. 3.39: Density at $T = 30$ (left), buffer lengths (middle) and optimal priority parameter (right) evolution on the time interval $[0, 30]$.

Figure 3.39 illustrates sample density, buffer length and optimal priority profiles for different inflows from the secondary incoming road of a roundabout at junctions during the simulation time interval $[0, 30]$.

Chapter 4
Modelling Pedestrians' Impact on the Performance of a Roundabout

4.1 Introduction

A wide variety of mathematical models describing traffic flow and separately pedestrians motion have been intensively investigated in the recent years using microscopic and macroscopic approaches as reviewed in chapter 1. In the present chapter, we are interested to present the relation between short stay of pedestrian on the crosswalk situated on entrance and exiting roads of the roundabout and its implication on the performance of the roundabout in regulating traffic flow problems. Compared to [10, 57], the model presented in this chapter use extended flux due to pedestrians motion on the crosswalk and focused on investigating the performance of the roundabout rather than optimizing the traffic flow.

Roundabouts can be seen as particular road network and can be modelled as alternatively periodic sequences of 2×1 and 1×2-type junctions. In the rest of the chapter, we consider a roundabout joining m-incoming and m-outgoing roads, $m \in \mathbb{N}$, $m \geq 2$, with pedestrian crosswalk situated both on the entrance and exit roads. The evolution of the traffic flow on the whole road network of the roundabout is described by nonlinear scalar hyperbolic partial differential equation (PDE) as discussed in chapter 3.

Here, we introduce three cost functionals that measure the total mass of vehicle, average velocity, and total flux on the network to analyze the performance of the roundabout with and without pedestrian through numerical simulation.

The chapter begins with reviewing existing literature on traffic and pedestrians flow modelling . In Section 4.2, we describe mathematical model for the road networks of the roundabout, governing equations and the solution of Rie-

mann problem at junctions. In Section 4.3 we detail numerical approximation and finally we close the chapter by presenting comparisons.

4.2 The Model

Consider a roundabout joining m-incoming and m-outgoing roads, $m \in \mathbb{N}$, $m \geq 2$, with pedestrian crosswalk situated both on the entrance and exit roads as illustrated in Figure 4.1.

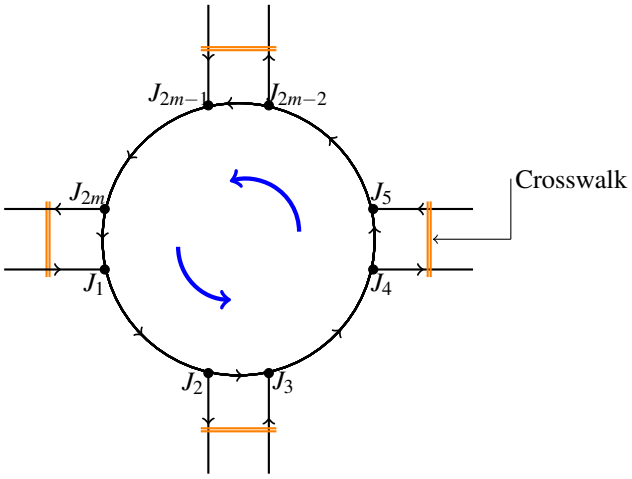

Fig. 4.1: Sketch of the roundabout considered in the chapter.

Such a roundabout can be described as a directed graph in which roads are represented by arcs and junctions by vertexices.The arcs are modelled by intervals $I_i = [a_i, b_i] \subset \mathbb{R}$, $a_i < b_i$, $i = 1, 2, \ldots, 2m$. In the case of incoming and outgoing roads either b_i or a_i can be extended to $+\infty$ or $-\infty$. Each junction J_i is described by its incoming and outgoing roads, where we denote the set of all incoming roads of junction J_i by $\mathrm{Inc}(\mathrm{J_i})$ and the set of all outgoing roads of junction J_i by $\mathrm{Out}(\mathrm{J_i})$ for $i = 1, 2, \ldots, 2m$. In this setting, the roundabout illustrated in Figure 4.1 can be decomposed into alternatively periodic sequences of 2×1 and 1×2-type junctions (compare Figure 4.2). This modelling approach is different from the model introduced in chapter 3 which consider the roundabout as a concatenation of 2×2- type junctions in addition to buffer on the external secondary roads.

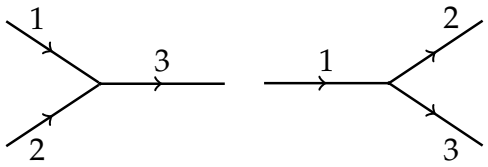

Fig. 4.2: A junction with two incoming and one outgoing road (left), and a junction with one incoming and two outgoing roads (right).

To recover the behavior of the roundabout we apply Coclite, Garavello and Piccoli (CGP) condition at each junction of the roundabout.

For the definition of road networks and detail description we refer to [30, 44].

Definition 4.1. A road network is a couple $(\mathscr{I}, \mathscr{J})$, where $\mathscr{I} = \{I_i = [a_i, b_i] \subseteq \mathbb{R}\}$, $i = 1, 2, \ldots, 2m$ represents a finite set of edges (roads), and $\mathscr{J}$ is the collection of vertexes. Each vertex J is a union of two non empty subsets **Inc(J)** and **Out(J)** of $\{1, 2, \ldots, 2m\}$ representing respectively, the incoming and the outgoing roads.

In this chapter, each junction can be identified as either 2×1 or 1×2 type. The evolution of the traffic flow on the road network of the roundabout is given by the scalar hyperbolic conservation law

$$\partial_t \rho_i + \partial_x f_i(\rho_i) = 0, \quad (t,x) \in \mathbb{R}^+ \times I_i, \quad i = 1, 2 \ldots, 2m, \tag{4.1}$$

where $\rho_i = \rho_i(t,x) \in [0, \rho_{\max}]$ is the mean traffic density and $\rho_{\max}$ the maximal density on the road. The flux function $f_i : [0, \rho_{\max}] \to \mathbb{R}^+$ is given by the following flux-density relation

$$f_i(\rho_i) = \rho_i v(\rho_i)$$

where $v : [0, \rho_{max}] \to \mathbb{R}^+$ is a smooth decreasing Lipschtiz continuous function denoting the mean traffic speed. As given in [44], the basic assumption we will make for the evolution of traffic on the roundabout is that the velocity function only depends on the density ρ of the cars. The mean traffic speed v attains its maximal value v_{max} for small density and when ρ increases to some maximum capacity ρ_{max}, the mean traffic speed vanishes. This means that when traffic is light on the road, cars will drive at maximum speed and as the road gets more congested, the cars will have to slow down until they come to a complete stand-still as the traffic stands bumper to bumper. The simplest example of velocity function [37] ensuring these assumption is

$$v(\rho) = v_{max}(1 - \rho)$$

where v_{max} is the maximal speed of vehicles on the road. For future use we normalize the vehicle density $\rho(t,x)$ so that $0 \leq \rho \leq 1$. Furthermore, as presented in [30], we make the following assumption on the flux function

(A_1) f_i is smooth strictly concave C^2 function.
(A_2) $f_i(0) = f_i(1) = 0$.

Assumption (A_1) and (A_2) guarantees the existence and uniqueness of critical density $\rho_c \in (0,1)$ such that $f_i'(\rho_c) = 0$. A typical example of flux function satisfying assumption (A_1) and (A_2) is

$$f(\rho) = \rho v_{max}(1-\rho) \tag{4.2}$$

which is commonly referred as fundamental diagram in the transportation literature(compare Figure 4.3).

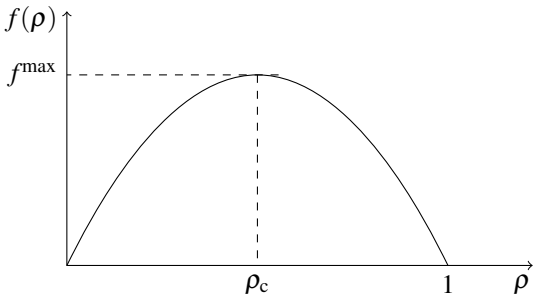

Fig. 4.3: Flux function considered.

More recently, the coupling of traffic flow networks with pedestrian motion on the street has been investigated in [6, 7] using scalar hyperbolic conservation laws in combination with the solution of the eikonal equation.

In this chapter, we are interested to investigate the relation between short stay of pedestrian motion on the crosswalk on entrance and exiting roads of the roundabout and its implication on the performance of the roundabout in regulating traffic flow problems. To achieve this goal, we assume that the crosswalk is a two-dimensional space orthogonal to the driving direction and extend the traffic flux at the exit and entrance by

$$\tilde{f}(\rho_i) = \rho_i v(\rho_i) g(p), \quad i = 1,2,\ldots,m \tag{4.3}$$

where the function g is defined by

$$g(p,t) = \begin{cases} 0 \text{ if p = 1}, t \in [t_1, t_2] \\ 1 \text{ if p = 0} \end{cases} \tag{4.4}$$

and $p \in \{0,1\}$. The state $p = 1$ denotes the presence of pedestrians certainly on the crosswalk while the state $p = 0$ corresponds to the absence of pedestrians on the crosswalk. The time t_1 and t_2 are randomly chosen. The duration $t = t_2 - t_1$ is the time taken by pedestrians to cross the road. The situation $g(p,t) = 0$ indicates the occupancy of road by pedestrians and the interruption of traffic flow. The state $g(p,t) = 1$ corresponds to the absence of pedestrians on the crosswalk at the exit and/or entrance of the roundabout and the traffic flow behaves normally as given in the LWR model as presented in the previous chapters. We solve the Cauchy problem

$$\begin{cases} \partial_t \rho_i + \partial_x \tilde{f}(\rho_i) = 0, \ (t,x) \in \mathbb{R}^+ \times I_i, \\ \rho_i(0,x) = \rho_{i,0}(x) \quad x \in I_i, \quad 1,2,\ldots,2m. \end{cases} \tag{4.5}$$

on each I_i where $\rho_{i,0}(x)$ is the initial density on the road network of the roundabout.

A weak solution of the network and Riemann problem has been given in [30, 44] and references therein as a solution in the sense of distributions with test functions, which are smooth at the junctions. We use entropic solutions on each of the single roads of the roundabout in the sense of the following definition.

Definition 4.2. Consider a roundabout as in Figure 4.1. Let A be a distribution rate at a fixed junction of the roundabout as given in Definition 3.2. A collection of function

$$\rho = (\rho_i)_{i=1,\ldots,2m} \in \prod_{i=1}^{2m} \mathscr{C}^0 \left(\mathbb{R}^+; \mathbf{L^1} \cap \mathrm{BV}(I_i) \right)$$

is an admissible solution to (4.5) if

1. ρ_i satisfies the Kružhkov entropy condition [50] on $(\mathbb{R}^+ \times I_i)$, that is, for every $k \in \mathbb{R}$ and for all $\varphi \in \mathscr{C}_c^1(\mathbb{R} \times I_i)$, $t > 0$,

$$\begin{aligned} &\int_{\mathbb{R}^+} \int_{I_i} (|\rho_i - k| \partial_t \varphi + \mathrm{sgn}\,(\rho_i - k)(\tilde{f}(\rho_i) - \tilde{f}(k)) \partial_x \varphi) dx dt \\ &\quad + \int_{I_i} \left| \rho_{i,0} - k \right| \varphi(0,x) dx \geq 0; \quad i = 1,2,\ldots,2m. \end{aligned} \tag{4.6}$$

2. $\tilde{f}(\rho_i(t, b_i^-)) = \sum_{j=1}^{n} \beta_{j,i} \tilde{f}(\rho_i(t, a_i^+))$, at each junction of the roundabout;
3. $\tilde{f}(\rho_i(t, b_i^-))$ must be maximized subject to (1) and (2).

Here b_i^- denotes left side of b_i in the interval whereas a_i^+ indicates the right side of a_i. Condition (1) is concerned with conservation of cars whereas condition (2)and (3) correspond to the preferences of drivers and the maximization procedure. In the definition , $n = 1$ or 2 depending on the junction type of the roundabout.

Definition 4.3. A Riemann solver for junction J is a map $\mathscr{RS} : [0,1]^2 \times [0,1] \to [0,1]^2 \times [0,1]$ that associates to the Riemann data $\rho_0 = (\rho_{1,0}, \rho_{2,0}, \rho_{3,0})$ at J to a vector $\hat{\rho} = (\hat{\rho}_1, \hat{\rho}_2, \hat{\rho}_3)$ such that the solution on the incoming road $I_i, i = 1,2$ is given by the wave $(\rho_i, \hat{\rho}_i)$ and on the outgoing road $I_j, j = 3$, the solution is given by the wave $(\hat{\rho}_j, \rho_j)$. Consistency condition: $\mathscr{RS}(\mathscr{RS}(\rho_0)) = \mathscr{RS}(\rho_0)$.

For a road $i \in Inc(J)$, the solution $\rho_i(t,x)$ over its spacial domain $x < b_i$ is given by the solution to the following Riemann problem

$$\begin{cases} \partial_t \rho_i + \partial_x \tilde{f}(\rho_i) = 0, & (t,x) \in \mathbb{R}^+ \times I_i, \\ \rho_i(0,x) = \begin{cases} \rho_{i,0} & \text{if } x < b_i, \\ \hat{\rho}_i & \text{if } x \geq b_i. \end{cases} \end{cases}$$

The Riemann problem for outgoing road is defined similarly except $\rho_i(0, x > b_i) = \rho_{i,0}$ and $\rho_i(0, x \leq b_i) = \hat{\rho}_i$. If $\rho = (\rho_1, \ldots, \rho_{n+m})$, $\rho_i \in [0, +\infty] \times I_i$ is a weak solution as in [30, 44] at the junction such that each $x \mapsto \rho_i(t,x)$ has a bounded variation, then precisely the conservation of cars through the junction J

$$\sum_{i=1}^{n} \tilde{f}(\rho_i(t, b_i)) = \sum_{j=n+1}^{n+m} \tilde{f}(\rho_i(t, a_j)) \tag{4.7}$$

holds where for a junction type 1×2, $n = 1, m = 2$ and for 2×1, $n = 2, m = 1$ in the context of the roundabout.

To ensure the uniqueness of solution at each junction we use priority rule as in the previous chapter. A parameter $p \in (0,1)$ is a priority parameter that defines the amount of flux that enters the outgoing main lane from each incoming road. In particular, when the priority applies, $p\tilde{f}(\rho(t, b^-))$ is the flux allowed from the incoming mainline into the outgoing main lane, and $(1-p)\tilde{f}(\rho(t, b^-))$ the flux from the incoming secondary road of the roundabout.

For a junction with 1×2 type, we consider traffic distribution rate as given in Definition 3.2 describing the distribution of traffic among outgoing roads depending on the preference of drivers at each junction J. We denote the Riemann initial data by $\rho_{i,0} = \rho_{i,0}(b_i)$ for incoming arcs and $\rho_{i,0} = \rho_{i,0}(a_i)$ for outgoing arcs for a single junction. Assuming a unique solution for the problem at the junction, we denote the solution at the junction, i.e., at $x = b_i$ for incoming and at

$x = a_i$ for outgoing roads, by

$$(\hat{\rho}_1, \hat{\rho}_2, \hat{\rho}_3).$$

Given the constant initial values $\rho_{i,0}$, we need to determine a unique solution $\hat{\rho}_i$ satisfying the coupling condition in the context of Coclite, Garavello and Piccoli (CGP) approach at junction. The possible values of $\hat{\rho}_i$ are necessarily as follows.

On the incoming road

$$\hat{\rho}_i \in \begin{cases} \{\rho_{i,0}\} \cup (\tau(\rho_{i,0}), 1] & \text{if } 0 \leq \rho_{i,0} < \rho_c \\ [\rho_c, 1], & \text{if } \rho_c \leq \rho_{i,0} \leq 1 \end{cases} \tag{4.8}$$

and on the outgoing road

$$\hat{\rho}_i \in \begin{cases} [0, \rho_c] & \text{if } 0 \leq \rho_{i,0} \leq \rho_c \\ \{\rho_{i,0}\} \cup [0, \tau(\rho_{i,0})) & \text{if } \rho_c \leq \rho_{i,0} \leq 1. \end{cases} \tag{4.9}$$

For further technical analysis we refer to [30]. The values of i are easily fixed depending on the junction type.

Remark 4.1. On the incoming road

- if $\rho_{i,0} < \rho_c < \hat{\rho}_i < 1$, $\tilde{f}(\rho_{i,0}) > \tilde{f}(\hat{\rho}_i)$, and $\rho_c < \rho_{i,0} < 1$, the solution of the Riemann problem consists of a shock wave with a negative speed and;
- if $\rho_{i,0} < \rho_c < \hat{\rho}_i < 1$ and $\tilde{f}(\rho_{i,0}) = \tilde{f}(\hat{\rho}_i)$, the solution consists of contact wave.

On the outgoing road

- if $\rho_{i,0} < \rho_c$ the solution of the Riemann problem consists of a shock wave with a positive speed.
- if $\hat{\rho}_i < \rho_c < \rho_{i,0} < 1$, the solution of the Riemann problem consists of a shock wave with positive speed and contact wave when $\tilde{f}(\rho_{i,0}) = \tilde{f}(\hat{\rho}_i)$.

For the following discussion we refer to [36, 40] for detail.

A. **Coupling conditions for junction type** 2×1

Let us consider a junction with two incoming arcs and one outgoing arc. Define the initial densities on each roads i by $\rho_{i,0}$ with $i = 1, 2, 3$. The corresponding flux on the roads as $\gamma_{i,0} = \tilde{f}(\rho_{i,0})$. Denote the maximum of the flux by $\tilde{f}(\rho_c)$. Then define the sets of valid resulting fluxes γ_i by Ω_i. For the incoming roads $i = 1, 2$, this is equivalent to saying that

$$\begin{aligned} &\rho_{i,0} \leq \rho_{\mathrm{c}} \Rightarrow \Omega_i = [0, \gamma_{i,0}], \\ &\rho_{i,0} \geq \rho_{\mathrm{c}} \Rightarrow \Omega_i = [0, f(\rho_{\mathrm{c}})]. \end{aligned} \tag{4.10}$$

For the outgoing road $i = 3$,

$$\begin{aligned} \rho_{i,0} \leq \rho_c &\Rightarrow \Omega_i = [0, \tilde{f}(\rho_c)], \\ \rho_{i,0} \geq \rho_c &\Rightarrow \Omega_i = [0, \gamma_{i,0}]. \end{aligned} \tag{4.11}$$

Moreover, we can define c_i such that

$$\Omega_i = [0, c_i].$$

Now after distinguishing two cases, we can compute precisely the fluxes at each junction of the roundabout in the following way.

(1) $c_1 + c_2 \leq c_3$: Then we have to look for γ_1, γ_2 such that

$$\begin{gathered} \max \gamma_1 + \gamma_2 \quad \text{w.r.t.} \\ 0 \leq \gamma_1 \leq c_1, \quad 0 \leq \gamma_2 \leq c_2, \quad \gamma_1 + \gamma_2 \leq c_3. \end{gathered}$$

The unique solution is found to be $\gamma_1 = c_1, \gamma_2 = c_2, \gamma_3 = c_1 + c_2$.

(2) $c_1 + c_2 \geq c_3$: Then we have to look for γ_1, γ_2 such that

$$\begin{gathered} \max \gamma_1 + \gamma_2 \quad \text{w.r.t.} \\ \gamma_1 = \tfrac{p}{1-p}\gamma_2 \\ 0 \leq \gamma_1 \leq c_1, \quad 0 \leq \gamma_2 \leq c_2, \quad \gamma_1 + \gamma_2 = c_3. \end{gathered}$$

where $p \in (0,1)$ is the priority parameter introduced at merging junction as given in [30]. Figure 4.4 illustrates feasible set for the solution of the Riemann solver. For detail theory regarding Riemann solver at junction we refer the reader to see [30] section(5.2.2). The purpose of the priority parameters is to neither impose insufficient flows nor send excess vehicles than the carrying capacity of the main link of the roundabout.

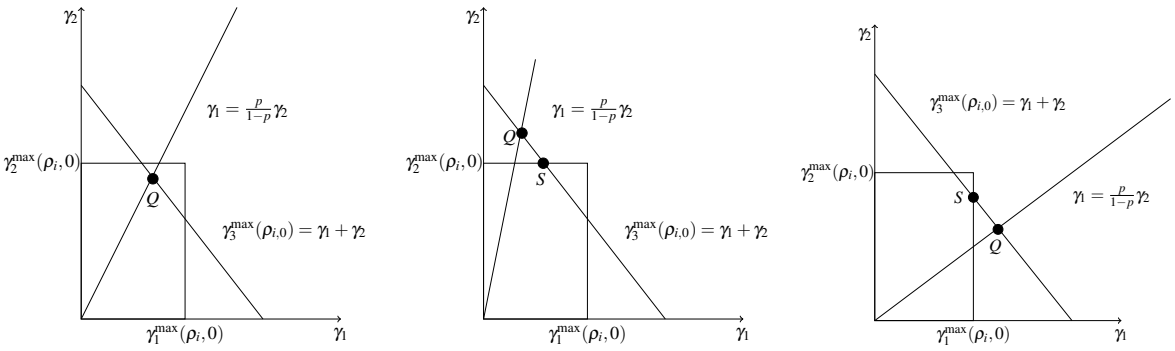

(a) Intersection inside Ω_i (b) Intersection outside Ω_i

Fig. 4.4: Solutions of the Riemann Solver at the junction.

Since $c_1 + c_2 > c_3$, $\hat{\gamma}_3 = \min(c_1 + c_2, c_3) = c_3$. For $c_2 > (1-p)c_3$ and $c_1 > pc_3$, we set $\mathrm{P}_1^i = 1 - \frac{c_2}{c_3}$ and $\mathrm{P}_2^i = \frac{c_1}{c_3}$ such that $\mathrm{P}_2^i - \mathrm{P}_1^i = \frac{c_1}{c_3} - (1 - \frac{c_2}{c_3}) > 0$. Under these conditions, the unique solution at junction is found to be

- $(\hat{\gamma}_1, \hat{\gamma}_2, \hat{\gamma}_3) = (c_3 - c_2, c_2, c_3)$ if $p \in (0, \mathrm{P}_1^i)$;
- $(\hat{\gamma}_1, \hat{\gamma}_2, \hat{\gamma}_3) = (pc_3, (1-p)c_3, c_3)$ if $p \in [\mathrm{P}_1^i, \mathrm{P}_2^i]$;
- $(\hat{\gamma}_1, \hat{\gamma}_2, \hat{\gamma}_3) = (c_1, c_3 - c_1, c_3)$ if $p \in (\mathrm{P}_2^i, 1)$.

B. **Coupling conditions for junction type** 1×2

In this case, we consider a junction with one incoming and two outgoing arcs. We use the same notation as before; i.e., we define $\gamma_{i,0}$ and the sets Ω_i depending on whether incoming or outgoing roads are considered. Using traffic distribution rates $\beta_{2,1}, \beta_{3,1} \in (0,1)$ with $\beta_{2,1} + \beta_{3,1} = 1$, then the CGP-conditions are

(1) $\gamma_1 \in \Omega_1, \beta_{j,1}\gamma_1 \in \Omega_j$ for j = 2,3;
(2) Maximize γ_1 w.r.t. (1);
(3) $\gamma_j = \beta_{j,1}\gamma_1, j = 2,3$.

Using $\Omega_i = [0, c_i]$, $i = 1,2,3$, we can obtain

$$\gamma_1 = \min\{c_1, \frac{c_2}{\beta_{2,1}}, \frac{c_3}{\beta_{3,1}}\}.$$

Remark 4.2. Condition (B) is exactly what is known as the FIFO (first in, first out) rule of a dispersing junction in the traffic engineering literature.

4.2.1 Analytical Study

In this subsection, we give analysis for traffic evolution on the roundabout network with and without the presence of pedestrians on the crosswalk. The analysis is only limited to a roundabout having four incoming and four outgoing roads for later numerical study and simplification purpose.

In the Absence of Pedestrians

Let $\tilde{f} = (\tilde{f}_1, \tilde{f}_2, \tilde{f}_3, \tilde{f}_4)$ be the traffic flux on the incoming roads towards the roundabout and $f(\rho_c)$ be the maximal traffic flux on the road network. Assume that $\beta f(\rho_c)$ of the traffic is flowing out of the main road of the roundabout through their corresponding existing roads while the remaining $(1-\beta)f(\rho_c)$ proceed to flow on the main road of the roundabout towards the next junction. Suppose that $p = (p_1, p_2, p_3, p_4)$ is the applied priority parameters at their respective

merging junctions of the roundabout where $\beta = (\beta_{ji})$ the splitting rate. In the case of supply limited situation,

$$\tilde{f}_i + (1-\beta) f(\rho_c) > f(\rho_c), \quad i = 1,2,3,4. \tag{4.12}$$

On the other hand from presentation under condition (A) we know that $(1-\beta) f(\rho_c) < c_1$ and $\tilde{f}_i \leq c_2$. Then we have the following conditions

(a) $p_i \in (0, \mathrm{P}_1^i)$
(b) $p_i \in [\mathrm{P}_1^i, \mathrm{P}_2^i]$
(c) $p_i \in (\mathrm{P}_2^i, 1)$, $i = 1,2\ldots,4$.

If $p_i \notin [\mathrm{P}_1^i, \mathrm{P}_2^i]$, $i = 1,2\ldots,4$, then either $p_i \in (0, \mathrm{P}_1^i)$ or $p_i \in (P_2^i, 1)$. If $p_i \in (0, \mathrm{P}_1^i)$, all the traffic on the incoming external roads of the roundabout enter the junction while excess vehicles waiting on the main link of the roundabout. In such a situation, backward propagating shock waves are produced on the main link of the roundabout while no wave on the incoming secondary road at each junction. On the contrary, if $p_i \in (\mathrm{P}_2^i, 1)$ all the traffic on the main link of the roundabout enter their corresponding junctions while queues are formed on the external incoming road of the roundabout. In both situation, the priority rule is violated due to the limited traffic demand entering the junction from either the main road of the roundabout or from the incoming external road of the roundabout. However, if $p_i \in [\mathrm{P}_1^i, \mathrm{P}_2^i]$ the priority rule is satisfied well due to sufficient demand from both main and the incoming secondary roads of the roundabout at each junction. In this case backward propagating shock will be formed on the network and congestion get raised. Furthermore, some of the junctions could be congested while the others stay demand limited. This fact is due to the volume of inflow traffic on the incoming edges.

Pedestrians Involvement

This situation includes all the previous cases in addition to the presence of pedestrian on the crosswalk. We assume that the crosswalk is situated both on the incoming and outgoing roads of the roundabout without any traffic light.

Consider vehicular traffic and pedestrian flow during peak hours. Assume for short period of time the crosswalk on the exit arm of the roundabout is occupied by pedestrians. Consequently, the original traffic flux is altered and behaves as given by equation (4.3). For the random duration $t_1 \leq t \leq t_2$ the flux is equal to zero on the crosswalk since the road is occupied by pedestrians. The interruption in flux function on the outgoing road results in a backward propagating shock waves. Thus, depending on the amount of traffic volume and

duration of the pedestrians staying on the crosswalk, the operational performance of the roundabout could be reduced.

On the contrary, when the pedestrians occupy the crosswalk on the entrance arm of the roundabout in the random time interval $t_1 \leq t \leq t_2$, queue would be formed on the incoming edge behind the crosswalk while the roundabout operate with less traffic compared to its carrying capacity. Further, when the probability of the pedestrians to be on the crosswalk both at entrance and exit road of the roundabout equal to 1, some of the circulatory road of the roundabout becomes congested due to backward propagating shock wave being demand limited on the entrance side. Also, as a result of priority parameter, drivers wait at the give-way lines for appropriate acceptable gaps between vehicles already circulating on the roundabout. This could also contribute in producing a backward propagating shock wave. However, under low traffic flow, any vehicle can proceed through the roundabout without delay.

From these scenarios, one can infer that traffic congestion plays a fundamental role in the formation of delay because vehicles spend longer periods of time near the roundabout while queuing, decelerating or accelerating due to the presence of pedestrian on the crosswalk. This shows the fluctuation on the performance of the roundabout in regulating traffic flow problem.

4.3 Numerical Approximation

In this section, we consider the traffic regulation problem for a network as the one in Figure 4.1. We analyze the impact of pedestrians' motion on the traffic evolution on the networks of a roundabout. In particular, we want to compare the performance of a roundabout with and without the involvement of pedestrians during peak hours.

4.3.1 Network Topology

The roundabout will be modelled by:

- 8 roads from the circle: $\mathscr{I}_5, \mathscr{I}_6, \mathscr{I}_7, \mathscr{I}_8, \mathscr{I}_9, \mathscr{I}_{10}, \mathscr{I}_{11}, \mathscr{I}_{12}$ coupled with CGP condition;
- 8 roads connecting the roundabout with the rest of the network: 4 incoming roads and 4 outgoing ones.

4.3.2 Numerical Scheme

From the topology, it can be noted that all the junctions in the roundabout can be represented as alternatively periodic sequences of 2×1 and 1×2-type for which it might be necessary to define respectively a right of way parameter p and distribution rate β. The first step is then to discretize the junction model. We define a numerical grid in $(0,T) \times \mathbb{R}$ using the following notation.

- Δx is the fixed space grid size;
- Δt is the grid size, given by the CFL condition;
- $(t^n, x_j) = (n\Delta t, j\Delta x)$ for $n \in \mathbb{N}$ and $j \in \mathbb{Z}$ are the grid points.

Each road is divided in to N + 1 cells numbered from 0 to N. The first and last cell of an edge are always a junction and we assume that these cells are ghost cells.

4.3.3 Godunov Scheme

We apply exactly the Godunov scheme briefly discussed in subsection 3.4.1. Under the CFL condition

$$\Delta t \max_{j \in \mathbb{Z}} \left| \lambda^n_{j+\frac{1}{2}} \right| \leq \Delta x, \tag{4.13}$$

the waves generated by different Riemann problems do not interact where, $\lambda^n_{j+\frac{1}{2}}$ is the wave speed of the Riemann problem solution at the interface $x_{j+\frac{1}{2}}$ at time t^n. Under the condition (4.13) the scheme can be written as

$$\rho_i^{n+1} = \rho_i^n - \frac{\Delta t}{\Delta x}(F^G(\rho_i^n, \rho_{i+1}^n) - F^G(\rho_{i-1}^n, \rho_i^n)), i = 2,3,\ldots,\mathrm{N}-1 \ \forall n \tag{4.14}$$

where the numerical flux F^G takes the following expression:

$$F^G(u,v) = \begin{cases} \min(f(u), f(v)) & \text{if } u \leq v, \\ \max(f(u), f(v)) & \text{if } v < u \ < \rho_c \vee \rho_c < v < u, \\ f(\rho_c) & \text{if } v < \rho < u. \end{cases} \tag{4.15}$$

for concave flux f.

In the following we introduce cost functionals that indicate the total mass of vehicle on the road networks of the roundabout, average velocity, and flux respectively to analyze the performance of the roundabout with and without pedestrian motion on the crosswalk.

$$
\begin{aligned}
J_1(t) &= \sum_{i=1}^{m} \int_{I_i} \rho(t,x)\, dx, \\
J_2(t) &= \sum_{i=1}^{m} \int_{I_i} v(\rho_i(t,x))\, dx, \\
J_3(t) &= \sum_{i=1}^{m} \int_{I_i} \tilde{f}(\rho_i(t,x))\, dx
\end{aligned}
\tag{4.16}
$$

For a fixed time horizon $[0,T]$ our aim is to compare $\int_0^T J_1(t)dt$, $\int_0^T J_2(t)dt$, and $\int_0^T J_3(t)dt$ for an appropriate fixed distribution matrix and priority parameters. We do not treat optimization problem in this chapter. We left it for future work.

Comparison of roundabout with and without pedestrian motion

We consider approximation obtained by Godunov scheme with space step size $\Delta x = 0.333$ and the time step determined by the CFL condition. The traffic and pedestrian flow on the road network is simulated in a time interval $[0, T_{max}]$, where $T_{\max} = 10$. For the initial condition on the roads of the network, we assume that at initial time $t = 0$ all the roads are empty and influx at boundary of incoming edges equal to 0.2.

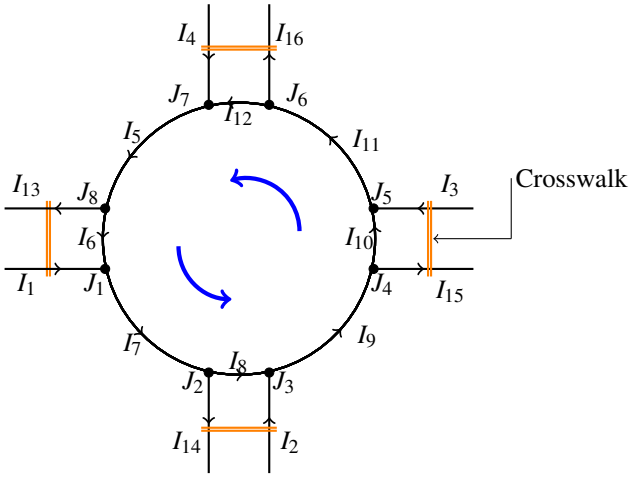

Fig. 4.5: For comparison.

In order to show the different state of traffic evolution on the network, we assume that the crosswalk is marked orthogonally at the midpoint of incoming and outgoing external roads. There is no crosswalk on the main roads forming the roundabout under consideration. Further we assume that the crosswalk on the incoming and outgoing roads are occupied by pedestrians for short period

of time $t = t_2 - t_1$, see Figure 4.5. We now compare the results of the traffic flow with and without the pedestrians. The corresponding pictures on all the external incoming and outgoing roads, roads forming the roundabout look the same and therefore we just compare one from each of them.

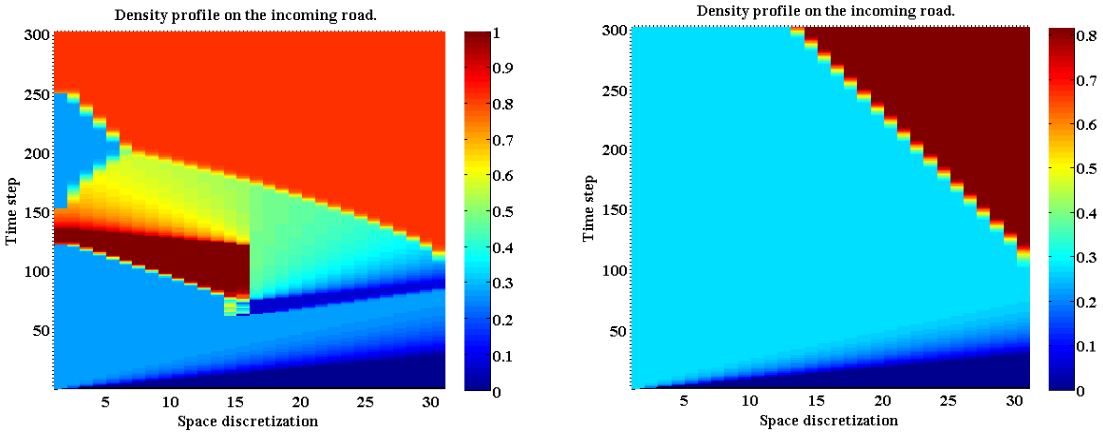

(a) Roundabout with pedestrians on the crosswalk.

(b) Roundabout without pedestrians on the crosswalk.

Fig. 4.6: Traffic evolution on the incoming roads of the roundabout.

For the first few time steps $t < 62$, the evolution of traffic on the incoming roads behave similar in both cases due to the absence of pedestrians on the crosswalk. As soon as the pedestrians interrupt flow on the incoming roads at cell position $x = 15$ at time step $t = 62$, the situation is immediately changed as illustrated in Figure 4.6. Different colors in the figure correspond to different states of traffic evolution over simulation period. The blue color corresponds to demand limited case whereas the red color corresponds to congested state. The shock occurred due to pedestrians motion on the crosswalk propagating back on the incoming road. The part of the road between crosswalk and roundabout stay demand limited until the pedestrians cleared on the road at time step $t = 77$. Then rarefaction wave fill this portion of the road. Due to priority at merging junctions of the roundabout, new shock wave is produced on the incoming road. This shock wave moves back on the incoming road as depicted in Figure 4.6a.

Traffic congestion can occur at merging junctions in the case of roundabout without pedestrian involvement, see Figure 4.6b. Similar to the other case shock wave propagating back on the incoming roads. Comparing these two states of

the roundabout one can easily observe the difference in the magnitude of traffic jam. Shock formed due to priority at merging junction do not reach the influx boundary in the absence of pedestrian involvement.

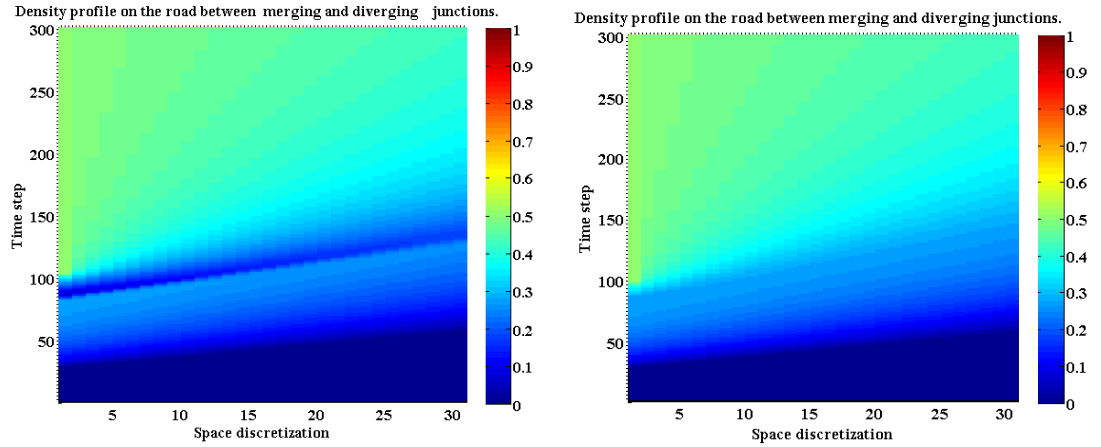

(a) Roundabout with pedestrians on the crosswalk.

(b) Roundabout without pedestrians on the crosswalk.

Fig. 4.7: Traffic evolution on the main road between merging and diverging junctions of the roundabout.

In Figure 4.7a, the blue color at about time step $t = 100$ reveals that the interrupted flow reach the main road between merging and diverging junctions of the roundabout. Rarefaction waves on the main road between merging and diverging junctions of the roundabout increases the density to its critical density. The evolution of traffic on this portion of the roundabout remains smooth.

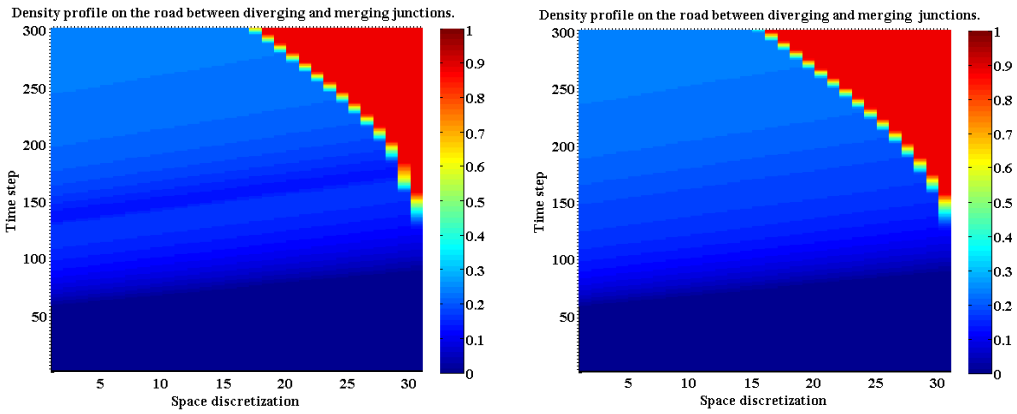

(a) Roundabout with pedestrians on the crosswalk.

(b) Roundabout without pedestrians on the crosswalk.

Fig. 4.8: Traffic evolution on the main road between diverging and merging junctions of the roundabout.

Traffic congestion appearing on the main road forming the roundabout at merging junctions. The shocks moving back as it can be seen from Figure 4.8. Further, the impact induced by pedestrians do not clearly reflected in this portion of the roundabout. This could be due to βf of the traffic exist the roundabout through outgoing roads and the influence of priority at merging junctions.

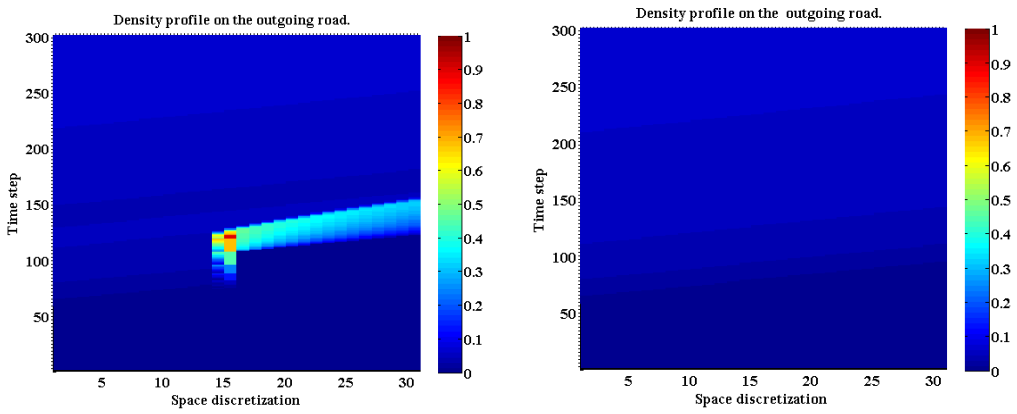

(a) Roundabout with pedestrians on the crosswalk.

(b) Roundabout without pedestrians on the crosswalk.

Fig. 4.9: Traffic evolution on the outgoing roads of the roundabout.

Traffic jam on the outgoing edges when pedestrians moving on the crosswalk arises (compare Figure 4.9). The influence due to this jam on the traffic circulating on the inner road of the roundabout is insignificant because of short stay of pedestrians on the croswalk. The outgoing secondary roads of the roundabout without pedestrians interference remains demand limited.

Comparison

In this subsection we compute changes in total density, average velocity and total flux of the cost functional introduced in equation (4.16). That is, in the case of traffic evolution on the roundabout without pedestrian and pedestrian involvement. More precisely, we consider fixed distribution rate in both cases and different simulations cases which vary according to the values of the priority parameter $p \in \{0.2, 0.3, 0.4, 0.5, 0.6, 0.7, 0.8\}$. Then we compute separately the values of the cost functional and take their respective differences for comparison.

p	$\sum_{t=0}^{T} J_1$	$\sum_{t=0}^{T} J_2$	$\sum_{t=0}^{T} J_3$
0.2	36.1013	119.0809	19.1204
0.3	36.1013	119.0809	19.5410
0.4	36.1013	119.0809	19.6240
0.5	36.1013	119.0809	19.4765
0.6	36.1013	119.0809	19.2031
0.7	36.0878	119.0944	18.988
0.8	36.0877	119.0945	18.9765

(a) In the absence of pedestrians

p	$\sum_{t=0}^{T} J_{1P}$	$\sum_{t=0}^{T} J_{2P}$	$\sum_{t=0}^{T} J_{3P}$
0.2	43.6625	111.5197	19.0936
0.3	43.6625	111.5197	19.1127
0.4	43.3753	111.8065	18.9086
0.5	42.6935	112.4887	18.6102
0.6	42.3726	112.8096	18.3428
0.7	42.2879	112.8943	18.1639
0.8	42.2879	112.8943	18.1574

(b) In the presence of pedestrians

Table 4.1: Sum of values of cost functional over time horizon. J_1, J_2 and J_3 respectively denotes cost functionals that measure total density, average velocity and total flux. The subscript p is used to indicate pedestrian.

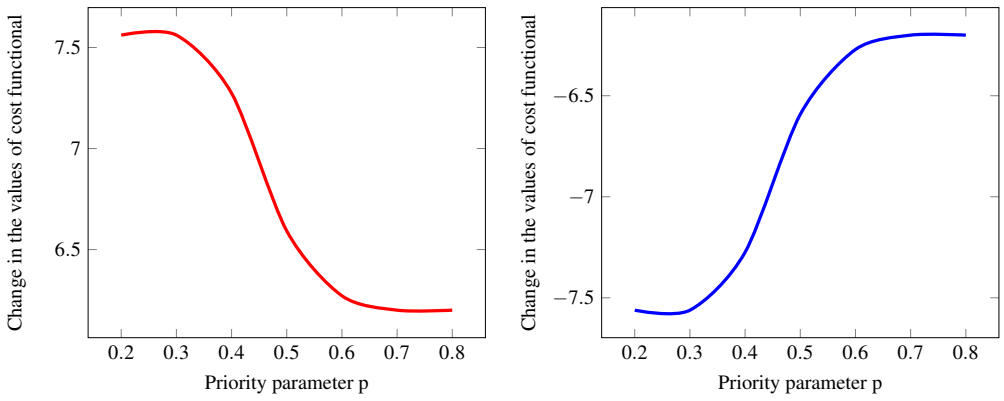

(a) Change in total density

(b) Change in average velocity

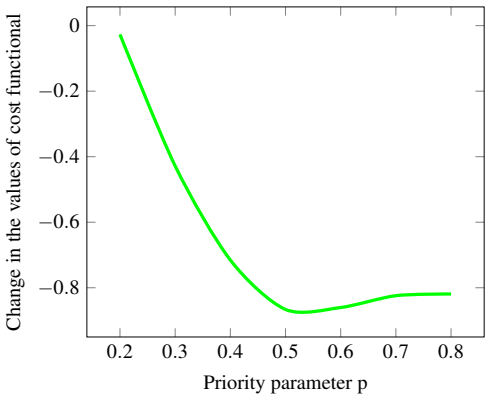

(c) Change in total Flux

Fig. 4.10: Difference in the values of cost functional measuring total density of vehicles, average velocity and total flux on the network.

From Table 4.1 one can easily infer that due to presence of pedestrian on the crosswalk there are more vehicles waiting on the network. In the case of roundabout without pedestrian involvement the role played by priority parameters are insignificant in altering total density. This is due to the fact that congestion which propagate backwards on the incoming roads do not reach the other end over the given time interval. In the contrary, in the case of roundabout with pedestrian involvement the priority parameter plays remarkable role in reflecting changes in the cost functionals.

To minimize traffic congestion, we give more priority for cars circulating on main road of the roundabout in both cases. Consequently, the change in the total density of vehicles initially constant and then it start decreasing, see Fig-

ure 4.10a. Furthermore, for $p \geq 0.7$ the change in the total mass of vehicles on the network becomes constant. Similarly, the change in the average velocity of vehicles initially constant and then it start increasing as depicted in Figure 4.10b. Figure 4.10c describe the change in the total flux due to priority parameters on the whole network.

Comparing these tables we can deduce that the interruption due to pedestrian decreases the average velocity of vehicles on the network, also see Figure 4.10b. Similarly it reduces the traffic flux on the whole network as it can be seen from Figure 4.10c. Thus, the simulation result indicates that the presence of pedestrians on the crosswalk influences the performance of the roundabout in controlling traffic flow problem. Since this reflects some what the validity of our model, the optimization and further analysis is still work in progress.

Chapter 5
Conclusion

In this dissertation, the issue of traffic congestion and its socio-economic impact is presented briefly. The advantages and disadvantages of modeling approaches were recalled before giving detail analysis. The use of traffic flow models were also briefly discussed and more emphasis was given to the macroscopic approach in particular the LWR model for this study. In Section 1.2 we reviewed some of the existing related literature.

The main results of this dissertation can be summarized as follows. In Section 3.2, the roundabout has been modelled as a concatenation of 2×2 junctions. The incoming roads have been modelled by a buffer of infinite capacity for the entering flux and with an infinite sink for the exiting one. The evolution of traffic flow on the whole road networks of the roundabout was described by nonlinear scalar hyperbolic partial differential equation (PDE). At each junction, the Riemann problem was uniquely solved using a right of way parameter and solutions were constructed exactly via wave front tracking method (cf. Subsection 3.3.1).

In Section 3.5, an optimization problem was solved where the optimal control acts on the priority parameters, which assigns right of way among incoming roads. Two cost functionals that measures the total waiting time and total travel time on the network were introduced. The cost functionals were computed analytically for a single junction in subsection 3.5.1. The approach was numerically tested on a simple roundabout with three incoming and three outgoing roads. Two different choices of parameters were considered: instantaneously locally optimal and a well chosen but fixed values. The local optima parameter value outperform the other choices, in improving the performances of the network. The simulation results have shown the effectiveness of the optimization strategy compared to the case of fixed constant right of way parameters.

In subsection 3.3.2, the construction of Riemann solver was extended to a roundabout with arbitrary m entrances and m existing roads. First the hyperbolic PDE was discretized via the Godunov scheme and the ODE using an explicit Euler first order integration method. Then the Godunov scheme was adapted in subsection 3.4.2 to fit to the settings considered.

In subsection 3.5.2, a cost functional was introduced that measures the total travel time spent by drivers on the roundabout in discrete form. Then the gradient of the cost functional was computed instantaneously at each time step t^n and the optimal priority parameters were found.

Numerical tests were conducted for a roundabout with four incoming and four outgoing roads in subsection 3.5.2. The simulation results show that gradient based instantaneous optimal choice of the priority parameters produce better results in improving the performance of the roundabout compared to the fixed choices of priority parameters. In the case of fixed priority parameters, larger fixed values are better in optimizing traffic flux on the main lane of the roundabout relative to smaller values.

In chapter 4, the performance of a roundabout in regulating traffic flow problems was studied in the presence and absence of pedestrians on the crosswalk located at entrances and existing roads. Roundabouts can be seen as particular road network and can be modeled as alternatively periodic sequences of 2×1 and 1×2-type junctions. The evolution of traffic flow on the whole road networks of the roundabout was described by nonlinear scalar hyperbolic partial differential equation (PDE).

Then the PDE was discretized again via the Godunov scheme and the time evolution of traffic on the network was studied through numerical simulation in subsection 4.3.3. Additionally, cost functionals were introduced that measures the total mass of vehicles on the road networks of the roundabout, average velocity and total flux for both cases and the values of the functionals were computed. Then, the sum of values of these cost functionals were compared. The simulation result indicated that, the presence of pedestrians on the crosswalk reduces the performance of roundabout in controlling traffic flow problem. The design of suitable optimization strategy for a roundabout involving pedestrians motion on the crosswalk and probablistic incoming flow require a future consideration. Multi-lane roundabout cases are also challenging and can be considered as future work. Furthermore, validation of the models with real data would be considered in the future work.

Bibliography

[1] A. AW and M. Rascle. Resurrection of second order models of traffic flows. *SIAM J. Appl. Math*, 60:916–938, 2000.

[2] M.K. Banda, M. Herty, and A. Klar. Gas flow in pipeline networks. *Netw. Heterog. Media.*, 1(1):41–56(electronic), 2006.

[3] M. Bando, K. Hasebe, A. Nakayama, A. Shibata, and Y. Sugiyama. Dynamical model of traffic congestion and numerical simulation. *Physical Review E.*, 51:1035–1042, 1995.

[4] C. Bardos, A. Y. le Roux, and J.-C. Nédélec. First order quasilinear equations with boundary conditions. *Comm. Partial Differential Equations*, 4: 1017–1034, 1979.

[5] N. Bellomo and Dogbe. C. On the modeling of traffic and crowds: A survey of models, speculations and perspectives. *SIAM J. Appl. Math*, 53(3):409–465, 2011.

[6] R. Borsche and A. Meurer. Interaction of road networks and pedestrian motion at crosswalks. *Discrete Contin. Dyn. Syst.*, 7(3):363–377, 2014.

[7] R. Borsche, A. Klar, S Kühn, and A. Meurer. Coupling traffic flow networks to pedestrian motion. *Mathmatical Models and Methods in Applied Sciences*, 24(2):359–380, 2014.

[8] A. Bressan. *Hyperbolic systems of conservation laws: The one dimentional Cauchy Problem.* Oxford Lecture Series in Mathematics and Its Application, 2000.

[9] G. Bretti, N. Natalini, and B. Piccoli. Numerical algorithms for simulations of a traffic model on road networks. *Jour. comput. Appl. Math.*, 210:71–77, 2007.

[10] A. Cascone, C. D'Apice, B. Piccoli, and L. Raritá. Optimization of traffic on road networks. *Mathematical Models and Methods in Applied Sciences*, 17: 1587–1617, 2007.

[11] A. Cascone, C. D'apice, B. Piccoli, and Luigi. Circulation of car traffic in congested urban areas. *Commun. Math. Sci.*, 6:765–784, 2008.

[12] Y. Chitour and B. Piccoli. Traffic circles and timing of traffic lights for cars flow. *Discrete and Continuous Dynamical Systems Series B*, 5:599–630, 2005.

[13] G.M. Coclite, M. Garavello, and B. Piccoli. Traffic flow on a road network. *SIAM J. Math. Anal.*, 36(6):1862–1886, 2005.

[14] R. Colombo. Hyperbolic phase transitions in traffic flow. *SIAM Journal on Applied Mathematics*, 63(2):708–721, 2002.

[15] R. Colombo and Rosini M. D. Pedestrian flows and non-classical shocks. *Math. Meth. Appl. Sci.*, 28:1553–1567, 2005.

[16] R. M. Colombo, P. Goatin, and B. Piccoli. Road network with phase transition. *Journal of Hyperbolic Differential Equations*, 07:85–106, 2010.

[17] A. Cutolo, C. D'Apice, and R. Manzo. Traffic optimization at junctions to improve vehicular flows. *International Scholarly Reaserch Network Applied Mathematics*, 1:1–19, 2011.

[18] A. Cutolo, B. Piccoli, and L. Raritá. An upwind-Euler scheme for an ODE-PDE model of supply chains. *SIAM J. Sci. Comput.*, 33:1669–1688, 2011.

[19] C. M. Dafermos. *Hyperbolic Conservation Laws in Continuum Physics*. Springer−Verlag Berlin Heidelberg, 2010.

[20] C. F. Daganzo. Requiem for second-order fluid approximations of traffic flow. *Transportation Research Part B*, 29(4):277 –286, 1995.

[21] C. F. Daganzo. A behavioral theory of multi-lane traffic flow. part i: Long homogeneous freeway sections. *Trans. Res. Part B: Methodological*, 36(2): 131–158, 2002.

[22] C. d'Apice and B. Piccoli. Vertex flow models for vehicular traffic on networks,. *Math. Models. Methods Appl. Sci.*, 18:1299–1315., 2008.

[23] C. D'apice, R. Manzo, and B. Piccoli. Packet flow on telecommunication networks. *SIAM J. Math. Anal.*, 38(3):717–740, 2006.

[24] M. L. Delle Monache, L. L. Obsu, P. Goatin, and S. M. Kassa. Traffic flow optimization on roundabouts. In *EWGT2013– 16th Meeting of the EURO Working Group on Transportation*, volume 111, pages 117–136. Elsevier Ltd, 2014.

[25] M. L. Delle Monache, J. Reilly, S. Samaranayake, W. Krichene, P. Goatin, and A. M. Bayen. A PDE-ODE model for a junction with ramp buffer. *SIAM J. Appl. Math.*, 74(1):22–39, 2014.

[26] L.C. Evans. *Partial Differential Equations: Graduate Studies in Mathematics*. American Mathematical Society, Vol. 19, 1998.

[27] Y. Feng, Y. Liu, P. Deo, and H.J. Ruskin. Heterogeneous traffic flow model for two lane roundabouts and controlled intersection. *International Journal of Modern Physics C*, 1:107–117, 2007.

[28] M. Garavello and P. Goatin. The Aw-Rascle traffic model with locally constrained flow. *Joural of Mathematical Analysis and Applications*, 378:634–645, 2011.

[29] M. Garavello and P. Goatin. The Cauchy problem at a node with buffer. *Discrete Contin. Dyn. Syst.*, 32:1915–1938, 2012.

[30] M. Garavello and B. Piccoli. *Traffic Flow on Networks: Conservation Laws Model*. American Institute of Mathematical Sciences, 2006.

[31] M. Garavello and B. Piccoli. Traffic flow on a road network using the aw-rascle model,. *Commun. Partial differential Equations*, 31(2):243–275, 2006.

[32] D. C. Gazis, R. Herman, and R. Rothery. Nonlniear follow the leader models of traffic flow. *Operational Research*, 9:545–567, 1961.

[33] P. Goatin. The Aw-Rascle vehicular traffic flow model with phase transitions. *Math. Comput. Modelling*, 44:287–303, 2006.

[34] G. Gomes and R. Horowitz. Optimal freeway ramp metering using the asymmetric cell transmission model. *Transportation Research Part C: Emerging Technologies*, 14.4:244–262, 2006.
[35] S. Göttlich, M. Herty, and A. Klar. Modelling and optimization of supply chains on complex networks. *Commun. Math. Sci.*, 4(2):315–330, 2006.
[36] S. Göttlich, A. Klar, and P. Schindler. Discontinuous conservation laws for production networks with finite buffer. *SIAM J. Appl. Math*, 73:1117–1138, 2013.
[37] B. D. Greenshields. A study of traffic capacity. *Highway Research Board*, 14: 448–477, 1935.
[38] M. Gugat, M. Herty, A. Klar, and G. Leugering. Optimal control for traffic flow networks. *Journal of optimization theory and applications*, 126:589–616, 2005.
[39] D. Helbing. Traffic and related self-driven many particle systems. *Rev. Modern phys.*, 73:1067–1141, 2001.
[40] M. Herty and A. Klar. Modeling, simulation, and optimization of traffic flow networks. *SIAM Journal on Scientific Computing*, 25:1066–1087, 2003.
[41] M. Herty and M. Rascle. Coupling conditions for a class of second order models for traffic flow. *SIAM J. Math. Anal.*, 38:595–616, 2006.
[42] M. Herty, C. Kirchner, and A. Klar. Instantaneous control for traffic flow. *Math. Meth. Appl. Sci.*, 30:153–169, 2007.
[43] M. Herty, J.P Lebacque, and S. Moutari. A novel model for intersections of vehicular traffic flow. *Networks and Heterogeneous Media, American Institute of Mathematical Sciences*, 4:813–826, 2009.
[44] H. Holden and N.H. Nisebro. A mathematical model of traffic flow on a network of unidirectional roads,. *SIAM J. Math. Anal.*, 26:997–1017, 1995.
[45] H. Holden and N. H. Risebro. *Front tracking for Hyperbolic Conservation Laws*. Springer− Heidelberg Dordrecht London New York, 2011.
[46] Godunov S K. A finite difference method for the numerical computation of discontinuous solutions of the equations of fluid dynamics. *Matematicheskii Sbornik*, 47:271–290, 1959.
[47] B. S. Kerner. Congested traffic flow: Observation and theory. *Transportation Research*, 1678:160–167, 1998.
[48] A. Klar and R. Wegener. Enskog-like kinetic models for vehicular traffic,. *Journal of Statistical Physics*, 87:91–114, 1997.
[49] D. Kröner. *Numerical Schemes for Conservation Laws*. Jointly by John Wiley and Sons Lts, 1997.
[50] S. N. Kružhkov. First order quasilinear equations with several independent variables. *Mat. Sb. (N.S.)*, 81 (123):228–255, 1970.
[51] J. P. Lebacque. The godunov scheme and what it means for first order traffic flow models. In *Transportation and Traffic Theory, 647–77*, 1996.

[52] R. J. Leveque. *Numerical methods for conservation laws. Lectures in Mathematcs ETH Zürich.* Birkhäuser Verlang, 1992.
[53] M. J. Lighthill and G. B. Whitham. On kinematic waves II. a theory of traffic flow on long crowded roads. *Proceedings of the Royal Society of London. Series A. Mathematical and Physical Sciences*, 229:317–345, 1955.
[54] R. M. M. Mattheij, S. W. Rienstra, and J. H. M. ten Thije Boonkkamp. *Partial Differential Equations, Moding, Analysis, Computations*. SIAM, 2005.
[55] A. Meister and J. Struckmeier. *Hyperbolic partial Differential Equations, Theory, Numerics and Applications*. Vieweg, 2002.
[56] P. Nelson. A kinetic model of vehicular traffic and its associted bimodal equilibrium solutions,. *Transport Theory and Statistcal Physics*, 24:383–408, 1995.
[57] Legesse L. Obsu, M. L. Delle Monache, Paola Goatin, and Semu M. Kassa. Traffic flow optimization on roundabouts. *Mathematical Methods in the Applied Sciences, DOI: 10.1002/mma.3283*.
[58] O. Oleinik. Discontinuous solutions of non–linear differential equations. *Uspekhi Mat.Nauk*, 12(3):3–73, 1957.
[59] H. J. Payne. Models of freeway traffic and control, in mathematical models of public systems. In *Simulation Council Proceedings, 1:51–61*, 1971.
[60] J. Reilly, W. Krichene, M. L. Delle Monache, S. Samaranayake, , P. Goatin, and A. M. Bayen. Adjoint-based optimization on a network of discretized scalar conservation law pdes with application to coordinated ramp metering. Preprint, October 2013.
[61] Paul I Richards. Shock waves on the highway. *Operations research*, 4:42–51, 1956.
[62] Hughes R.L. A continuum theory for the flow of pedestrians,. *Trans. Res. Part B: Methodological*, 36:507–535, 2002.
[63] D. Schrank, T. Lomax, and B. Eisele. Urban mobility reports. Technical report, Texas Transportation Institute, 2011.
[64] J. A. Trangenstein. *Numerical Solution of Hyperbolic Partial Differential Equations*. Cambridge University Press, 2007.
[65] G.B. Whitham. *Linear and nonlinear waves*. John Wiley and Sons, New York, 1974.

Declaration

This dissertation is my original work and has not been presented for a degree in any other university, and that all sources of the material used for the dissertation have been duly acknowledged.

Legesse Lemecha Signature .....

Dr. Semu Mitiku (Supervisor) Signature .....

Dr. Paola Goatin (Supervisor) Signature .....